Nanomaterial Processing Using Self-Assembly - Bottom-Up Chemical and Biological Approaches

Rajagopalan Thiruvengadathan[1,2], Venumadhav Korampally[3], Arkasubhra Ghosh[4], Nripen Chanda[5], Keshab Gangopadhyay[1,2,6] and Shubhra Gangopadhyay[1*]

[1]*Department of Electrical Engineering, University of Missouri, Columbia, Missouri, 65211- USA.*
[2]*NEMS/MEMS Works, LLC. 8850 Westlake Road West, Columbia, Missouri, 65202 - USA.*
[3]*Department of Electrical Engineering, Northern Illinois University, Dekalb, Illinois - 60115 USA.*
[4]*Molecular Signalling and Gene Therapy, Narayana Nethralaya, Narayana Health City, Bangalore - 560099 INDIA.*
[5]*Micro System Technology, CSIR – Central Mechanical Engineering Research Institute, Durgapur – 713209 INDIA*
[6]*Nuclear Science and Engineering Institute, University of Missouri, Columbia, Missouri - 65211 USA*
***Corresponding Author**: *gangopadhyays@missouri.edu*; **Tel**: +1 573-882-4070; **Fax**: + 1 573-882-0397

Abstract

Nanotechnology is touted as the next logical sequence in technological evolution. This has led to a substantial surge in research activities pertaining to the development and fundamental understanding of processes and assembly at the nanoscale. Both top-down and bottom-up fabrication approaches may be used to realize a range of well-defined nanostructured materials with desirable physical and chemical attributes. Among these, bottom-up self-assembly process offers the most realistic solution towards the fabrication of next-generation functional materials and devices. Here, we present a comprehensive review on the physical basis behind self-assembly and the processes reported in recent years to direct the assembly of nanoscale functional blocks into hierarchically ordered structures. This article emphasizes assembly in the synthetic domain as well in the biological domain, underscoring the importance of biomimetic approaches towards novel materials. In particular, two important classes of directed self-assembly, namely, (i) self assembly among nanoparticle-polymer systems and (ii) external field-guided assembly are highlighted. The spontaneous self-assembling behavior observed in nature that leads to complex, multifunctional, hierarchical structures within biological systems is also discussed in this review. Recent research undertaken to synthesize hierarchically assembled functional materials have underscored the need as well as the benefits harvested in synergistically combining top-down fabrication methods with bottom-up self-assembly.

Key Words: *Self-Assembly; Nanotechnology; Nanomaterials; Bottom-Up; Directed Self-Assembly; In situ Characterization; Self-Assembled Monolayers; Nanopatterning; Block Copolymers; Biological Systems; Biomimetics*

1. Introduction

Nanotechnology has drawn a great deal of interest in the past two decades owing to its potential in the creation of novel materials and device structures with extraordinary physical and chemical properties.[1-11] Considerable resources have been invested in the research and development of these materials to realize drastic improvements in the device/material performance. However, challenges persist, preventing application of these technologies to real-world problems. While a general wish list for the desired material/device properties has been identified through simulations of specific nanoscale architectures, translating these findings to reproducible fabrication of functional macroscopic structures on a scale feasible for industrial production is far from a trivial undertaking. Self-assembly stands out as the most attractive, technologically feasible, and cost-effective strategy to address these challenges. Self-assembly is essentially a bottom-up process, wherein atoms, molecules, or particles associate into well-defined and functional geometries under specific, controllable thermodynamic conditions. Nature has devised clever means to circumvent a number of challenges through application of self-assembly and examples of the effectiveness of this concept are ubiquitous. The scientific community has long attempted to replicate this idea, with early examples including colloidal assembly of large objects reported as early as the 1940s.[12] Others have followed suit as the ability to probe into the nanoscale has improved, and now, self-assembly of metal and semiconductor nanoparticles [13-17], polymers [18-22], and biological systems [23-26] is well-documented and the subject of intense on-going research. It is also known that nature prefers the bottom-up approach exclusively, to generate self-assembled hierarchical systems exquisitely by manipulating the local conditions using a very limited repertoire of available molecules. Such self assembly occurs typically in the liquid phase under normal temperature, pressure and pH to generate a variety of materials with wide ranges of strength, elasticity and function. Thus the basic tenets of biological assembly are being investigated vigorously to apply them to modern manufacturing processes for higher efficiency as well as development of novel, functionalized nanomaterials.

The key to self-assembly in a variety of systems such as colloidal suspensions, micro- and nano-emulsions, and biological systems lies in achieving force balance between various attractive and repulsive interactions.[27] It is imperative to gain a thorough understanding of the nature and complexity behind these processes to manipulate the arrangement of nanoparticles in a desired manner. Depending on the nature and cumulative effect of these interactions, the net association between objects may be either isotropic or anisotropic. While most of the aggregations observed in non-biological systems are isotropic in nature and result in the formation of non-hierarchical structures, the aggregation behavior observed in many biological (DNA, RNA, and proteins) and bio-mimetic (synthetic amino acids, carboxylic acids,

and dendric polymers) systems can be highly anisotropic in nature, leading to well-defined, directional, and ultimately functional assemblies.

The main objective of this review is to present a detailed overview of various aspects of self-assembly from the perspectives of fundamental science and resulting applications. This review begins with an introduction to self-assembly and its scientific and technological implications. This is followed by a detailed discussion on the physics of self-assembly. Specifically, the forces and force balance conditions responsible for the self-assembly of nanoscale elements in a particular manner are presented. Readers are referred to standard references for detailed mathematical treatment of the interaction forces in their appropriate sub-sections. In the last decade, there has been a flood of scientific developments in the field of directed self-assembly (DSA), where nanoscale building blocks are guided to assemble in a predetermined fashion under the influence of external fields or templates, which has enabled realization of hierarchical macroscopic structures with novel structural, optical, electronic, and magnetic properties. Another attractive means towards self-assembly is to exploit the thermodynamic interactions (entropic-enthalpic interplays) within nanoparticle and polymer systems. Recent literature has shown that such interactions may be utilized to govern the spatial organization of the nanoparticles within the system. Therefore, an attempt is made to provide a comprehensive review of DSA in both synthetic and biological systems with illustrations from pioneering works reported recently. Particular emphasis has also been placed on approaches that combine top-down lithography and bottom-up self-assembly towards fabrication of hierarchically ordered structures. Such combinations often overcome the distinct limitations of each and highlight the potential complementary nature of the two approaches.[28, 29]. Recent efforts have further demonstrated the tremendous potential of integrated approaches in the generation of self-assembled structures at all length scales (from nano- to macro-scales).[30-35]. The final section is devoted to description of various *in situ* characterization techniques developed in the past decade to grasp the science of DSA. Catching glimpses of the self-assembly processes as it occurs is expected to provide new insights and advance our fundamental understanding of the assembly process. Through this review, we hope to stress the importance of understanding the concepts of self-assembly for future work at the nanoscale and help the reader gain a fascination for the field and its progress from the viewpoint of both fundamental science and technological development.

2. Self-Assembly: Origins and Importance

Self-assembly is a process by which discrete components are driven to organize spontaneously into well-defined geometries by specific interactions. These interactions may arise due to the intrinsic properties of the individual elements composing the system or under the influence of applied external fields.[36, 37] Self-assembly is originally believed to be associated with thermodynamic equilibrium; the

organized structures being characterized by minima in the system's free energy.[38] However, deeper inspection suggests this definition is broad and not always appropriate given the recent emergence of concepts such as DSA, where the building units are driven to assemble through the application of external forces such as electric, magnetic, or flow fields as well as combinations of these fields.[39]

Self-assembly, especially at the molecular level, is omnipresent in nature. Complex biological structures such as lipid membranes, higher-order structured proteins and nucleic acids, and multi-component protein aggregates present in living cells are formed almost exclusively through self-assembly and are central to the very existence of life.[24, 26, 38, 40] Synthesis of man-made materials using the concepts of molecular self-assembly was first adopted by synthetic chemists in the 1980s.[41] Subsequent emergence of interdisciplinary sciences involving the concepts of physics, chemistry, biology and materials science led to the development of producing materials at the nanoscale with tunable dimensions, morphology, and functionality.[26] Examples of these forms include nanospheres, nanorods, nanowires, nanodiscs, core-shell nanostructures, and nanocages.[7, 25, 42] In addition to the synthesis of nanoscale objects, the concept of self-assembly has been further exploited to arrange and assemble these objects in an orderly manner at pre-determined locations.[30-35, 37, 43] A number of interactions, namely, electrostatic, van der Waals (vdW), steric, and hydrophobic forces, may be used to organize colloidal nanomaterials on different surfaces. We discuss these interactions in detail with suitable illustrations in the following section.

3. Physics of Self-assembly: Interaction Forces

The assembly of nanoscale components into macroscopic hierarchical structures depends on the manipulation of inter-particle interactions governed by various forces as will be described shortly. Specifically, the free energy of the system is a quintessential parameter governing self-assembly within a colloidal suspension. Free energy is a net contribution from both enthalpic and entropic terms. The nature of the dominant force driving the assembly depends on a number of parameters, including, but not limited to the relative and total concentrations of the constituents composing the system, the separation distances between them, their relative and actual size, solvent composition, temperature, and other environmental conditions.

What drives such a system toward an ordered or disordered state? Unfortunately, there is no simple, all-encompassing answer to this question. The length scale of different interaction potentials, the relative magnitudes of short-range and long-range interactions, and the nature of interactions involved are just a few of the many factors involved in the formation of ordered assemblies. It is often thought that careful tailoring of the interactions between nanomaterials can lead to the formation of equilibrium structures corresponding to the minimum free energy state, subsequently leading to ordered self-

assembly.[38] In reality, processes more often occur under non-equilibrium conditions. Prominent examples of self-assembly dominated by non-equilibrium conditions include glass and gel formation as well as protein folding.[44-46] In general, non-equilibrium events compete with relaxation processes that may lead to amorphous states.[36, 46] It may therefore be necessary to exploit long-range interactions relative to the size of the assembling components to be able to form ordered self-assembled structures. Unfortunately, many common attractive interactions act appreciably over only the scale of molecular dimensions. Larger, colloidal particles interacting through such short-range attractive forces would likely aggregate to form a disordered phase. However, nearly all examples of colloidal crystallization overcome this limitation by using long-range interactions (electrostatic and depletion) or through entropic processes at high volume fractions.[36] The objective of this section is to introduce the basic concepts clearly and restrict the discussion to qualitative highlights with suitable illustrations for each type of interaction. We attempt to provide the readers some details on the magnitude and the length scale of these interactions as well as discuss how these interactions scale with particle size and inter-particle distance.

3.1 Van der Waals Forces

Van der Waals (vdW) force arises due to the interactions between two or more permanent and/or induced dipoles. The vdW force encompass three possible configurations: (i) Keesom interactions that describe interactions between two permanent dipoles, (ii) Debye interactions between a permanent dipole and an induced dipole, and (iii) London forces between two or more induced dipoles of polarizable objects. The vdW attractive interaction potential between dipoles may be expressed by the well-known expression, $U(r)_{vdW} = -{C_{vdW}}/{r^6}$, where r is the distance between dipoles and C_{vdW} is the proportionality constant.[47] The constant takes into account the three different types of interactions mentioned above. Originally, the potential was derived for inter-atomic or inter-molecular interactions. In the case of colloidal particles where the inter-particle separation is less than 10 nm, vdW forces play a significant role in inter-particle interactions. However, the inverse sixth-power dependence indicates that vdW forces between dipoles decay rapidly as the distance between particles increases. Hence, it is considered a short-range force only.

A repulsive aspect to dipole interactions also exists, which has an inverse twelfth-power dependence on dipole separation. The combined expression for the attractive and repulsive forces forms an analog to the Lennard–Jones (LJ) potential, which describes the interactions between two spherical atoms. The LJ potential accounts for both attractive and repulsive interactions between atoms arising from the overlap of their electron orbitals.[47] In the case of systems composed of many atoms (i.e. nanoparticles), an analogous potential can be obtained by summing the LJ potential across all atom-atom

pairs.[48] Henderson *et al* [48] estimated the potential for two interacting particles with sizes from atomic (few Å) to nanoscopic (few tens of nm) dimensions (**Figure 1**). Despite variations in particle size, the potential reaches a minimum corresponding to an equilibrium state when the particles are separated by only a few Å, confirming that the length scale of the interaction is always of the order of atomic dimensions.[36] The relationships governing the calculation of the LJ potential can also be applied to other types of interaction potentials where the length scale of interaction is much smaller than the dimensions of particles. Similar principles may further be applied for non-spherical bodies.[49, 50] Here also, the magnitude of the interaction increases linearly with the size of the particles and the length scale of the interaction is independent of particle size. Detailed mathematical treatment of these calculations with derivations and interpretations are given in these published works.[36, 47-50]

The three main theoretical approaches to describe the vdW interactions are (a) Hamaker integral approximation [51], (b) Dzyaloshinskii–Lifshitz–Pitaevskii (DLP) theory [52], and (c) Coupled dipole method (CDM) [53, 54]. The Hamaker integral approximation is the simplest method to determine the magnitude of vdW interactions between objects composed of several constituents. It is in essence a pair-wise summation (or integration) of the molecular interactions throughout the volumes of the two bodies, which is very similar to the one described earlier for the LJ potential. The values of C_{vdW} estimated using the Hamaker coefficient for various material systems are close to those calculated using more meticulous methods such as the DLP theory and the CDM.[47] The nearly identical values of C_{vdW} between the three methods suggest that the Hamaker method is a good first-order approximation of both the magnitude and distance dependence of the vdW interaction potential across vacuum.

The expression for the interaction potential clearly indicates that the Hamaker coefficient should be positive for the interactions to remain attractive in nature. Indeed, it is always positive for identical colloidal particles interacting through a solvent, confirming the attractive nature of these forces.[27] When non-identical colloidal particles are interacting through solvent, the sign of the Hamaker coefficient is dictated by the relative dielectric properties of the solvent and two interacting particles and can be either positive or negative under certain circumstances.[27, 55, 56] In particular, the Hamaker coefficient becomes negative when the dielectric property of the solvent lies in between the dielectric properties of the two interacting non-identical particles, in turn implying that the vdW interactions can move from attractive to repulsive by changing one of these properties.[27, 36] For example, repulsive vdW interactions are experienced by systems such as thin liquid hydrocarbon films on alumina flakes and different types of polymers dissolved in organic solvents. [57, 58]

It is evident from our initial discussion that the Hamaker integral approximation method ignores the influence of neighboring molecules, thus failing to take into account many-body effects between

atoms/molecules composing the two objects. A molecule in the system with a permanent dipole or charge may influence the effective polarizability of neighboring molecules, which may, in turn, introduce orientational effects that will cause notable error in the estimation of the coefficient and potential. These effects are significant at the nanoscale, where the shape and size of a particle and the arrangement of its constituent atoms can influence the vdW interaction at both large separations [53] and near contact.[54] Two approaches have been developed to address this issue, namely, continuum DLP theory [52] and the discrete CDM.[53, 54] The continuum DLP approach accounts for many-body effects by including the bulk dielectric response of the interacting materials and the surrounding medium. Meanwhile, the CDM follows a discrete approach akin to the Hamaker pairwise summation, but accounting for all possible many-body effects.[53, 54]

The significance of DLP theory in relation to the Hamaker integral approximation can be understood from the plot of the Hamaker coefficient as a function of surface separation, *L*, calculated using the DLP theory for two semi-infinite gold surfaces separated by *L* and interacting across water (**Figure 2(a)**).[59] The interaction energy per unit area determined using the Hamaker integral approximation is given as, $U_{Ham}(L) = -A/12\pi L^2$, where the Hamaker coefficient, *A*, is a constant. According to the DLP theory, *A* is not constant, but a function of the separation distance between the surfaces. The interaction energy is therefore expressed as $U_{Ham}(L) = -A(L)/12\pi L^2$. For $L > 10$ nm, the vdW interactions become much weaker than those estimated by the Hamaker integral approximation, suggesting that vdW forces would not play a significant role in nanoscale self-assembly when the surface separation exceeds 10 nm.[36] For smaller separations, however, the DLP-calculated Hamaker coefficient is nearly constant. Meanwhile, the discrete CDM method provides a more appropriate calculation since it combines the discrete Hamaker pairwise summation with a more rigorous mathetmatical treatment of many-body effects.[53] This method could be useful for extremely small nanoparticles for which the dielectric response is significantly different from the bulk.

In general, it is difficult to isolate the contribution of vdW forces to the self-assembly of nanoparticles from other types of interactions that are simultaneously present. However, there are still examples in the literature where vdW forces have been noted as the dominant effect in triggering the self-assembly of both spherical and non-spherical nanoparticles.[27, 36, 60-63] For spherical nanoparticles, the self-assembly has resulted in close-packed structures in two and three dimensions [60, 61]. Interestingly, the self-assembly of nanoparticles driven by vdW forces is often also accompanied by size and shape selectivity, as seen in **Figure 2(b)**.[63] In particular, the potential energy is minimal when the largest particles are at the center of the assembled structure and the smallest particles are at the periphery.[62] In the case of anisotropic nanoparticles such as nanorods, directional interactions are observed

favoring assembly in a side-by-side configuration as opposed to end-to-end configuration (**Figure 2(c)**) owing to larger vdW forces in the side-by-side orientation [63]. Thus, the aspect ratios of the particles in question become an important parameter in dictating the final configuration of the assembly of anisotropic nanoparticles.

3.2 Electrostatic Forces

Electrostatic forces play a significant role in many self-assembly processes. Unlike vdW forces, which are mostly attractive except under certain conditions as discussed in the preceding sub-section, electrostatic forces can be either attractive or repulsive depending on the charge of the interacting species. For colloidal systems, the chemical nature (i.e. dielectric property) of the solvent and the concentration of any counter-ions dictate the magnitude and length scale of these interactions.

The Coulomb force describes the electrostatic interaction between atoms, ions, or molecules in vacuum or medium. This interaction is a long-range force (up to 50 nm) and very strong (typically 500 – 1000 kJ/mol) when compared to vdW interactions (~1 kJ/mol). Electrostatic forces are especially relevant to polar systems. For example, a surface in contact with an aqueous solution can become charged through either physisorption or chemisorption of ions. In the case of a negatively charged surface, the area in proximity to this surface will attract positively charged ions from solution. At relatively greater distances from this surface, the negatively charged ions will diffuse into the region, providing an effective reduction in the number of positively charged ions per unit volume. An equivalent picture can be drawn for a positively charged surface. The models developed to explain this situation hypothesize formation of two layers namely, (i) the Stern layer [64] and (ii) the Gouy-Chapman diffuse layer.[65, 66] The net charge of the medium outside these layers can be assumed to be neutral due to the gradual move to equivalent concentrations of the two oppositely charged ions. The double layer represents the two parallel layers of charge surrounding the surface.

The Debye-Hückel and Gouy-Chapman theoretical models present the same qualitative representation of the electric double-layer potential. In general, this potential is defined by the Debye-Hückel equation $U = U_O \mathrm{e}^{-\kappa x}$, where U is the potential at a distance of x and U_o is the potential as that distance approaches zero. As seen, the potential U decreases exponentially with increasing distance from the surface. The symbol κ^{-1} represents the screening length (Debye length) or the thickness of the double layer. For mono-, bi-, or tri-valent electrolyte systems with concentrations less than 0.1 M, this value can be up to 10 nm. When two surfaces with the same type of charge approach each other, the diffuse layers (the potentials) from each surface overlap, generating a repulsive force often referred to as electric double-layer repulsion.[12] The potential in the diffuse layer and, therefore, the double-layer repulsive

force is affected by the surface geometry (spherical or non-spherical), the electrolyte concentration, and the type of electrolyte. Duval *et al* discusses the effect of non-uniform surface charge density and surface roughness on the electrostatic interaction between electric double-layers.[67]

More often than not, interactions between curved surfaces are encountered in colloidal or biological systems. For spherical particles separated by a distance larger than κ^{-1}, the interaction potential is well-approximated by the DLVO (Derjaguin, Landau, Verwey, and Overbeek) potential for screened electrostatic interactions.[12, 68] However, when the separation distance between the interacting charged particles is smaller than κ^{-1}, this theory fails to describe the interactions adequately. As a consequence, there will be qualitative deviations between the experimentally observed self-assembled structures and the theoretically predicted ones. However, it is possible to obtain a reasonable solution for the interaction potential under certain boundary conditions. The Derjaguin approximation is one such approach, which relates the force between two curved surfaces to the interaction free energy per unit area between two planar surfaces.[49] This makes the Derjaguin approximation a very useful tool, since it is usually easier to derive the interaction energy for two planar surfaces rather than for curved surfaces. This approximation is valid so long as the range of the interaction and the separation distance are much smaller than the radii of the curvatures of the interacting surfaces. In the case of colloidal solutions, it is applicable when the thickness of the electric double-layer is much less than the radii of the curvatures (i.e. micron-scale particles). However, the approximation becomes invalid for nanoscale self-assembly systems and biomolecules in biological systems as the Debye length (100 nm for 10 µM aqueous electrolytes) is on the same order or larger than the size of the nanoscale colloids (typically 0.5 to 50 nm).[69] Thus, a more reliable numerical approach must be developed in order to establish a deeper understanding of the electrostatic interaction potentials for the self-assembly of nanoscale objects. Bhattacharjee *et al* began that work by reporting a novel approach to describe the interaction between a particle and a flat surface, where the value obtained for the potential is far more reasonable than the one predicted by the Derjaguin approximation.[70] There is ample opportunity for further improvement in the area of mathematical modeling and simulations to enable quantitative determination of the self-assembly processes driven by electrostatic forces, especially for nanoparticles with different sizes and shapes (morphologies) with screening length comparable to the size of the nanoparticles.

In reality, both the electric double layer force and the vdW forces act together in driving the self-assembly of colloidal nanoparticles. In fact, it is quite possible that a number of other forces (steric, hydrophobic, and hydrogen bonding) may be acting on the nanoparticles as will be explained in subsequent sub-sections. However, the following example demonstrates self-assembly through predominantly electrostatic interactions. Grzybowski *et al* reported the self-assembly of charged, nearly

equally sized, gold and silver nanoparticles (8.36 to 8.6 nm) to form large, diamond-like crystals with a variety of morphologies, in which each nanoparticle has four oppositely charged neighbors.[71] **Figure 3** shows one such morphology of an octahedron and the insets show the {111} and {100} faces. The as-synthesized gold and silver nanoparticles were coated with self-assembled monolayers of 11-mercaptoundecanoic acid (MUA) and N,N,N-trimethyl(11-mercaptoundecyl)ammonium chloride (TMA), respectively. The resultant self-assembled crystalline structure (diamond-like ZnS or NaCl) is reported to depend on the separation distance between the charged particles vis-à-vis the screening length.

3.3 Steric and Depletion Forces – Role of Entropy

Ordered assemblies need not always form when only strong attractive forces of interaction are present. For well-controlled assembly, it may be necessary to have some form of repulsive interactions between the constituents of the system to prevent premature system collapse into an undesirable disordered state. This concept is most commonly encountered in the folding of polypeptide chains into higher order structures. For colloidal systems, the absence of any repulsive interactions manifests in an undesirable precipitation or flocculation among the dispersed components. Entropic interactions through steric and depletion forces could be helpful, even essential in this context.[27]

Steric forces are long-range attractive or repulsive forces induced by the adsorption or grafting of polymers, polyelectrolytes, and biomacromolecules on the surface of the interacting objects. In solutions, a number of interactions such as polymer-polymer, polymer-solvent, and polymer-colloid coexist and contribute to the magnitude of this force. Besides, the nature of the solvent (good or poor for the polymer), temperature, and nature of the polyelectrolyte, if used, could also affect the force [27]. It must be kept in mind that polymer induced forces can be attractive or repulsive depending on various experimental factors.

When the colloidal particle surfaces are saturated with adsorbed polymers in a good solvent, the particle interactions are effectively repulsive as a result of overlapping of the polymer layers. Specifically, when the solvent used in the colloidal system is a good solvent for the polymer, the solvent-polymer interaction dominates. As two or more colloidal particles coated with the polymer chains come in contact with each other, the solvent molecules are constrained near the polymer chains as a result of their affinity for the polymer. There could be loss of entropy due to restriction on the molecular motion or orientational freedom of the polymer, provided the number density of the polymer chains per unit area of the surface of the colloidal particles is high. This entropically driven repulsive interaction is induced by contact [72]. There is also another instance of repulsive interaction when the colloidal particles coated with polymer

approach each other. The elasticity of polymer coils causes the conformational entropy change in this case [27, 73, 74].

Repulsive steric forces have been produced upon compression of neighboring polymer ‘‘brushes’’ in many applications. One of the major applications of polymer brushes is the enhanced stability in colloidal dispersions realized through tethering long-chain molecules onto the surface of colloidal particles. Other applications include artificial joints, transplants, drug delivery by biodegradable micelles, and diagnostics of mutations through attachment of polymers to DNA microarrays [75-78]. Detailed discussion on theoretical approaches to polymer brushes and its applications is beyond the scope of this review. However, interested readers in this field are referred to several approaches such as scaling theory [79, 80], self-consistent field theory [81, 82], and Monte Carlo simulations [81-85] that have been put forward to explain the concepts of “polymer brushes”.

When the colloidal system is composed of colloidal particles with polymer chains in a poor solvent, polymer-polymer interaction is preferred to polymer-solvent interaction, as a result, the colloidal particles coated/adsorbed with polymer on their surfaces experience a net attractive force. This is often referred to as ‘*bridging attraction’ [86]*. Temperature is a significant factor besides the number density of polymer chains in this case. On the other hand, if a non-adsorbing polymer is present in the colloidal system, attractive depletion interactions could occur. When the distance between the interacting colloidal particles is large, an even distribution of polymer chains (micelles in solutions) is expected. If this distance becomes small ($< 2R_g$,) as the colloidal particles come into contact with each other, there is a region in the vicinity of this contact volume where the amount of polymeric chains are depleted. The osmotic pressure force exerted by the solvent molecules present on the outside of this depletion volume is higher. This will induce a net attractive force between the colloidal particles. This kind of interaction is known as depletion attraction [87]. The strength of this attractive interaction is dependent on the concentration and molecular weight of the polymers, but is generally weaker than vdW or electrostatic forces of attraction. Interestingly, depletion attraction forces are independent of the size and the morphology (shape) of the interacting colloidal particles. For example, the depletion attraction from a sphere-rod interaction has been studied in detail in recent years, where a strong attractive depletion force is experienced owing to both translational and rotational degrees of freedom [88]. The question arises - what happens when the colloidal particles and/or the polymer are charged? In this case, electric double-layer repulsion and depletion attraction oppose each other [89-91]. The net force is dependent on the size of the polymer (molecular weight) and the concentration of colloidal particles (distance between them).

Having discussed the steric repulsion and depletion attraction qualitatively, let us now consider a few examples of self-assembling nanoparticles using these forces. Yan and co-workers demonstrated the

synthesis of complex tubular architectures of gold (Au) nanoparticles using DNA-mediated assembly with various conformations and chiralities by exploiting the steric and the electrostatic repulsion effects that the Au nanoparticles lined up on the DNA array experience [92]. Importantly, precise placement of Au nanoparticles on the DNA structures enables one to image 3D conformations of DNA tubes and overcome the limitations of electronic microscopic imaging techniques (**Figure 4**). Also, self-assembly of Au nanoparticles into tubular structures using DNA tiles could lead to interesting properties for nanoelectronics and photonics applications.[92] Depletion attraction forces between CdSe/CdS hydrophobic colloidal nanorods of semiconductors dispersed in an organic solvent in the presence of an additive have been tailored to form 2D monolayers of close-packed hexagonally ordered arrays directly in solution [93]. Depletion attraction forces were also found to be effective in the shape-selective separation of nanorods from binary mixtures of rods and spheres.[93] The experimental procedures employed in this work provide a basis for cost-effective fabrication approaches for devices from nanoscale building blocks.

3.4 Hydrophobic Effect

Studies on hydrophobic interactions continue to attract constant attention as they play a pivotal role in understanding molecular self-assembly. The hydrophobic effect is central to our understanding of many biological processes, including protein folding [94], formation of lipid bilayers [95], and insertion of membrane proteins into the nonpolar lipid environment [96]. It is believed to result from the tendency of nonpolar substances to aggregate in aqueous solution and exclude water molecules. Both entropy and enthalpy contribute to this effect. When a nonpolar substance with limited aqueous solubility (e.g. hydrocarbons or long-chain poly-amines) comes in contact with water, the tetrahedral bonding sites of water molecules are disrupted around the solute-water interface or at the surface of the solute. In other words, the dynamic hydrogen bonds between water molecules are disrupted by the presence of nonpolar substances. According to the theory of iceberg formation, water molecules form a network like structure around the solute molecules [97-99]. The degree of translational and orientational motions of water molecules is restricted, leading to a loss of entropy that makes the process unfavorable in terms of free energy of the system, given as $\Delta G = \Delta H - T\Delta S$, where ΔH is the change in enthalpy, T is the temperature, and ΔS is the change in entropy. At the same time, nonpolar molecules tend to come together to form aggregates, in turn breaking the network structure and leading to an increased motion of the water molecules. One may also consider the fact that by aggregating together, nonpolar molecules reduce the surface area exposed to water and minimize their disruptive effect. So, although there is a loss of entropy due to the confinement of nonpolar molecules, the overall the system gains a significant amount of entropy as a result of the motion of water molecules. In summary, hydrophobic interaction is understood

as an entropic effect originating from the disruption of highly dynamic hydrogen bonds between molecules of liquid water by the nonpolar solute.

The theory of iceberg formation to explain the genesis of the hydrophobic effect has been questioned by many scientists all over the world. For the sake of providing a complete picture to the readers, we summarize here the results from critical works. The fundamental goal of all these works is to unravel the mystery of long-range interactions of hydrophobic forces that extend up to 100 nm from the nonpolar surface. Yamaguchi and co-workers provided evidence for iceberg-like structure as well for the decreased mobility of water molecules.[98] At the same time, their study did not reveal any exact correlation of the decreased mobility of water molecules with the formation of the iceberg-like structure. There have also been many experimental observations as well as simulation studies for this purpose. One of the critical experimental observations is the appearance of nanobubbles on the surfaces of hydrophobic molecules. Attard *et al* have argued that the growth of these nanobubbles followed by their bridging through capillary action could explain the origin of the force. The bridging meniscus would then pull the surfaces together to form aggregates [100]. Their AFM observation of the formation of pancake-shaped nanobubbles lends credibility to their arguments [101]. More recent experimental works with neutron and X-ray reflectivity studies show depletion of water density at the interface. A surface layer 2–5 nm thick with a density about 6–12% lower than that of bulk D_2O was observed by Steitz *et al* [102]. The authors noted that the use of AFM in previous works might have nucleated the bubbles so they used neutron reflectivity to look at the interface. Neutrons are strongly scattered by deuterium (D) and, therefore, they employed D_2O, in contact with deuterated polystyrene, a hydrophobic polymer. In another work reported by Jensen *et al* X-ray reflectivity measurements of the interface of a heavy-alkane monolayer floating on the surface of water also reveals a similar depletion zone of 1.5 nm thickness with a density of around 10% of the bulk water density [103]. Thus, it is suggested that lower fluid density at the interface could lead to the formation of gas-like water more so than ice-like water [104].

3.5 Hydrogen Bonding

The unusual physical properties of water, especially its low molecular weight, high boiling point, maximum density at 4 °C, and increasing dielectric constant upon freezing of water into ice, are understood to originate from its hydrogen bonding structure [47]. Hydrogen bonds are also present in other molecules apart from water. These bonds are formed between hydrogen and highly electronegative atoms such as oxygen, nitrogen, fluorine, chlorine, and others. The electron cloud of the hydrogen atom is attracted by these atoms, making the hydrogen atom positively polarized. The positively charged hydrogen atom can, in turn, interact with the electronegative atoms in its vicinity. In a sense, hydrogen

bonds are believed to be electrostatic in nature, whereby a proton mediates the attraction of two larger atoms with partial negative charges. Magnitudes of individual hydrogen bonds range from 10 to 40 kJ per mol and, therefore, it is weaker than a covalent bond (~ 500 kJ/mol), but stronger than vdW interactions (around 1kJ/mol). Hydrogen bonds are directional in nature. In other words, the molecules capable of forming a hydrogen bond interact only through specific bonding sites. Hydrogen bonding can occur within the same molecule (intramolecular) as well as between molecules (intermolecular). Both the strength and the directionality of the hydrogen bond are responsible for the formation and stability of the DNA double helical structure, integrity and function of biological membranes, and cell functions such as cellular transport.

Beyond supramolecular systems, hydrogen bond interactions have been extended to the self-assembly of nanoscale materials [105-107]. Metal nanoparticles functionalized with thiol molecules (HS–C_6H_4–X where X = OH, COOH, NH_2) are reported to self-assemble through hydrogen bond formation and the extent of assembly is dependent on the strength of hydrogen bonds formed [106]. End-to-end self-assembly of anisotropic nanostructures has been realized through the attachment of hydrogen bonding functionalities to the ends of the Au nanorods [105, 107]. When the functional groups are acidic, strong hydrogen bond interactions were observed at low pH and repulsive electrostatic interactions were experienced at higher pH [107]. Meanwhile, when the pH values are intermediate, vdW interactions could come into play, leading to side-by-side assembly [36].

4. Bottom-up Approaches

Having summarized the various fundamental interaction forces responsible for self-assembly among discrete nanoscale elements, we will now focus on the various approaches towards the fabrication of nanoscale organized structures. In contrast to the use of expensive equipment and cumbersome processing methodologies often employed for top-down fabrication, bottom-up approaches rely on imparting specific interactions between molecules or nanoparticles often using simple chemistry to drive an autonomous self-assembly process once the precursors are mixed together under appropriate conditions. The sheer number of choices available to fine tune the interactions between the nanoscale elements (interaction forces, molecular structure, nanoparticle shape, size, and surface characteristics) makes this especially promising for nanofabrication. For example, tunable nanostructures can be created by simply controlling the process parameters such as temperature, humidity, pH, and chemistry of sacrificial templates. We refer the interested readers to several detailed reviews written in this area.[108-119] The scope of this article is limited to highlighting the ground breaking achievements in directed self-assembly (DSA) with suitable examples from recently published works.

4.1 Directed Self-Assembly

Spontaneously self-assembled structures formed through thermodynamic interactions between individual components is a rapidly growing area of research as it offers facile means to fabricate uniquely tailored nanostructures. Approaches involving the use of nanoparticles as individual building blocks for realization of such systems are especially relevant.[120-133] Such bottom-up fabrication methodologies offer unprecedented control on fine tuning the optical, mechanical and electrical properties of the resultant material. Evaporation-induced self-assembly (EISA) [132, 134-139] is one such example for this type and when combined with templating, it may be used to produce well-controlled nanostructures with long-range order. In order to successfully exploit nanoparticle self-assembly in technological applications and to ensure efficient scale-up, a high level of direction and control is required. The methods concerning DSA can again be classified into three broad categories: (i) template-guided self-assembly (ii) entropic – enthalpic interplay driven self-assembly within nanoparticle-polymer systems, and (iii) field-guided self-assembly with subsets within these categories.

4.1.1 Template-Guided Self-Assembly

A template may be defined as a scaffold onto which molecules or particles can be arranged into a structure with a morphology that is complementary to that of the template. A variety of elements, such as single molecules [140], nanostructures (*e.g.*, carbon nanotubes[141, 142] and mesoporous silica [143]), or block copolymers (BCP) [132, 139, 144, 145], can serve as soft and hard templates. Hard templates include mesoporous materials [139], porous alumina [146], proteins[147], carbon nanotubes [141, 142], and porous polymer films [148]. Soft templates are generally micelles, reverse micelles and vesicles formed by the aggregation of surfactant molecules. Therefore, BCPs and biomolecules can serve as a soft template. The soft template provides cavities in dynamic equilibrium, and substances can diffuse into the cavity through the cavity wall, while the hard template provides static pore channels, and substances can only enter the pore channel from its opening. Soft templates are reported to provide a uniform spatial distribution of active reactive sites to allow controlled periodicity in the placement of nanoparticles and hierarchical structures. Hard templates with chemically modified surfaces allow assembly of nanoparticles and the template-directed growth of nanostructures, such as nanowires, nanorods, nanotubes, and others. As this field has matured rapidly, some outstanding reviews on this topic have been already written and interested readers are referred to these publications.[39, 149-151]

4.1.2 Directed Self-Assembly through Interplay of Entropy-Enthalpy in Polymer-Nanoparticle Systems

4.1.2.1 Nanoparticle - Polymer Systems

One of the evolving fields of research in directed self-assembly has been that of assembly in nanoparticle–polymer systems. In such systems, nanoparticle distribution within the polymer is determined primarily by the interplay between entropic and enthalpic effects between the dispersed nanoparticles and the polymer chains. A great deal of research has been accomplished on using nanoscopic filler elements in various composites to enhance the electrical, mechanical and optical properties of materials [152-159]. Segregation of the nanoparticles is often undesired under these circumstances and achieving and maintaining a uniform distribution of the nanoparticles within these composites through appropriate surface modification becomes extremely important to preserve the structural integrity of the composite materials. However, segregation, when finely directed, could lead to exotic structures opening up new avenues to use nanoparticles as nanoscale building blocks for bottom-up assembled structures at multiple length scales. For example, we have recently reported a novel process of synthesizing dye-doped nanoparticles and facilitating their controlled segregation to form fluorescent supra-nanoparticle clusters (~22 nm), with each supra-nanoparticle cluster made up of ~200 unit nanoparticles and each unit nanoparticle (~3 nm) in turn encapsulating on average a single dye molecule.[160, 161] Beyond the demonstration of the assembly process, there is a functional advantage to this architecture, which lends itself a unique solution to the long-standing problem of self-quenching among dye molecules when encapsulating them in high number within nanoscale volumes (e.g. within a single nanoparticle).

Controlled segregation of nanoparticles may also lead to interesting macroscale architectures. Nanoparticle distribution and dispersion stability within a polymer matrix are governed primarily by the enthalpic factors between the nanoparticles and the polymer chains [162]. For maintaining a uniform distribution of the nanoparticles, it becomes critically important to minimize the enthalpic contact energies between the nanoparticles and the polymer chains [163]. This is easily attained when nanoparticle is of the same chemical make-up as the polymeric matrix in which it is dispersed. Alternatively, the nanoparticle surfaces may be grafted with appropriate surface ligands that are miscible with the polymer matrix [120, 164]. The latter approach is more attractive as it lends greater flexibility in incorporating nanoparticles that are fundamentally different in their chemical, electronic, optical, and/or mechanical properties than the polymers in which they are dispersed, thereby substantially influencing the properties of the final composite material.

Towards self-assembled systems using nanoparticles as individual building blocks, the nature of the surface ligands on the nanoparticles plays an important role. It is well known that in multicomponent polymeric systems, the component with the lowest surface energy tends to segregate to the air interface to

minimize the surface energy of the system [164]. Thus, nanoparticles that are surface grafted with low surface energy ligands may be selectively driven to the air interface. This aspect enables fabrication of smart coatings wherein the surface functionality of the coatings is predominantly determined by the nature of the ligands on the nanoparticles and those of the nanoparticles themselves.

In addition to enthalpic factors, entropy also plays an important role in determining the nanoparticle distribution within the polymer matrix. Maintaining a uniform distribution of the nanoparticles within a polymer matrix imposes an entropic penalty on the polymer chains as the polymer chains have to extend and stretch across the nanoparticles [120, 164-166]. Thus, the larger the nanoparticle, the greater the entropic penalty levied on the polymer chains [165]. A careful control of the enthalpic and entropic factors therefore allows one to direct self-assembly within polymer-nanoparticle composites. For this, the nanoparticle size, the surface groups on the nanoparticles, and the polymer matrices used are all parameters that may be fine-tuned to obtain desired structures. To initiate self-assembly, the nanoparticle-containing polymer films are often subjected to an annealing step at the glass transition temperature of the polymer. This makes the polymer chains mobile while imparting energy to the nanoparticles for their thermodynamically-directed segregation.

An exquisite example of self-assembly within nanoparticle-polymer systems has been reported by Krishnan *et al* [167]. Here they have demonstrated various instances where the nanoparticle localization may be predicted accurately and controlled experimentally within multi-layer polymeric thin films (**Figure 5(a)).**[164]. By choosing polystyrene nanoparticles dispersed within linear polystyrene, the authors have effectively minimized the enthalpic contribution to the self-assembly process. Segregation of the nanoparticles to the substrate interface was observed under these conditions primarily due to the entropic effects. By expelling the nanoparticles to the substrate interface, the linear polystyrene chains gained conformational entropy at the cost of loss of translational entropy of the nanoparticles. Segregation to the air interface was demonstrated with the use of CdSe nanoparticles surface-grafted with oleic acid molecules. Here, in contrast to the behavior exhibited by the polystyrene nanoparticles, enthalpic terms dominated. The low surface energy of the oleic acid brushes promoted the segregation of the CdSe nanoparticles to the air interface to minimize the total energy of the system. Regardless of the contributing term to the segregation of the nanoparticles, multilayer formation of the self-assembled systems was demonstrated.

A relevant immediate application of this behavior, as reported in [168], is to be able to limit dewetting of ultra-thin polymer films on low surface energy substrates. Irrespective of the manner in which the nanoparticles segregated (either to the substrate interface or air interface) the segregation of the nanoparticles promoted stabilization of thin polymer films on low surface energy substrates. This is a

significant development as dewetting in ultra-thin polymer films is a consistent problem, which usually requires surface energy matching of the substrate or modification of the polymer functionality itself to limit dewetting.

Recently, there has been a surge of interest in fabrication of thin films/coatings that can sense and self-heal in response to damage [154, 156, 165, 169]. Towards this, the concepts of self-directed nanoparticle assemblies become especially relevant. Controlled localization and on-demand release of nanoparticles within polymer systems can lead to the next generation self-healing coating technologies. An example of such a self-healing thin film was reported by the Balazs group (**Figure 5(b) and 5(c)**) [165]**.** It was predicted theoretically and experimentally that in a multilayered composite system consisting of a nanoparticle-filled polymer layer topped with a brittle inorganic film, nanoparticles may be entropically driven to fill up cracks developed within the overlying brittle film, thereby effectively repairing the damage [156]. Practical demonstration of this thermodynamically driven self-assembly process was done using CdSe nanoparticles surface-grafted with polyethylene oxide (PEO) brushes and blended within PMMA thin films. The good miscibility of PEO and PMMA ensures that the enthalpic contributing terms are minimal and that any assembly of the nanoparticles within this system is driven predominantly by system entropy. The authors demonstrated successful segregation of the nanoparticles to the exposed PMMA surface in cracks initiated in a brittle SiO_x layer upon annealing this system to above the glass transition temperature of PMMA. Further, the extent of this segregation was shown to be dependent on nanoparticle size as larger nanoparticles incur a larger entropic penalty on the polymer chains, which translates to a greater propensity of the polymer chains to expel the nanoparticles.

4.1.2.2 Block Copolymer–Nanoparticle Systems

BCPs are a classic example of synthetic systems capable of undergoing spontaneous self-assembly to give rise to a myriad of different, ordered nanostructures with well-defined geometries. The exceptional self-assembling propensity of these molecules may be attributed to their unique molecular make-up. These are often amphiphilic molecules and are composed of multiple covalently linked blocks of chemically distinct polymer segments. The amphiphilic nature owing to the differential wetting characteristics of the individual blocks of the copolymer lends itself to spontaneous self-assembly into ordered domains (i.e. spheres, cylinders, lamellar structures, etc.) similar to self-assembly among surfactant systems [170, 171]. The use of these assemblies as templates for the fabrication of ordered mesoporous inorganic materials is widely documented [139, 143, 172-174]. A particular advantage of BCPs lies in the enormous degree of flexibility it offers in the choice of the different blocks and their individual molecular weights that are often the key factors governing self-assembly among these systems

[175]. Casting these molecules as thin films, the ensuing ordered assemblies may be further utilized as patterning templates; this technique also referred to as block-copolymer lithography [144, 171, 175]. A brief overview of BCP nanolithography is described in section 7.3.

We have discussed previously that the nanoparticle assembly within polymer systems is governed primarily by their entropic-enthalpic interplay; the nanoparticle surface ligands playing an integral role in the assembly process. By controlling the wettability of the nanoparticle surfaces such that the nanoparticles are dispersible within only one block of the BCP, researchers have demonstrated their controlled localization within specific domains of the BCP [166, 176-178]. This is achieved by tailoring the ligands to have favorable enthalpic interactions (i.e. ionic, hydrogen bonding, dipole-dipole, hydrophobic interactions, etc.) with the particular BCP block [132].

In this regard, Chiu *et al* demonstrated a simple and robust procedure for the exquisite control of the nanoparticle location within a diblock copolymer [166]. By taking poly(styrene-*b*-2 vinylpyridine) (PS-PVP) diblock copolymer as a model system, they have demonstrated differential segregation behavior of gold nanoparticles surface modified with PS, PVP, or a combination of both within the BCP domains. While nanoparticles coated with the single homopolymer (PS/PVP) segregated to the central portion of the respective domains, co-localization of PS and PVP molecules on the nanoparticles led to their segregation to the PS-PVP interface within the BCP (**Figure 6(a) and 6(b)**).[166] As in the nanoparticle-polymer systems discussed previously, the segregation of the nanoparticles coated with single homopolymer to the respective domains is driven primarily by the need to minimize their enthalpic contact with the alternate domains of the BCP. Following in line with our previous discussion, although localization of the nanoparticles at the central regions of the corresponding blocks result in loss of translational entropy for the nanoparticles, this loss is offset by the gain in the conformational entropy of the corresponding domains. The segregation of the nanoparticles that are surface modified with both PVP and PS to the PS-PVP interface within the BCP, although rationalized by taking into consideration the interfacial effects, still remains a subject of further investigation [166].

Extending the nanoparticle-BCP assembly to the fabrication of 3-dimensionally ordered mesoporous materials was demonstrated by Warren *et al* [132]. Although BCPs assemblies have been reported extensively as sacrificial templates for the fabrication of ordered mesoporous metal organic frameworks, fabrication of these structures that are purely metallic remains a significant challenge. High surface energies associated with pure metals make it more favorable for them to assume shapes of low surface areas [132]. By utilizing Pt nanoparticles surface modified with ionic liquid ligands, ultra-high loading of the nanoparticles (~79% by volume) within the hydrophilic domains of the copolymer was demonstrated. Cooperative assembly between functionalized nanoparticles and BCPs can further lead to

hierarchically ordered thin film structures. Such an assembly was elucidated by Lin *et al* where they have demonstrated that incorporation of low surface energy tri-n-octylphosphine oxide-(TOPO)-covered CdSe nanoparticles within a PS-PVP diblock copolymer leads to the formation of hexagonally ordered, vertically oriented (normal to the substrate) PVP domains with the nanoparticles segregated within these domains and concentrated at the film-air interface (**Figure 6(c) and 6(d)**).[127] This is despite the fact that PVP domains had preferential wetting to the substrate. The control samples showed contrasting architectures wherein cylindrical microdomains assembled parallel to the substrate substantiating the role the nanoparticles played in the self-assembly process.

More recently, the cooperative self-assembly process between functionalized nanoparticles and BCPs to yield 3D multi-layered, in-plane hexagonally ordered nanoparticle sheets was demonstrated by Kao *et al* [179]. In this work, it was demonstrated that the self-assembled structures observed in the bulk nanoparticle-BCP systems may be translated to thin film configurations with high fidelity. For example, by optimizing the solvent annealing conditions to orient lamellae parallel to the substrate, low surface energy nanoparticles assembled within the interiors of the BCPs were effectively kinetically trapped from segregating to the air interface. Extending such cooperative self-assembly to anisotropic nanoparticles can have many technological implications. One-dimensional nanostructures such as nanorods and nanowires are increasingly being considered for use as novel filler elements within polymer composites. The ensemble arrangement of the nanowires/nanorods and their spatial distribution within the polymeric system can have a significant impact on the overall properties of the composite. Further, using polymeric templates to direct their self-assembly wherein the spatial order, orientation on the substrate and rod-rod/wire-wire spacing may be controlled accurately is desirable for applications spanning photovoltaics, plasmonics, sensing, and others [180-182]. In the case of anisotropic shapes such as nanorods, the rod-rod energetic interactions gain prominence and are on the same order as the other thermodynamic interactions (entropic and enthalpic) present within typical nanoparticle-polymer systems[145]. Thorkelsson *et al* reported on these aspects and how previously described energetic interactions–depletion interaction and dipole-dipole interactions–may be coupled synergistically with those occurring between the nanorods and the BCPs to control the nanorod organization [145]. The additional parameter–aspect ratio of the nanorods–among other things played a vital role in the final self-assembly process.

BCP self-assembly on chemically and/or structurally patterned surfaces presents yet another route towards directed organization of nanoparticles on substrates [175, 183]. The underlying basis of this organization stems from the fact that, on a chemically patterned substrate with contrasting surface energies, preferential interfacial interactions of the individual blocks with the chemical patterns leads to well-defined organization provided commensurability between the surface patterns and the BCP lamellae

period is satisfied. This principle was further extended to include assembly on irregularly shaped patterns by using a ternary blend of diblock copolymers and homopolymers by Stoykovich *et al* demonstrating that this was a viable technique towards achieving large scale device oriented patterns [175]. In the follow-up to this work, Kang *et al* adapted the cooperative self-assembly between nanoparticles and BCPs upon chemically patterned substrates and demonstrated both theoretically and experimentally, fabrication of ultra-low defect arrays of nanoparticles at sub-40 nm length scales with exceptional control on the local distribution (at the length scale of few nanometers) of the nanoparticles within individual arrays [183]. It was further demonstrated that a fine control on the local distribution of the nanoparticle within each array may be made by controlling the period of the striped chemical patterns and/or the composition of the ternary BCP blend. When the periods were commensurate, single lines of nanoparticles were obtained, consistent with the segregation behavior observed within the bulk state. However, when the period of the striped pattern exceeded that of the BCP lamellae, aggregated nanoparticles were obtained within the PS domains. This was attributed to the extension in the chain configuration brought about by interfacial surface effects. This fine level of control demonstrated by the authors is significant as this can lead to well-controlled nanoparticle assemblies over large areas, controllably and inexpensively.

4.1.2.3 Nanoparticle–Polymer Systems at High Temperatures

A particularly interesting scenario occurs when the nanoparticle-polymer systems are examined at high annealing temperatures (i.e. temperatures beyond the decomposition temperature of the polymer). When nanoparticles possessing high temperature stability are utilized, this leads to the condition where the nanoparticles, initially confined within the polymer chains, experience a sudden increase in entropy due to the decomposition of the polymer matrix. The thermal input provided to the system further imparts energy to the nanoparticles that are in continuous random Brownian motion. Our group previously reported that a rapid thermal annealing step at high temperature in systems using poly(methylsilsesqioxane) nanoparticles dispersed within poly(propylene) glycol (PPG) polymer leads to the formation of highly porous nanoparticulate films [184]. Interestingly, the properties of these films, even for set nanoparticle weight fractions, were highly temperature dependent. Contrary to conventional logic, these films exhibited increasing pore volume fractions and decreasing thicknesses at higher temperatures, suggesting that these were not constant mass systems. A significant fraction of nanoparticles, namely, those that were not cross-linked, simply escape (i.e. fly-off) from the composite film upon annealing at high temperature due to their increased associated kinetic energies (**Figure 7(a)**). Using this novel approach, reproducible synthesis of nanoporous, high surface area films with refractive indices as low as 1.05 was demonstrated [184].

The system behavior of such high temperature processed nanoparticle-polymer composite films on chemically patterned substrates presents another interesting scenario. Substrate surface energy plays a dominant role in this case since, unlike low temperature processed systems where the substrate effects are effectively shielded from the bulk film through the formation of a segregated monolayer of the wetting phase at the interface, decomposition-led depletion of the segregated labile phase results in the domino effect for high temperature processed systems. This leads to profound morphological changes in the bulk film. Here, surface energy was used to gate the formation of porous and collapsed pore films. By chemically patterning the surfaces to contain low and high surface energy patterns, we had demonstrated spontaneous patterning of nanoporous films. Preferential wetting of the PPG phase on high surface energy patterns led to collapse of pores in the bulk film. Films present on the low surface energy regions on the other hand retained the high porosity (**Figure 7(b)**) [185].

4.1.2.4 Anisotropic Self-Assembly of Nanoparticles

Recent literature is inundated with reports on the synthesis and fabrication of various anisotropically-shaped nanoparticles and bottom-up assembled nanostructures.[115, 117, 118, 186-189] In most of these instances, anisotropic growth of nanoparticle superstructures is brought about by the directional interactions among anisotropically shaped nanoparticles,[190-194] the anisotropic properties of the nanoparticles themselves and/or under the influence of external manipulation (Electric field, magnetic field etc)[195]. Directional interactions between common, isotropic nanoparticles, however, present a unique challenge, which was addressed recently by Kumar and co-workers.[196, 197] This work, which may be considered an extension of the previously discussed literature on nanoparticle-polymer systems, examined the directional assembly of nanoparticles grafted with macromolecules and dispersed within their corresponding homopolymer matrices. By taking polystyrene chain-grafted silica nanoparticle–polystyrene polymer composites as the model system, it was demonstrated that silica nanoparticles self-assembled into a myriad of different anisotropic assemblies; the final self-assembled morphology critically dependent on the grafting density of the polymer chains on the nanoparticles, its molecular weight, and the molecular weight of the homopolymer matrix. Self-assembled morphologies ranged from spherical aggregates (under the limiting case of bare nanoparticle dispersed within the polymer matrix) to thick sheets, thin sheets, strings, and well-dispersed nanoparticles as the grafting density and/or the molecular mass of the grafted polymer increased progressively. The authors showed both experimentally[196] and computationally[197] that such a behavior was indeed expected for these systems and was rationalized by considering the entropic–enthalpic interplay between the grafted nanoparticles; the short-range inter-particle attraction forces and entropic penalty of distorting the

polymer brush chains due to the approaching nanoparticles. The interplay among these forces essentially leading to the final aggregated morphology of the lowest free energy. Similar anisotropic self-assembly of isotropic nanoparticles was recently demonstrated by Mang *et al*[198]. Here, it was demonstrated that spherical gold nanoparticles, surface-grafted with mixed monolayers of mesogenic molecules and alkyl thiols led to anisotropic self-assembly of the nanoparticles; the volume fractions of the surface-grafted molecules determining the extent of anisotropy in the final assembly.

4.1.3 Field-Directed Self-Assembly

The use of external influences and fields to control particle suspensions is well-known for tailoring the mechanical, optical, and electronic properties of materials in several applications. External fields have been applied to direct the assembly of colloidal and nanoparticle systems. Electric and/or magnetic fields are suitable choices for field-directed assembly. Also, assembly in fluid flows and even electromagnetic fields in the form of spatially-patterned optical traps have shown tremendous promise to direct assembly. Macroscopic viscous flows have been demonstrated to produce ordered assembly of nanoparticles from a solution containing a disordered suspension of nanoparticles. However, shear rate and shear strain, particle volume fraction, particle interaction potentials, and polydispersity are factors that affect flow-induced ordering and these need to be controlled and tuned appropriately and accurately. A number of methods employing external fields used to produce structures from a solution phase of precursor particles will be reviewed in this section. Field-directed assembly promises to be a key tool in the bottom-up fabrication of novel functional nanostructures that will enable new materials and devices.[39]

4.1.3.1 Electric Field Induced Self-Assembly

Electric field-induced self-assembly can be accomplished using either DC or AC fields. Most of the works reported in literature, however, employ AC fields in order to overcome electro-osmotic and electrochemical effects associated with DC fields. Self-assembly induced by electric fields in colloidal and nanoparticle systems have been studied in detail over the past three decades.[199-205] Particle polarization is the key phenomenon behind this type of field-induced assembly owing to the differences in the dielectric properties of the particles and the surrounding medium (i.e. solvent). The charges present in the electrostatic double-layer also contribute to the polarization in response to the external field.[199] In this respect, the behavior of electrorheological (ER) fluids under the influence of an external field has been studied in detail to understand the interactions and the resulting structural evolution as a function of applied field and particle concentration [201, 206]. ER fluids are defined as colloidal suspensions of

highly polarizable particles in a nonpolarizable solvent [206]. The induced field formed results in strong dipole-dipole interactions, forming first dipolar chains and then leading to the gradual formation of minimum energy structures at longer times such as a body-centered tetragonal (bct), hexagonally close-packed (hcp), or face-centered cubic (fcc) lattices, depending upon the particle, concentration, and field. If the interaction energies were high, kinetically jammed states of percolated chains were observed [39].

In a recent work reported by Lumsdon *et al* self-assembly of micrometer-sized polymer latex particles and silica particles was directed by application of an AC electric field using coplanar electrodes (field parallel to the interface), resulting in the formation of two-dimensional hexagonal crystalline arrays (**Figure 8(a-d)**) [207]. The directed self-assembly was enabled due to the role played by two complementary forces, namely, (i) induced dipole–applied field and (ii) dipole–dipole interactions. While the former caused the movement of the particles towards the surface of the electrode, the latter caused the aggregation and 2D crystallization into hexagonal phases. Fields of intensities in the range of 40-100 V with coplanar electrodes separated at 1 mm apart at a frequency of 200-20,000 Hz (typically 500 Hz) were used to assemble the crystals. The remarkable aspect of this field-induced assembly is the reversible switching between ordered and disordered states [39, 207].

Apart from the dipole-dipole interactions, localized electrohydrodynamic (EHD) flows generated by AC electric fields can also enable formation of 2D superlattices and, in some cases, complex assembled structures. Ristenpart *et al* reported that the frequency of AC field and the particle concentration dictate the type of 2D planar superlattices formed (triangular or square) in case of a binary colloidal suspension composed of silica and polystyrene particles.[204] Interestingly, the aggregation at low frequency (< 3 kHz) is dominated by attraction resulting from EHD flow while that at high frequency (20–200 kHz) the EHD flow is negligible and the aggregation is instead driven by attractive dipole-dipole interactions.[204] Absence of superlattice formation at intermediate frequencies (3–20 kHz) has been attributed to domination of repulsive interactions (causing lateral displacements) transverse to the applied field. While there is no dependency on the field strength at low frequencies (< 3 kHz), the aggregation behavior at high frequency is strongly dependent on field strength. The reported absence of field strength dependence at low frequencies is attributed to the identical scaling of the repulsive and attractive interaction forces scale with field strength. The authors further reported that monodisperse suspensions exhibit similar trend at lower frequencies and hence the cause of aggregation is not intrinsically linked to a binary character. This work is an excellent contribution to the study of electric field-directed self-assembly of colloidal particles. The extent of resultant self-assembled complex structures depends upon the orientation of the applied field (parallel or perpendicular to the assembly plane) and the proximity of the colloidal particles with respect to the electrodes.[208] The degree of confinement (through varying

spacing between the electrodes) of colloidal suspensions is also reported to dictate the assembly.[209] It must be noted that diverse self-assembled structures are possible depending upon the field frequency, the field strength, and the particle concentration.

4.1.3.2 Magnetic Field Induced Self-Assembly

Magnetic nanoparticles (MNPs) with tunable characteristics such as size, shape, magnetic properties, and composition have been synthesized for wide-ranging applications such as data storage media [210], catalysis [211], and biomedicine [212]. From an applications point of view, MNPs are generally dispersed within a polymer with random distributions and orientations. It is expected that achieving precise control over the spatial organization of MNPs within the polymer matrix will enable the production of smart, switchable materials or magnetic devices with enhanced performance parameters. Formation of 1D, 2D and 3D assembled structures of MNPs through self-assembly requires an understanding of the inter-particle and intermolecular forces that are present. It is evident that the extent or the length scale of the self-assembly of MNPs will be influenced by the nature of magnetic properties (paramagnetic or ferromagnetic) associated with the particles. MNPs are generally coated with an organic functional layer to prevent them from aggregation and to remain soluble in solvents. Therefore, spatial organization of these MNPs with surface functionalized groups within a polymer matrix require favorable intermolecular interactions such as hydrogen bonding, electrostatic attraction, hydrophobic interactions, and vdW forces.[213] Alternatively speaking, surface functionality of MNPs needs to be tailored suitably to allow favorable interactions with the polymer for self-assembly.

In general, materials respond to magnetic fields, but the direction and magnitude of their response is what defines the various types of magnetic materials. Diamagnetic materials are weakly repulsive to an external field with a negative susceptibility on the order of of 10^{-5} to 10^{-6}. Paramagnetic materials, on the other hand, are weakly attractive to the field with a positive susceptibility in the range of 10^{-3} to 10^{-5}. Ferromagnetic and antiferromagnetic materials are magnetic even in the absence of external magnetic fields. The molecular composition and nature of the coupling interactions between the electrons within the materials distinguishes these three classes of materials. Typical MNP compositions include Fe and Co metal particles, iron oxides (Fe_3O_4), spinel ferrimagnets such as $CoFe_2O_4$ or $MnFe_2O_4$, and intermetallic alloys such as $CoPt_3$ or FePt. Since the scope of this article is limited to self-assembly, interested readers are referred to some excellent review articles and the references therein for information on the synthesis, characterization, and applications of MNPs.[214-217]

Similar to the electric field-induced assembly discussed in the preceding sub-section, the main driving force for self-assembly of MNPs is attributed to magnetostatic dipole–dipole interactions. These

interactions could be attractive or repulsive depending upon whether the dipoles are aligned in parallel or antiparallel directions, respectively. It has been reported that application of external magnetic fields facilitate self-assembly of nanoparticles into array structures even for ultrafine particles, which do not aggregate easily in the absence of field.[218] This kind of field-assisted self-assembly process may be reversible, dependent on the interaction energy of the nanoparticles. In addition to magnetic interactions, attractive vdW forces are also likely to play a significant role in the self-assembly of ultrafine nanoparticles. The energy of vdW interactions scales linearly with particle radius while that of magnetic dipole interactions is proportional to the particle's volume. Therefore, vdW interactions dominate for sufficiently small particles and small inter-particle distances, while the long-range magnetic interactions play a crucial role in the presence of an external magnetic field as exemplified in the self-assembly of γ-Fe_2O_3 nanoparticles with 10 nm average diameter.[218] Thus, the magnetic interactions drive the self-assembly of these nanoparticles in the presence of a strong external field (≈0.6 T).

Magnetic dipole–dipole interactions are directional in nature. A variety of structural morphologies such as linear chains, ring structures, and others are possible from colloidal self-assembly of nanomagnets.[219-223] The final morphologies of self-assembled structures are dictated by the interplay of magnetic dipolar interactions with thermal fluctuations. In the presence of an external magnetic field, well-ordered superlattice structures with body-centered tetragonal symmetry have been achieved by the self-assembly of nanoparticles driven by stronger dipolar interactions.[224] Bliznyuk *et al* reported the observation of spontaneous self-assembly of Ni nanoparticles into an interconnected network of nanochain structures on a Si surface in the presence of a magnetic field.[225] The AFM images shown in **Figure 9 (a & b)** reveal the formation of such assembled structures with the inset showing the arrangement of individual nanoparticles into a chain.[225] Likewise, Zeng *et al* reported the formation of necklace-like chains of Co nanostructures when an external magnetic field was applied *in situ* during the chemical synthesis.[226] Furthermore, by using the pre-assembled 1D structure of Co nanoparticulate chains as a sacrificial template, they demonstrated the synthesis of hollow nanoparticle chains of gold, platinum, and palladium (i.e. noble metals) with tunable optical properties (**Figure 10 (a-c)**). The length of the chains was shown to determine the positions of surface plasmon resonance (SPR) absorbance/coupling peaks. The remarkable feature of this work is the observed tunability of the SPR peak from 577 nm to nearly 850 nm by merely varying the external field strength during the synthesis of the sacrificial Co nanostructures. The SPR behavior of hollow Au nanoparticles was shown to differ significantly from that of Au nanotubes and Au nanorods, indicating the utility of magnetic field-directed self-assembly to obtain previously unattainable structures by more traditional means.[226] By extension,

a number of works in the last decade have been reported on the synthesis of periodic arrays of 1D and 2D patterns of magnetic nanoparticles and other related structures.[227-229]

We will conclude this sub-section with a few remarks on the usefulness of self-assembled MNPs in relation to real-world applications and future directions. Self-assembly can facilitate synthesis of hierarchically-ordered nanoparticle structures with extremely narrow distributions of size and electromagnetic properties. MNPs are also used extensively in biomedical applications such as targeted drug delivery and as contrast agents in a number of MRI applications. For these applications, a high degree of control in the synthesis of MNPs is required to achieve well-defined homogeneous magnetic properties. Lastly, this kind of DSA could be useful in the areas of smart, switchable materials and for making materials with highly asymmetric mechanical and optical properties. Since the magnetic properties are also dependent on the shape of the nanoparticles, future focus should be directed towards developing self-assembly-based methods leading to shape-controlled synthesis with tailored and desired magnetic properties.

4.1.3.3 Flow-Induced Self-Assembly

Colloidal dispersions are used extensively in a number of industries ranging from paints, cosmetics, and inks to food and pharmaceuticals. The macroscopic properties of these dispersions are strongly dependent on the micro- and nano-structures that result from the spatial organization of the colloidal particles under the influence of various interactions. In general, colloidal particles are subjected constantly to inter-particle interactions, Brownian motion, and hydrodynamic forces. The inter-particle forces can be attractive as well as repulsive.[230] Brownian motion represents the random motion of colloids in a fluid due to thermal effects. Hydrodynamic interactions result from the force experienced by the colloid in a flow field induced by the motion of a given particle. Thus, the resultant structure is determined by a delicate balance achieved through the interplay of all these forces. In this sub-section, we will limit the discussion to key developments reported on flow-induced self-assembly.

Considerable efforts have been invested in the study of the evolution of microstructures as a function of shear rate in colloidal suspensions of polystyrene spheres (with size from about 100 nm to a few microns) using a variety of analytical techniques such as X-ray scattering, neutron scattering, and optical microscopy.[230-242] The key result is the observation of disorder to order transitions by modulating the shear flow appropriately and the observed microstructural changes show correlation with rheological behavior of these colloidal suspensions as a function of shear rate.[231, 236-238, 243] Studies carried out on diblock copolymer micelle systems confirm the transition from a polycrystalline state to a (111) slipping layer under the influence of steady shear.[236, 237] These works are significant from the

perspective of forming flow-induced self-assemblies of nanoparticles. In general, it is concluded that a variety of parameters such as shear rate, shear strain, particle volume fraction, and the particle interaction potentials affect flow-induced ordering.[241, 242, 244] In these examples, the colloidal particles were suspended either in water or decane, which exhibit Newtonian fluid behavior. In these Newtonian systems, alignment of particles has not been reported at volume fractions below 0.54 for hard spheres. Moreover, high shear flow strengths are required to assemble nanoparticles.[242]

Let us now discuss the situation in which the particles are dispersed in a polymeric matrix or in highly concentrated surfactant solutions. Typically, nanoparticles are employed as fillers in these systems and, therefore, this type of system is essentially a dilute system. Such material systems exhibit complex rheological characteristics. Several studies have been reported in the literature to investigate the effect of shear flow vis-à-vis self-assembly of nanoparticles in the matrix. Vermant and co-workers reported the formation of 1D string-like structures along the flow direction from a dilute suspension of polystyrene spheres (volume fraction of 0.008) when subjected to shear flow.[245] The same group reported the self-assembly of particles into 2D crystalline patches aligned in the flow direction.[246] The self-assembly of particles into ordered structures in viscoelastic fluids is attributed to two possible reasons: (i) layers of fluid sheared at different rates may form through the gap thickness between the parallel plates leading to preferential particle migration toward layers with lower shear rates and (ii) the observed differences in the normal stress in the sheared suspending medium. In the case of non-spherical nanoparticles, anisotropic stresses come into play. Study on the flow-induced alignment of anisotropic particles revealed the observation of complex orientational transitions, which are highly sensitive to aspect ratio and medium rheological properties.[235] The system of carbon nanotubes (CNTs) is a typical example of an anisotropic constituent where the study of flow-induced alignment of the CNTs dispersed either in polymer matrix or surfactant solutions presents some interesting behavior.[247, 248] The behavior of CNTs under shear flow is reportedly very interesting and of technical importance. Below a certain critical shear rate, the dispersed state of CNTs becomes unstable leading to aggregation among CNTs. [249-253] There is plenty of room for exploiting the flow-induced assemblies of nanoparticles in complex fluids especially from the viewpoint of applications. This subject is relevant in large scale applications, where complex flows are routinely observed. For example, the flows encountered in coating technology direct self-assembly of nanoparticles from dilute suspensions. More details about flow-directed self-assembly with recent developments can be found in these publications.[39, 254]

4.1.3.4 Capillary Force-Directed Interfacial Self-Assembly of Nanoparticles

Capillary interaction forces are either attractive or repulsive forces that arise whenever colloidal particles make contact with liquid-based interfaces such as a liquid-liquid interface, wetting liquid film, or foam film. They can also exist between the colloidal particles themselves and between the colloidal particles and a solid surface. The extent and direction of the forces are dictated by the surface properties of the colloidal particles such as their wetting behavior, surface roughness, and the resulting interface. The direction of the capillary force can be lateral or normal with respect to the particle–liquid contact line (wetting line). Kralchevsky *et al* have written excellent reviews on these aspects of interactions induced by capillary forces [255]. The three major types of capillary forces are: (i) immersion, (ii) flotation, and (iii) bridge. For the benefit of non-specialists in this area of research, we define briefly these different types of capillary forces.

Immersion capillary forces arise when the particles are partially immersed in the liquid film. This liquid film can be a wetting film on a solid substrate or a free-standing film. Wetting of a solid substrate causes the formation of menisci around the particles. The direction and scale of the forces exerted on the particles by the menisci are dependent on the wettability of the liquid to the substrate. When the menisci from the neighboring particles interfere in such a way that the deformation on the menisci induced by the wetting is minimized, an attractive capillary force arises between the particles. On the other hand, if the deformation is maximized, the force is repulsive. In the case there is no deformation induced by the particles on the liquid interface, no immersion force interaction would exist to direct assembly.

Flotation capillary forces arise between colloidal particles when they are afloat on the surface of liquid. Besides the interaction force exerted on the particles by the menisci, gravity and buoyant forces acting on the particles also come into play. When the balance between these forces is achieved through reduced inter-particle distance, it means, an attractive force is generated. On the other hand, if the inter-particle distance increases, it means the net force is repulsive. The size and the density of the particles are important parameters.

Bridged capillary is induced when a liquid or gas phase connects or bridges the particle–particle or particle–substrate. Surface properties are extremely important in this case. For example, when the solid surface is hydrophobic, the bridge phase must be a gas or oil. In contrast, if the surface is hydrophilic, then the bridged phase should be water or an aqueous phase. While capillary condensation occurs when the bridged phase is water, capillary cavitation occurs when the bridged phase is gas. The bridged phases between solid particles form curvatures, pointing towards the bridged phases as a result of which a pressure difference is generated across it. This pressure difference induces the interaction between the particles causing them to move towards each other. Furthermore, the surface tension also acts in the same

direction. Therefore, the bridged capillary force is always attractive. The capillary forces are orders of magnitude stronger than vdW and electrostatic forces, and can therefore be exploited to direct self-assembly, overcoming the presence of any repulsive interactions.[27, 255, 256]

In this respect, we briefly outline the developments in the area of capillary force-mediated self-assembly at liquid interfaces. The driving force behind the self-assembly of particles at the interface is attributed to the reduction in interfacial energy. The abundance of literature in directing the self-assembly through exploitation of capillary forces is remarkable, with special emphasis in recent years on assembly of anisotropic particles such as rods and ellipsoids.[257-260] The orientation of anisotropic particles and the extent of packing into assembled structures at the interfaces are dependent on a number of factors such as solvent evaporation rates, particle concentration, and characteristics such as the aspect ratio and surface properties of the particles.[261] Particle shape is also important as the undulation of the contact/wetting line may lead to shape-dependent capillary forces.[257, 259] Such interactions can direct assembly of particles in preferred orientations.[258] Loudet *et al* recently reported a beautiful work wherein capillary forces were exploited to direct the assembly of anisotropic polystyrene (PS) particles (ellipsoids) with and without silica shell at an oil-water interface.[259] It was observed that the silica-coated PS particles interact with each other forming aggregates side-by-side and the PS ellipsoids interact end-to-end forming open structures or chains through strong, long-range capillary attractions that exceeded k_BT, where k_B is the Boltzmann constant. The morphology of the aggregated structures was found to depend on particle surface chemistry (**Figure 11 (a & b)**). The motion of interacting pairs of ellipsoids far from other particles was monitored and recorded *in situ* using optical microscopy. A plot of the center-to-center separation between two ellipsoids versus time was best fitted by a power law, holding good for both end-to-end and side-by-side interactions. Interestingly, spheres with the same surface chemistry behave differently, highlighting the importance of particle shape in capillary interactions. Though the interaction energies seemed to be comparable to k_BT, the motion trajectories were chaotic and the spheres could approach one another very closely without contacting and then separate again. The authors attribute the difference in behavior to the shape anisotropy of the ellipsoids, which may produce more complex interfacial distortions, leading to stronger capillary interactions. These observations could not be explained by attractive vdW interactions since they are much smaller than k_BT at distances larger than 1µm.[47] As per theoretical predictions, even very small interfacial undulations of a few tens of nanometers are enough to cause long-range capillary interactions greater than $1000k_BT$. [256, 262]

The assembly of spherical nanoparticles at interfaces has the potential to provide rapid self-assembled systems due to the highly dynamic nature of the assembly process enabling rapid error corrections[263]. Such an assembly is essentially an extrapolation of the “Pickering emulsion effect” that

has been known for well over 100 years. Pickering emulsions are emulsions between two immiscible phases (e.g. oil and water) that are stabilized by the segregation of micron-sized particles to the liquid–liquid interfaces driven by the need to minimize the high interfacial energy [263, 264]. The nature of assembly of the nanoparticles is dictated by the minimization of the Helmholtz free energy ($\Delta \boldsymbol{E}$) accompanying placement of a single nanoparticle at the interface. Taking the example of an oil-water system, the expression for $\Delta \boldsymbol{E}$ is given by: $\Delta \boldsymbol{E} = -\frac{\pi \boldsymbol{R^2}}{\boldsymbol{\gamma_{O/W}}}[\boldsymbol{\gamma_{O/W}} - (\boldsymbol{\gamma_{P/W}} - \boldsymbol{\gamma_{P/O}})]^{\mathbf{2}}$, where R is the effective particle radius, $\boldsymbol{\gamma_{O/W}}$ is the interfacial energy of the oil-water interface, $\boldsymbol{\gamma_{P/W}}$ the energy of the particle–water interface, and $\boldsymbol{\gamma_{P/O}}$ the energy of the particle–oil interface [264]. The segregation of the particles to the interface, resulting in their loss of entropy, must therefore be compensated by yielding a negative change in $\Delta \boldsymbol{E}$ in order to reduce the total free energy of the system; a larger negative value of $\Delta \boldsymbol{E}$ yielding a more stable assembly at the interface. This equation has several implications regarding the interfacial assembly process. The R^2 dependence of $\Delta \boldsymbol{E}$ implies that larger nanoparticles favor more stable assemblies, yielding larger negative values of $\Delta \boldsymbol{E}$. As the size of the nanoparticle shrinks, the smaller associated $\Delta \boldsymbol{E}$ becomes comparable to the thermal fluctuations of the nanoparticles, leading to progressively less stable assemblies. Consequently, larger nanoparticles tend to selectively displace smaller nanoparticles at the interface in dispersions containing a heterogeneous mixture of particle sizes [264].

Experimental verification of the above equation was reported by Russel *et al* through the use of fluorescent quantum dots (CdSe nanoparticles) surface-modified with tri-n-octylphosphine oxide (TOPO) ligands and dispersed in toluene [264]. Introducing water droplets to this mixture, the authors demonstrated assembly of the nanoparticles at the water interfaces, stabilizing the water droplets. Furthermore, when two different sized quantum dots (2.8 nm and 4.6 nm CdSe nanoparticles) with size-dependent fluorescence emission were utilized, the larger nanoparticles categorically displaced the smaller nanoparticles at the interface, as evidenced by the shift in fluorescence emission to that corresponding to the larger quantum dots at the water interface. The use of this fluorescence probing technique further allowed the authors to determine the time constant for the displacement process simply by measuring the rate of shift in fluorescence emission. The authors also demonstrated photo-induced reaction of the hydrophobic TOPO ligands on the nanoparticles at the interface, thereby transferring the nanoparticles from the toluene phase to the water phase.

The nature of ligands attached to the nanoparticles also affects the assembly process as these have a primary effect on the interfacial energies $\boldsymbol{\gamma_{P/W}}$ and $\boldsymbol{\gamma_{P/O}}$. For instance, the degree of hydrophobicity or hydrophilicity of the surface-attached ligands determines the spatial localization of the nanoparticles at

the interface; more hydrophobic ligand-modified nanoparticles preferring the oil phase over the water-phase and vice versa [263, 265]. Interfacial reactions may therefore be carried out conveniently by exploiting this phenomenon for the surface modification and transfer of the nanoparticles from one phase to the other. This interfacial assembly also paves way for the synthesis of heterodimeric nanoparticles or Janus nanoparticles consisting of two or more distinct material faces. The assembly of the nanoparticles at the liquid–liquid interface described above may also be extended to the cost-efficient formation of free-standing, closely packed nanoparticle membranes through controlled evaporation of the solvents. Further, 'nanoalloys', membranes consisting of a mixture of different nanoparticles, may also be fabricated easily. Reports include membranes consisting of close-packed arrangements of Au, Ag, and γFe_2O_3 nanoparticles [265] as well as membranes made up of self-assembled biological (virus) particles [266].

The interfacial self-assembly process need not be confined to liquid–liquid interfaces. Liquid–solid [267] and liquid–air [268-270] interfaces have also been exploited for obtaining self-assembled systems of nanoparticles through carefully chosen boundary conditions. While droplets of colloidal solutions leave behind the commonly observed coffee ring patterns upon drying due to the highly non-equilibrium fluid flow and solvent evaporation processes, Bigioni *et al* demonstrated that exceptional long-range ordering of nanoparticles over macroscopic length scales was still possible under these conditions[268]. The authors observed that the key factors required for such an assembly were rapid evaporation of the solvent and promoting attractive interactions between the particles and the liquid–air interface. This leads to segregation of the nanoparticles to the interface from which 2D nucleation and growth of the particle islands take place, eventually covering the entire surface with monolayer close-packed assembly of nanoparticles (**Figure 12(A)**). Dodecanethiol-modified gold nanoparticles dispersed in toluene were shown to assemble with monolayer perfection over areas as large as 3 mm × 4 mm upon drop-casting followed by rapid drying **(Figure 12(B)).** Interestingly, the assembly process was also critically dependent on the presence of excess, unligated dodecane molecules in the solution, the absence of which led to nanoparticles concentrating and depositing at the substrate edge. The ease of formation of these monolayered structures with exquisite long-range order provides an attractive means to produce self-standing 2D nanoparticle lattice sheets [267, 269, 270]. Further, the inter-particle separation within the assemblies may be controlled easily by changing the length of the surface ligand groups. Beyond alkyl molecular ligands, DNA molecules [271, 272] and polymeric ligands [269, 270] were also utilized to control the inter-particle spacing, critical for applications where tailored optical/electrical properties of the sheets are desired.

Extending these concepts to anisotropic nanoparticles, Khee Chaw *et al* recently reported the fabrication of free-standing, monolayered gold nanorod (GNR) superlattice sheets (**Figure 12(C &**

D)).[269, 270] The anisotropy of the GNRs caused the resultant assemblies to assume different structural morphologies (e.g. disordered assemblies, horizontally-aligned packing and vertically-aligned packing) as a function of temperature, aging time (in solvent-rich environment), and the length of the polymeric ligands attached to the nanorod surfaces. Increasing temperature or annealing time under the saturated solvent environment favored the formation of vertically-aligned packing in contrast to horizontal packing at lower temperatures or shorter annealing times for the same GNR dispersions. This was rationalized by taking into account the Tirodo model relating the diffusion constants of cylindrical particles to temperature and shear viscosity, giving the GNRs more time to assume the most thermodynamically stable vertical alignment of the GNRs.

4.1.3.5 Self-Assembly Under the Application of Combinations of Fields

In order to realize hierarchically ordered structures, it may be necessary to develop novel procedures wherein a variety of external fields are combined together to direct nanoparticle self-assembly. Such a method would allow achievement of a high degree of control required for realizing desired structures assembled at multiple length scales. This sub-topic within the family of self-assembly is still a nascent area of research. However, some efforts have been reported in the literature, which suggest an enormous potential for this method. We will highlight the key results here. For example, electric or magnetic fields have been applied during deposition of films to manipulate the orientation of the nanoparticles within the films and the resulting tunable properties.

Mittal *et al* employed AC electric field *in situ* to assemble and control the orientation of anisotropic (ellipsoid) TiO_2 nanoparticles during film formation by convective flow of the colloidal suspension confined in a suitable experimental cell.[273] Briefly, as the solvent evaporates, the particles are transported towards the drying front (**Figure 13**). Simultaneous application of the AC field induces the orientation of the nanoparticles either parallel or perpendicular to the field direction depending on the magnitude and frequency of the field. The films exhibit a high degree of birefringence ($\Delta n \approx 0.15$) and high packing fraction of 0.75 ± 0.08 on AC field orientation of the nanoparticles while the packing fraction in the absence of electric field was only 0.44 ± 0.06, confirming that orientation yields denser films. Interestingly, cracks in the film propagate along the direction of the electric field, leading to anisotropic mechanical properties. Thus, a remarkable approach to tailor the properties of nanostructured films *in situ* during the deposition process has been demonstrated.[273] In another work by Ding *et al* fabrication of 3D photonic crystals by convective self-assembly of magnetic γ-Fe_2O_3/SiO_2 core-shell ellipsoids in the presence of magnetic field was reported.[274] Application of a static magnetic field *in situ* during the convective flow of ellipsoids towards the glass slab resulted in long-range positional and orientational ordering as shown in the SEM images (**Figure 14**). While the convective flow-induced self-

assembly was responsible for the close packing, the presence of a magnetic field ensured that the ellipsoids were not oriented in random directions. The strong, selective reflectance observed at certain wavelengths is attributed to the periodicity of the sample induced by synergetic effects of the convective flow and magnetic fields. A similar method based on a combination of flow-assisted assembly and electric fields has been extended to organic nanocrystals. Employing electric field-assisted shear assembly, orientation and degree of alignment of rod-like cellulose nanocrystals can be controlled by the magnitude and frequency of the electric field applied to the substrate.[275] In another recent work, electric field-induced alignment of more complex structure composed of organic-inorganic composite dumbbells, specifically, a titania/silica core coated with PMMA and a polystyrene lobes, has been demonstrated.[195] The direction of the alignment of these anisotropic particles either parallel or perpendicular to the direction of field depends on the interplay between the forces due to inter-particle interaction and the torque that the induced dipoles experience in the external electric field.[195] Together, these works show the tremendous potential of employing a combination of external fields in controlling the placement, orientation, and alignment of nanoparticles in a desired manner. As we have seen in the examples above, the orderly arrangement of nanoparticles has the potential to provide tunable optical and mechanical characteristics. There is a wide scope for further research in this area of directed self-assembly. For instance, the ability to modify inter-particle interactions rapidly with the application of pulsed fields is yet to be demonstrated.

The kinetics of DSA (structural evolution as a function of time) needs to be explored *in-situ* with advanced *state-of-the-art* tools. Unfortunately, there are experimental limitations in using tools like electron microscopy for this purpose. Especially, when dealing with the study of self-assembly of nanoparticles with size below 10 nm to form hierarchical structures at multiple length scales, it is necessary to develop appropriate instrumentation that can facilitate in-situ monitoring to study the kinetics of self-assembly. Some important advancement has been made using X-ray and neutron scattering methods over the past decade. We therefore present a detailed review on the application of *in-situ* characterization methods to probe DSA of colloidal nanoparticles in section 7.

5. Self assembly in Biological Systems

Self assembly processes in living structures remain a constant source of stimuli for the development of nanomaterials. Biological systems provide a rich variety of ordered structures. Some common examples are self-assembly of lipids to bilayers that forms the boundary of all living cells and intracellular organelles, four heme subunits forming functional hemoglobin, ribosomal RNA and proteins interacting to form a functional ribosome or the honeycomb like structure formed by fibers that form the

lens of the eye (**Figure 15 (D)**). Proteins, in particular vary in structural properties and provide a scaffold that can generate a massive array of materials with unique properties such as keratin, collagen, shell, pearl, coral, microlenses and optical waveguides .Molecules, including proteins, nucleic acids and lipids can self-assemble into supra-molecular architectures such as motors [276-280], arrays [281-283], pumps, membranes, valves [284, 285] cytoskeletal filaments (**Figure 15 (B & C))**[116, 286, 287], lipid raft signaling complexes and light harvesting and electron transport machinery for organ level structures like bones (**Figure 15 (A))**[288], hearts or kidneys etc.

Nature uses the bottom-up approach at the nano- and meso-scales to constitute such complexes. Molecular self assembly occurs ubiquitously by spontaneous association of individual biomolecules or "monomers" under physiological conditions into structurally well-defined, complex and functional aggregates via non-covalent interactions such as hydrogen bonding, hydrophobic forces, vdW forces and/or electrostatic interactions. The physics of these interaction forces are described in section # 3. Since self assembly constitutes an increase of order in a system, this process is unfavorable from an entropic point of view. However, as they are formed from the reversible association of various molecules using the aforementioned weak interactions, the balance between enthalpy and entropy plays an important role in their formation. [26] Nicholas and Prigogine showed that non-linearity combined with non-equilibrium constraints can generate multiple solutions through bifurcation and thus allow for more complex behavior in an open system.[289] The biosphere absorbs energy from the sun's radiation, exchanging energy and materials with the earth, thereby constituting an open system. Thus, nanoscale self assembly processes utilize the principles of irreversible thermodynamics to construct ordered, hierarchical structures. Research efforts for understanding these processes have laid the foundation for the first biologically inspired self assembly processes that have considerable technological potential as exemplified by self-assembled monolayers (SAMs) [290] and GEPIs.[291] . Most importantly, the complementarity of the shapes and chemical natures of the interacting molecular surfaces drive the energetic stabilization of the resulting nanostructures. Although the basic polymers that constitute biological systems are quite weak, they often display mechanical properties beyond those achieved thus far by synthetic materials.[292] Furthermore, despite the limitations of the self assembly being forced to occur at ambient temperature, aqueous environment, processing and limited availability of elements (primarily C, N, Ca, H, O, Si, P), living systems produce complex structures from composites that are organized in terms of composition and structure, containing both inorganic and organic components. Additionally, biological nanoscale structures have built-in capacity to self-heal as well as evolve over time. That may be a direct result of the bottom up self-assembly process, since the structural growth is not directed by any overarching design but occurs locally due to individual molecules sensing and responding to its immediate environmental

effectors. Hence these nanoscale structures can undergo structural and functional adjustments according to cellular requirements.

Living systems thus accomplish a myriad of functions by having a broad range of mechanical properties from limited resources and locally directed bottom up self assembly. The mechanical strength of mineralized biological materials is connected to its nanostructure and to the scale, which limits the sizes of existing flaws to the level close to the theoretical strength of the mineral. This was recently demonstrated by Gao *et al*.[293] However, this is only part of the story, and hierarchical aspects play a key role. In bone, crack bridging, which occurs via local deposition and restructuring to maintain strength, is utmost importance in determining the toughness, and representative of a unique property of biological nanostructures –"self-healing".[294] These mechanical properties of the self-assembled biological structures are explained through Ashby maps. These maps denote strength and Young's moduli as functions of density, thereby revealing certain defining features such as having five orders of magnitude for the range of Young's moduli and strength despite the average density(<3) being lesser than that of synthetic materials. Thus understanding the physics behind such properties of bio-nanostructures might be useful in process development of synthetic mechanical or electronic devices.

5.1 Biological self assembly – Its application in the development of nanomaterials.

A model to explain the specific and unique properties of biological systems has been proposed by Arzt [295] that has five components: self assembly, ambient temperature and pressure processing, functionality, hierarchy of structure and evolution/environmental effects. These features have been studied to develop variety of systems such as (i) bioinspired (or biomimicked) materials: approaches to synthesizing materials inspired on biological systems, (ii) biomaterials: these are materials (e.g., implants) specifically designed for optimum compatibility with biological systems and (iii) functional biomaterials and devices.

A large body of literature has demonstrated that biomolecules and polymers in general, are capable of self-assembling into a wide diversity of structures with distinct nanoscale architectures [296, 297]. Clearly, deeper understanding of such processes controlling diverse biological self assembly can provide important clues that may help shape powerful biomimetic technology with higher levels of functionality and specificity and also be cost effective. For example, Morse and co-workers [298] derived inspiration from spicule formation to develop a manufacturing process for semiconductor thin films. Enzymes onto gold surfaces are used as templates on which semiconductor films could grow. Throughout this section we have provided examples of many similar instances, where the biological nanoscale assembly processes have taught us about the physical nature of various materials and structures that will have a profound effect on everyday applications and process design. The ingenious design of

nanomachines in nature has helped to inspire and accelerate the pace of development of biomimetics for nanodevices.[299-301]. Therefore, current research efforts are focused on making these machines as viable and effective as possible outside of their native environment.[302, 303]. It should be noted that while the synthesis of nanomaterials is typically accomplished under equilibrium conditions, within the biological systems, such synthesis is far from equilibrium and is driven by various biomolecular stimuli as discussed previously.

A significant progress has been made in the application of biological materials for generating nanodevice systems for applications in the driving of molecular sorters, building of intricate arrays and chips for diagnostics, molecular sensors [304, 305], novel actuators[306-308] , delivery of drugs [302] and therapeutic macromolecules [309], in nanoelectromechanical systems (NEMS) [310, 311], and in new electronic and optical devices. Hierarchical structures and compartmental organizations are integral to biological functions and are conserved across biological systems. At a simplistic level, compartmentalization accounts for spatial separation and confinement of ions and molecules within and throughout biological systems. Selective and dynamically changing permeability of these compartments enables control over the flow of energy, information, and molecular raw materials in support of complex biochemical processes. Conversely, the study of such hierarchical processes can be harnessed for generating complex nanodevices [312, 313] and may provide instances of “top-down” approaches in nature. The combination of biological molecules and novel nanomaterials is of great importance in the process of developing new nanoscale devices for future biological, medical, and bioelectronic applications.[7, 314]The chemical modification of enzymes with redox-relay groups [315], the immobilization of enzymes in redox polymers [316] and the conjugation of biomolecules to metal nanoparticles (NPs) [317] and carbon-based nanomaterials [318] were reported as means to establish electrical communication between redox proteins and electrodes.

5.2 Protein- and peptide-based bio-nanomaterials

Proteins are especially attractive candidates due to their well-defined structure and the feasibility of structural modification by genetic engineering [319]. Enzyme-NP complexes based on a protein molecular scaffold displaying hundreds of enzymes in one catalytic unit [320] have potential applications in the food industry as well as for drug delivery. Fabrication of such structures typically require highly stable proteins such as SP1,[321] that acts as a molecular scaffold to tether NPs [322] and protein domains, while selectively and controllably binds to surfaces. The ability of such protein scaffolds to self-assemble into three-dimensional nanostructures, combined with the precision to connect to NPs and enzymes, provides a promising approach for the self-organization of composite nanostructures. Other enzyme hybrid structures, such as the conjugation of enzymes with metal-NPs or carbon nanotubes, have

also been reported. The system is based on laterally nanostructured arrays with high local concentration of enzyme on the electrode surface. However, the immobilization of biological molecules on carbon nanoscaffolds, such as carbon nanotubes, is limited by the fact that their closed shell does not allow for a high degree of functionalization, since adsorption or covalent immobilization can be achieved only at the functionalized end of the opened tubes.

In cyanobacteria and plants, sequential energy transfer between the different complexes of the photosynthetic machinery is essential to trigger electron transfer that drives photosynthesis [323, 324] and generate molecules containing high energy bonds. Sophisticated self-organization of the natural photosystems serves as a model for artificial photosynthetic systems that require efficient energy and electron transfers. Accordingly, the synthesis and supramolecular self-assembly of a variety of pigments have been widely explored with the aim of constructing photochemical and photoelectronic devices, including photovoltaics, nonlinear optical materials, and photoswitching conductors. To mimic bacterial light harvesting systems, dendritic systems have been widely studied for multi-pigment arrays; although it may be currently challenging and time-consuming to produce such complex molecules with high yield.[325-327] Similarly, biological materials such as virus coat protein structure can serve as templates guiding nanoscale organization of pigments via chemical linkage or electrostatic interactions. [328]. The highly ordered coats of viruses represent one of the most well studied and exploited examples of directed biological self assembly of proteins. The first to be studied in extensive detail was the Tobacco Mosaic Virus (TMV). The 300nm by 18nm TMV virus particle is composed of exactly 2130 identical protein units arranged in a spiral shaped hollow shell enclosing the RNA genome.[329, 330] The assembly process utilizes a very limited set of reversible, non-covalent, binding interactions between the proteins and the individual disc sub-assemblies that generate the entire viral particle, allowing it to self-edit or correct any errors. Later, we will show in section # 6.2.2, how the self-assembly behavior of TMV has been exploited to achieve hierarchical 3D nanostructures for the fabrication of functional materials.

The study of the self-organization properties of peptides has emerged in recent years as an active and diverse field of research, ranging from biomedicine and biotechnology to material science and nanotechnology. Although self-assembly of polypeptides into aggregates such as amyloid fibrils is often associated with human medical disorders such as Alzheimer's disease, type II diabetes and Crutzfeld-Jakob disease [331, 332] and microbial physiological processes [182, 333], such peptide nanofibers are very well ordered displaying helical periodicity and possessing regularity. These self-organization properties of peptides have been exploited for the formation of bio-inspired assembled structures, including nanotubes, nanospheres, nanofibers, nanotapes and hydrogels (**Figure 16 (A & B**)).[23, 334-338] Structural elements as short as dipeptides can form well-ordered assemblies at the nanoscale [43].

Ionic self-complementary peptides can form β-sheets and β strand structures with regular repeat pattern of alternating hydrophilic and hydrophobic groups. The hydrophobic residues shield themselves from water, with the hydrophilic groups exposed to surface thereby driving the self-assembly. The complementary ionic sides of these polypeptide nanostructures have been classified to several moduli on the basis of the number of alternating positive and negatively charged amino acids on their hydrophilic faces. Another important physical property driving ordered self assembly processes is the chirality of the peptides. For example, in the 8-residue peptide FKFEFKFE [339] the innate right handed twist of the beta stranded peptide in the beta-sheet conformation leads to the formation of a nanoscale, ordered, left-handed, double helical ribbon (**Figure 16(C & D**)). Thus, peptides serve as excellent building blocks for bionanotechnology owing to the ease of their synthesis, small size, relative stability and chemical and biological modifiability. Understanding the physicochemical determinants that trigger peptide self-assembly is a fundamental step, for the rational design of new nano building blocks for biotechnological applications or new drugs.

5.3 DNA assisted self-assembly of nanoparticles

Efficiently controlled assembly of nanostructures is becoming increasingly important as building blocks in nanodevices, because of their unique optical, electronic, and mechanical properties.[340, 341] Several approaches such as optical, electron beam, or dip-pen-lithography are reported for assembling the nanostructures into higher-level devices, and systems of well-defined shapes, sizes, and functionality. All of these techniques have little or no control of assembling nanostructures into the functional nanosystems or devices. Biologically driven programmed assembly is an attractive alternative to assemble nanostructures because of highly specific nature of interactions among biomolecules. In this regard, deoxyribonucleic acid (DNA) based assembly is especially promising. [340-344]. This is because of the unique chemical make-up of these molecules enabling highly site specific controlled assembly of nanostructures. Moreover, DNA can easily be synthesized with different lengths, sequences, and functional groups. These unique properties in combination with the site-specific DNA adsorption on solid surface have been exploited by many research groups to develop functional devices poised with nanoscale materials in a high-throughput manner.[342-345] For example, Mirkin group has explained DNA based three-dimensional programmed assembly of gold nanoparticles for highly selective colorimetric detection of polynucleotide detection in solution.[342] In their study, the specific sequence of DNA molecules conjugated to the gold nanoparticle provided the required programming needed for the assembly process. Majumdar group has demonstrated DNA-mediated assembly to develop the array of gold nanoparticles functionalized with thiolated single-stranded DNA on a solid surface i.e. on a pre-patterned gold surface.[343] They have shown successfully the programmed assembly of nanoparticles with the help of

standard lithography, specific DNA strands and chemically inert PEG molecules directing nanostructures to develop in a specific region on a chip (**Figure 17**). The extraordinary specificity and selectivity make the fabrication process ideal for assembling gold nanoparticles on a defined gold pattern by masking the rest of the surface with polyethylene glycol molecules. Myung group approached highly specific and selective assembly of functional multisegmented nanowires of gold/palladium/gold on prepatterned gold electrodes using DNA hybridization.[345] **Figure 18** schematically explains the hybridization of two complementary DNA strands for the immobilization of metallic nanowires across the gold electrode. Two complementary single-stranded DNAs (DNA_1 and DNA_2) modified with thiol moiety adsorb on gold electrode and gold segments of nanowires, and enable the nanowires to selectively assemble across the electrode. From these discussions, it is clearly understood that programmed assembly of nanoparticles using DNA molecules is one of the best possible bottom-up nanofabrication approaches and can emerge as a powerful platform to assemble nanomaterials into a variety of complex structures.

5.4 RNA based bio-nanomaterials

RNA has a multitude of biological functions despite being more chemically labile than DNA, such as various forms of mRNAs, t-RNAs, small interfering and micro RNAs (siRNAs and miRNAs) [346] which are now being harnessed for medicine. Additionally, RNA also constitutes biologically active molecular machines such as ribozymes [347], regulatory aptamers [348] and nano-motors [348]. Therefore, RNA molecules can be designed and manipulated with a level of simplicity characteristic of DNA while possessing versatility in structure and function similar to that of proteins.This natural versatility of RNA might make it more attractive as building blocks and functional components of multifunctional therapeutic nano-scaffolds for nano-medicine [349] that have no counterparts in the present day DNA world for building. Elegant experiments have demonstrated that modular RNA units can form small multimeric particles of various sizes as well as programmable filaments and 2D and 3D nano-arrays and nanogrids consisting of RNA squares (**Figure 19 (A-C)**).[350-352]

RNA molecules are polymers made up of millions of nucleotides from four groups: adenosine (A), cystidine (C), guanosine (G), and uridine (U) (see Section 3). A 100-nucleotide RNA polymer may have as many as 4^{100} ($=1.6\times10^{60}$) different RNA molecules. Since the size of RNA ranges from the angstrom to the nanometer scale, bottom-up approaches are preferred for use with RNA in applications [353-355]. RNA self-assembly involves cooperative interaction of individual RNA molecules that spontaneously assemble in a predefined manner to form a larger two- or three-dimensional structure (**Figure 19 (A & B)**). Tertiary RNA structures or RNA folding is determined by repetitive structural features [356], commonly the double helix which is constituted by consecutively stacked pairs of complementary nucleotides which interact through hydrogen bonds. Structural motifs in RNA do not

necessarily require any long-range tertiary interactions [357] and a synthetic combination of such motifs can then be used to design novel nanostructures [358], including artificial ribosensors and RNA "Lego" (**Figure 19 (C-D**)). [359] Artificial RNA architectures also depend on the Watson-Crick pairing of RNA strands (hybridization of complementary base sequences) [353, 360]. RNA of diverse sequence complexity have been used to build complex RNA Lego as well as square- and cube-shaped self-assembled objects [350, 354] and their crystal structures analysed. Such sequence-dependent programmed self-assembly [353, 354] may serve as a nanoscale template for the directed combination of RNA scaffolds for biomimetic applications. Recently, RNA has been used in a variety of techniques including replication, molding, embossing, etc.,that allow the utilization of a variety of materials to enhance diversity and resolution of nanomaterials. It should eventually be possible to adapt RNA to facilitate construction of ordered, patterned, or pre-programmed arrays, construction of sensors, programmable packaging and cargo delivery systems for biomedical applications [347, 350, 352, 361]. Given the potential for 3D fabrication, the ability of self-repair, editing and replication, RNA self-assembly might play an increasingly significant role in integrated biological nanofabrication.

5.5 Lipid based bio-nanomaterials

The phospholipid bilayer membranes are one of the most ubiquitous forms of nanoscale biological self-assembly, conserved from bacteria to humans and are functionally required for all forms of life. These bilayers organize living matter into compartments providing physical barriers that partition the aqueous phase into several compartments that are spatially, chemically, and functionally distinct [362, 363]. Lipid molecules in bilayer membranes associate with various proteins to form functionalized complexes involved in maintaining compartment chemical composition, critical aspects of biosynthesis, energy transduction, information storage, and cellular recognition and signaling. [364]. Hence, whether engineering biomimetic technologies or designing therapies to interface with the cell, this adaptable membrane can provide the necessary molecular-level control of membrane-anchored proteins, glycopeptides, and glycolipids.

In the last few years, lipid bilayer vesicles with an internal aqueous core, called liposomes have been widely used for systemic (i.e intravenous) delivery of drugs and diagnostic reagents (**Figure 20 (A)).**[365, 366] They were discovered by Bangham [367] which were thought of as models for plasma membranes. Within a liposomes'outer hydrophobic shell (lipid bilayer) is contained the internal hydrophilic cavity enabling hydrophilic drugs or macromolecules to be encapsulated in the central aqueous compartment, while the hydrophobic molecules can be embedded in the membrane. Additionally, using chemical modifications, the liposome surface can be functionalized such that they can adsorb and carry specialized molecules or drugs. Typically, liposomes have properties like

biocompatibility, biodegradability, low toxicity and ability for surface and size modification that make them desirable carriers in biomedicine and made them suitable as nanoscale reaction vessels [368] as well.. However, they have steric instability, poor control of drug release and short half-life in circulation. Certain liposomes have been clinically approved for the delivery of Doxorubicin (Doxil) for cancer treatment [369]. The liposomes encapsulating Doxil was covalently modified with PEG to improve its circulation time and referred to as "stealth liposomes". Thus various tenets of materials science, cell biology and pharmacology have been put together to achieve higher drug retention and sustained release by external stimuli such as pH, magnetism, temperature and electromagnetic radiation at different radiofrequencies to control the triggering of drug release. An example is Thermodox, a thermally sensitive liposome encapsulating Doxorubicin to treat recurrent chest wall breast cancer and primary liver cancer *(http://celsion.com/docs/technology_thermodox)*. Such clinical success has led to the generation of hybrid nanoparticle-liposomes with multiple functionalities in therapeutics and diagnostics. For example, TOPO-capped QDs (quantum dots) were incorporated in lipid bilayers, and drugs loaded in the internal cavity were loaded efficiently to create a theranostic vector.[370]

Recently, cubosomes (cubosome dispersions) have raised interest as a drug nanocarrier due to their great potential as alternative drug delivery system compared to liposome. Specifically, cubosomes consisting of binary monoolein–water systems have been widely studied.[371] They are thermodynamically stable, aqueous surfactant systems which self-assemble into bicontinuous cubic liquid crystalline phases. Cubosomes that have a large internal surface area (~400 m^2/g) are viscous, isotropic and can load lipophilic, hydrophilic or amphiphilic drugs.[372, 373] Furthermore, their large interfacial area may provide for complex diffusion for sustained release of drug cargo.[374, 375] Some examples of cubosome mediated delivery are with somatostatin[376], insulin[377], indomethacin, and rifampicin. Furthermore, lipid vesicles that can be induced to release entrapped materials in response to an applied stimulus have also been developed. Elegant works from different groups have recently demonstrated that, discrete lipid particles, including reconstituted high density lipoprotein (HDL), can form ordered complexes with proteins to form nanodiscs (**Figure 20 (B**)[378]), which have been characterized by multiple biophysical techniques [379, 380]. The Nanodisc is a robust membrane bilayer vehicle for the stoichiometrically controlled incorporation and study of membrane proteins such as cytochrome P450 [381, 382], bacteriorhodopsin (bR) [383, 384], and G-protein-coupled receptors [385, 386]. In the recent past, lipid-based, monodisperse, self-assembled nanostructures termed nanodiscs, that are 10 nm in diameter have been developed and studied, often to understand structure and dynamics of membrane protein function. Nanodiscs typically consist of two molecules of a protein such as membrane scaffold protein 1 (MSP1) wrapped around the outside edge of a discoidal bilayer fragment consisting of ~160

saturated lipids. These nanobiomolecular assemblies can be generated using a broad range of amphipathic molecular constituents from synthetic or natural sources by harnessing the lipid-based self assembly processes. Such simple, self-assembled structures could theoretically stabilise amphipathic and hydrophobic elements capable of interacting with targets at biological or inorganic surfaces and may have use as biosensors. Nanodiscs are also of great value to the incorporation of larger molecular complexes, such as the enzymes involved in cellular energy metabolism, oligomers of integral membrane receptors, ion channels and transporter proteins [387] which may find applications in both diagnostic or therapeutic fields. The phospholipid membrane thus represents an ideal scaffold for a host of nanotechnology applications {Tanner, 2011 #460).

6. Integrating Top-Down Lithography and Bottom-Up Self-Assembly Methods

This section will begin with a brief discussion on the advantages and the limitations of both top-down lithography and self-assembly to emphasize the need for combining the top-down and bottom-up approaches to form hierarchically assembled functional structures on multiple length scales. We will then highlight some of the recent achievements to illustrate the importance of employing such an integrated approach.

6.1 Need for integrating top-down and bottom-up methods

Top-down fabrication methods are being used widely by semiconductor manufacturing industries, wherein patterned structures are accomplished by suitable photolithographic and ion-implantation techniques.[28, 388, 389] These methods are well-established in the production of silicon-based integrated chips. The major advantages of top-down methods include a high level of precision, reproducibility, and high-throughput capabilities. However, the physical limits of device dimensions realizable by ultraviolet, electron/ion beam, and soft X-ray lithographic techniques will be reached in the near future. Furthermore, relatively new nanostructured materials such as carbon nanotubes, graphene, and organic semiconductors may require bottom-up processing as they may not be able to withstand the harsh processing conditions of typical top-down approaches. The main disadvantages of the currently available top-down techniques are the high costs of equipment, limited access to fabrication facilities, restricted capacity to achieve three-dimensionality, and poor resolution below 20 nm. There are also some issues with the implementation of top-down approach concerning the biocompatibility of the materials that can be produced.[29]

On the other hand, bottom-up methods are versatile in many ways such as enabling generation of self-assembling building-blocks, assembling pathways, ordered structures, and functionalities. Molecular self-assembly techniques have been touted to be the most promising approaches towards cost-effective and practically realizable methods for large area nanolithography. In recent years, extensive research has been done in this regard both theoretically and experimentally, wherein custom molecular species have been devised and studied for their self-assembling characteristics. A wide variety of structures including tapes, belts, fibrils, tubes, vesicles, and bilayer membranes have been achieved by peptide and protein self-assembly.[390-393] Thus, the potential of peptide and protein-based self-assembly to create materials with unique nanoarchitectures is indeed enormous. The bottom-up method based on self-assembly is expected to enable miniaturization below the current limits possible using lithography techniques. Yet, this bottom-up self-assembly method has some disadvantages, which include inability to produce industrial-scale quantities of materials at reduced costs, and in some instances, purification and polydispersity limitations. Owing to these limitations, self-assembly alone cannot produce more complex structures. A promising alternative is the use of strategies that combine top-down methods with molecular self-assembly, exploiting their benefits and, at the same time, overcoming their limitations. This integrative approach employing peptides and proteins is particularly powerful because of the possibility of precision production at the molecular level, versatility, and functionality. Attempts to realize a high degree of control in directing the self-assembly with top-down methods using these molecular structures as building blocks are opening up unprecedented opportunities.

6.2 Illustrative Examples of Combined Assembly Methods

6.2.1. Biological Applications

In order to produce ordered hierarchical structures beyond the molecular or nanoscale, recent efforts have focused on the synergistic combination of the functionality, molecular resolution, and biocompatibility of peptides or proteins with top-down lithography-based techniques exhibiting a high level of precision and reproducibility. Three different ways to integrate the two approaches have been reported in literature: (i) implementing top-down processes before self-assembly, (ii) implementing self-assembly before top-down processes, and (iii) simultaneous implementation of top-down and self-assembly processes. In the first method, the patterns produced by photolithographic means define the areas or volumes where the subsequent self-assembly processes can take place.[394] Meanwhile, employing top-down methods after self-assembly helps with positioning or removing nanostructures from specific locations.[31] There are also a few published works that demonstrate the simultaneous or alternating application of top-down and self-assembly approaches, influencing both the assembly as well

the final structural properties.[395, 396] In order to appreciate this integrated approach to fabrication of functional structures, we limit our discussion to the development of two systems wherein thiolated and aromatic peptides have been used as self-assembling building blocks in conjunction with top-down lithography. For other systems using different building blocks such as polypeptides or amphiphilic peptides, the interested readers are referred to several published works.[397-401]

As we discussed earlier, the spontaneous assembly of thiol-terminated molecules onto gold surfaces is a mature field. The thiol group forms a strong bond with the gold whilst the rest of the molecule aligns with its neighbors. Zhang *et al* have developed a family of peptides capable of self-assembling on gold surfaces [393]. Microcontact printing was then employed wherein the inked PDMS stamp was placed on a gold substrate for approximately 1 minute and then peeled off carefully to transfer and engineer the surface patterns. While the bottom-up self-assembly ensured nanoscale organization and precise ligand display, the top-down microcontact printing defined the organization of the developed SAM at micro- and macro-length scales. **Figure 21** shows the thiol-terminated peptides and an example of a patterned surface using self-assembly and microcontact printing.[393] Subsequently, several similar works employing a combination of thiol-terminated peptides and top-down lithography methods to engineer patterned biological surfaces have been reported in the literature.[402-404] These works establish the potential of integrated approaches to produce tailored surfaces composed of precise patterns of bioactive molecules/ligands. Such patterned substrates could be useful for high-throughput analysis in biological applications.[405] Though the use of thiol-terminated peptides facilitates generation of high resolution surface patterns with functionality, these patterns lack assembly on a macroscale. On the other hand, the aromatic peptides offer a different route to self-assembly enabling localization of self-assembled peptide structures. For example, Gazit *et al* reported the synthesis of aromatic dipeptide nanotubes (ADNTs) with diameters of 50–300 nm and lengths up to microns using diphenylalanine.[43] The observed self-assembly is attributed to the π-stacking of the aromatic rings. In another work reported by Gazit *et al* an ink jet printer was employed to manipulate and position the ADNTs to produce surface patterns.[31] The same research group reported the self-assembly of diphenylalanine molecules into vertically aligned ADNTs employing evaporation-initiated growth from a surface. Here, top-down (evaporation) and self-assembly occurs simultaneously and enables macroscopic ordering and assembly of the nanotubes.[34] In yet another pioneering contribution by Gazit *et al* self-assembly of large arrays of aromatic peptide nanotubes using top-down vapor deposition method was observed (**Figure 22 (a-c)**).[30] The integrated approach based on simultaneous molecular self-assembly of peptide and top-down vapor deposition is shown to dictate the length and the density of nanotubes. In this study, a vapor deposition system supplied the diphenylalanine peptides from a gas phase, which initiated the growth of vertically

aligned ADNTs. Furthermore, this work revealed the potential of ADNTs in a variety of applications including high-surface-area electrodes for energy storage applications, highly hydrophobic self-cleaning surfaces, and microfluidic chips.[30] The electrical double-layer capacitance density (C_{DL}) estimated from **Figure 22(d)** and comparison of the values confirms that ADNT modified carbon electrodes exhibits much higher values for C_{DL} (480 μF/cm^2) with respect to unmodified carbon electrodes (16 μF/cm^2) and carbon nanotube-modified carbon electrodes (120 μF/cm^2).[30]

6.2.2 Integrated Approach for Hierarchically Ordered Energy Storage Devices

Small-scale power applications such as portable medical devices and implants, sensor networks, and contemporary commercial electronic gadgets demand the implementation of miniaturized batteries with increased energy and power densities. Development of battery architectures that combine a small footprint with enhanced performance is, therefore, highly desirable. Previously, two independent approaches based on MEMS and nanomaterials have been explored with the objective of realizing 3D microbattery electrodes with enhanced energy and power densities. MEMS-based approaches involving micron-size particles have been shown to improve energy density significantly.[406-409] However, there are some problems inherent with this technology owing to the non-uniform current density and the limitation in increasing the thickness beyond a certain limit as the diffusion pathway is still in the micron scale and full lithiation of the active material may not be achieved, resulting in reduced power density. On the other hand, the advantages of implementing nanomaterials for the development of microbattery electrodes include larger electrode/electrolyte contact area, improved mechanical stability, and reduced diffusion distances for electron transport and ion diffusion.[410-413] These attributes combined can enhance the power density and cyclic stability of the electrodes and address the shortcomings of thicker electrodes. Limitations related to nanostructured materials include the difficulty in synthesis and integration as well as performance concerns such as undesired reactions with the electrolyte. However, the main critical bottleneck in their practical use in micropower sources is the limited energy density. Thus, there is a need for the development of a novel approach for the fabrication of hierarchical electrodes that combine benefits of both length scales (nano- and micron-scales).

Gerasopoulos *et al* recently demonstrated the advantage of combining bottom-up self-assembly approach with top-down micromachining to fabricate 3D microbattery electrodes, which are composed of self-assembled, virus-templated nanostructures conformally coating 3D microfabricated gold pillars (**Figure 23**).[33] Self-assembly behavior of TMV virus (which has been discussed in the previous section on biological self-assembly) has been exploited in this work. Active battery material (V_2O_5) was deposited conformally using atomic layer deposition across the entire available surface. Electrochemical characterization of these electrodes indicated a three-fold increase in energy density compared to

nanostructures alone, while maintaining the high power characteristics of the nanomaterials. From the literature, the reported capacities of RF-sputtered 2D electrodes with thicknesses of 1.2 µm and 1.8 µm were 38 and 60 µAh-cm^{-2}, respectively.[414] Patrissi *et al* reported synthesis of V_2O_5 nanofibers (8 µm length, 600 nm diameter) in modified polycarbonate membranes that exhibit a capacity of 86 µAh-cm^{-2}.[415] In comparison, another work achieved a similar range of capacity values with 30-40 times thinner electrodes (30-60 nm).[33] This was achieved using the combination of high surface area nanostructures with 3D micropillars. In summary, these works highlight the importance of an integrated top-down and bottom-up approach in controlling both energy and power density with structural hierarchy. Additional merits of the work reported by Gerasopoulos *et al* include the potential to achieve even greater energy densities by increasing the aspect ratio of the micropillars and the facile possibility of extending this integrated approach to other active battery materials.[33]

Following the observation of spontaneous self-rolling of strained metal layers reported in 1909 [416], Mei *et al* recently demonstrated the ability to create ordered micro- and nano-structured building blocks of a wide variety of material combinations on a single chip through self-rolling of patterned thin layers.[417] Applying this technique further, Bof Bufon *et al* reported the fabrication of 3D ultracompact capacitors (UCCaps) based on rolled-up nanomembranes.[32] Capacitors that are self-wound and manufactured in parallel using semiconductor planar processing technologies are almost 2 orders of magnitude smaller than their planar counterparts and exhibit capacitances per footprint area of around 200 μF/cm^2. Furthermore, the UCCaps exhibit high power density (~2000 W/kg), which is characteristic of electrostatic capacitors, while reaching a specific energy of ~0.55 Wh/kg in the range of supercapacitors.[32] Briefly, the process steps to fabricate the self-wound ultracompact capacitor shown in **Figure 24** include: (i) fabrication of a planar strained multilayer nanomembrane by the sequential deposition of metal and dielectric thin films on top of a sacrificial layer and (ii) removal of the sacrificial layer leading to formation of the ultracompact 3D capacitor by stress-induced self-winding. The most important process consideration is the design of the bottom metallic layer to provide the necessary strain to force the roll-up of the nanomembrane. The SEM image in **Figure 24 (e)** shows an array of self-wound capacitors obtained in a controlled and reproducible fashion. The highlights of the integrated top-down and bottom-up self-assembly approach presented in this work include (i) compatibility of the process with organic materials, (ii) possibility to generate additional devices in the empty 2D area after sacrificial layer release, (iii) significant reduction in the footprint area leading to compact devices, and (iv) increase in the active capacitor area as a result of the rolling of the nanomembrane. The extension of the technology presented in this work to high dielectric constant materials such as HfO_2 and TiO_2 is expected to increase the performance several-fold. Owing to the compatibility of this process to organic materials,

incorporation of organic materials such as self-assembled monolayers into the multilayer structure (**Figure 24**) has enabled achievement of an increase in breakdown electric field. Furthermore, the SAM grown on top of the Al_2O_3 layer is shown to control leakage currents as a result of an additional high-gap barrier. In short, the UCCaps fabricated through top-down and bottom-up approach exhibit capacitances per footprint area higher than their state-of-the-art planar counterparts and specific energy comparable with supercapacitors.[32]

6.2.3 Nanopatterning

The ability to create well-defined nanoscale patterns is pertinent to continued device miniaturization to attain the resultant improvements to chip performance. Conventional top-down lithographic methods are well-established for fabrication of microdevices and they offer arbitrary geometrical designs and superior placement precision and accuracy. However, as the demand for improved resolution in lithographic processes increases, a point will come where conventional lithographic processes simply fail to keep up with demand. Although alternate techniques for nanopatterning are available, the cost and/or low associated throughput make them impractical choices for commercial-scale implementation, especially when sub-10 nm feature sizes are desired. On the other hand, BCPs are a well-known class of self-assembled materials, which form well-defined periodic domains from microphase separation. BCP thin films can generate line patterns as well as 2D periodic arrays of holes with periodicity from 10 to 100 nm. Both lateral and vertical ordering of the microdomains over large area has also been demonstrated. [418-421]

Self-assembly of BCPs is an inherently thermodynamic process that originates from the microphase separation of the chemically distinct blocks owing to their immiscibility in one another; the driving force coming from the need to minimize the enthalpy of contact between the individual co-blocks.[422-424] Meanwhile, macrophase separation is prevented as the two blocks are linked together chemically. The force balance between the repulsive intermolecular forces between blocks and the attractive restoring force is the key to the formation of regular periodic structures of microphase-separated domains. Tailoring the interactions between the surfaces and the polymer blocks is the key to achieving the desired orientation and alignment. Microphase separation in BCP systems has been investigated thoroughly for a long time from the viewpoint of fundamental and applied research [425-430] and, therefore, the scope of this sub-section is restricted to the salient features of BCP self-assembly in relevance to the physics of the nanopatterning process. We refer the interested reader to some excellent books and deep review articles for a comprehensive coverage on all aspects of BCP systems.[127, 426, 431-437]

The thermodynamics of microphase separation can be expressed as, $G_{mix} - G_{PS} = \Delta G_{SA} = \Delta H_{SA} - T\Delta S_{SA}$, where G_{mix} and G_{PS} represent the free energy of the mixed and phase-separated systems, respectively. ΔH_{SA} and ΔS_{SA} represent the enthalpy/entropy changes between the mixed and phase-separated states, respectively. The entropy change associated with mixing is usually quite small because of the random coil confirmation adopted by the polymer blocks. The intermolecular forces driving the microphase separation are normally of the hydrophobic type, where the attraction of more polar components forces the non-polar components to aggregate. This segregation of the blocks reduces the number of interactions between dissimilar blocks, thereby lowering the number of repulsive interactions between chains.

For a diblock polymer, the value of the interaction parameter (Flory-Huggins) resulting from the interactions between block A and block B is given by $\chi_{AB} = (Z/k_BT)((\varepsilon_{AB} - (\varepsilon_A+\varepsilon_B)/2)$, where ε_{AB} is the interaction energy per monomer units between A and B monomers, and Z is the number of nearest neighboring monomers to a copolymer configuration cell.[433, 435] The determination of whether a given BCP system will phase separate into ordered domains or a disordered state may be made based on the product $\chi_{AB}N$, where N is the degree of polymerization of each individual block. The segregation quantity χN determines the degree of microphase separation. Depending on χN, three different regimes are established: (i) the weak segregation limit (WSL) for $\chi N \leq 10$, (ii) the intermediate segregation region for $10 < \chi N \leq 50$, and (iii) the strong segregation limit (SSL) for $\chi N > 100$.[435] Further, the morphologies and the sizes of the individual ordered domains may be predicted based on (i) the degree of chemical disparity between the blocks, (ii) the degree of polymerization, and (iii) the relative volume fractions of the individual blocks. Temperature also plays an important factor in the assembly process due to the temperature dependence of χ. The phase diagram for a BCP system may be plotted by describing the various possible structures formed as a function of the product χN and the BCP composition. The phase diagram is separated into several regions, characterized by the relative stability of the structures formed and the dependency of the feature size on the degree of polymerization.[438] It is important to avoid the WSL regime for nanopatterning. Although WSL gives the smallest feature sizes, the thermodynamic driving forces for microphase separation are small, thereby giving rise to regions of disordered assemblies due to the dominance of thermal effects. Working in SSL regime may also pose problems because achieving thermal equilibrium for disorder reduction may require extended annealing as the driving force could be too strong.[425]

In the case of diblock copolymer, various structures may be formed depending on the composition of individual blocks. The phase diagram described by Matsen and Bates is symmetrical around the composition of $f_A = f_B = 0.5$, where f_A and f_B are the volume fractions of the two blocks.

[439] A lamellar structure is observed in this composition region. Upon increasing f_A to between 0.6 and 0.7, a bicontinuous gyroid phase of cubic symmetry consisting of interpenetrating tubules of the B block in the A block is formed. This phase has a relatively narrow stable composition range, particularly in the intermediate and strong segregation limits. At higher f_A values, hexagonal arrangements of block B cylinders in a matrix of A may be observed. Due to its structural complexity and a narrow stability range, the gyroid structure has only limited applicability. Among these various structures, the lamellar and hexagonal structures are most important in terms of patterning applications. In reality, more complex structures are possible because of the complexity of the intermolecular interactions in polymers. One such structure is the hexagonal-perforated lamellar structure, observed at the phase boundary between the lamellar and cylinder arrangements.[440] This perforated phase has become more important in thin film structures because it can be stabilized by surface reconstruction due to preferential interactions of one block with gas, liquid, or substrate interfaces.[441] Exploiting the microphase separation of BCP, many applications have been developed over the past few years.[119, 187, 435, 442-445] Among these, nanopatterning using BCP self-assembly continues to receive tremendous attention.

Patterning using BCP assemblies may occur in one of the following ways: (i) using BCP assemblies as sacrificial masks, (ii) using the assemblies themselves as functional elements of the final design, or (iii) using BCP thin films as sacrificial templates to order the assembly of nanoparticles on substrates. In the first method, imparting good etch selectivity between the co-blocks becomes necessary such that their degradation occurs at different rates when exposed to the etch environment. The final un-etched block may then be used as a sacrificial etch mask to pattern the underlying substrate. Several works on nanopatterning with BCP have focused on the study of the polystyrene-b-poly(methyl methacrylate) (PS-b-PMMA) system.[423, 431, 446] The typical patterning principle involves deep UV degradation and removal of PMMA domains along with cross-linking of the PS block. Typically, etch techniques that are already compatible with conventional microelectronic fabrication are used for this purpose, such as reactive ion etching (RIE)[447], UV-Ozone exposure[448, 449], wet-chemical etching[422], and others, thereby making this a readily adaptable technique without a significant infrastructure change. Thus, technologically relevant applications such as fabrication of nanoscale air gap interconnects [450], field-effect transistors [451], flash memory devices [452], sensors [453, 454], plasmonic structures [454, 455], and ultra-high density magnetic dot arrays [456] have all been demonstrated using BCP lithography, underscoring the substantial advancements made in this field.

In the second technique, employing the assemblies themselves as functional elements in the final design necessitates that the final formed assemblies are stable and robust akin to oxide structures, in addition to exhibiting good etch selectivity between the blocks. This has been accomplished through the

introduction of inorganic segments as one of the blocks of the BCPs. In addition to possessing higher χ values (thereby favoring ordered assemblies) and greater etch selectivity (due to the intrinsic chemical disparity between the inorganic and organic blocks of the co-polymer), incorporation of inorganic blocks facilitate formation of robust oxides upon oxygen plasma treatment or under high temperature annealing. A comprehensive handling of this topic has been done in a recent review article to which the readers are directed.[423]

Despite the promise of BCPs for nanolithography, spontaneously self-assembled, phase-separated domains typically are "polycrystalline" in their order, interspersed with a high density of defect sites.[419, 423] Also, achieving a high degree of control on the precise location of nanopatterns as well as forming a wide variety of lithographically defined patterns is essential for the fabrication of integrated circuits, patterned media, and other microdevices. Thus, a significant amount of research is dedicated to improving the long-range order and orientational control within BCP systems through directed self-assembly techniques integrating top-down and bottom up self-assembly techniques. While there are a number of reported techniques such as the use of electric fields [457], shear flow [458], chemical (epitaxial self-assembly)[419, 423, 459], and topological (graphoepitaxy) [422, 460, 461] approaches, patterned substrates to direct the ordering of the BCP assemblies, epitaxial, and grapho-epitaxial methods have proven to be the most promising in terms of registering long-range order among the phase-separated domains.

In epitaxial self-assembly, chemically pre-patterned substrates with pattern dimensions commensurate with the phase-separated domains of the BCPs are utilized to direct their ordering over large areas. Typically, chemical contrast is introduced to the patterns such that one block of the copolymer wets one of the regions of the pattern preferentially. The effectiveness of this technique was demonstrated by Stoykovich *et al* [175], wherein BCP assemblies were directed into non-regular device architectures. A particular shortcoming of this technique lies in the requirement for the additional lithographic step defining the chemical patterns [461]. As the chemical patterns are constrained to be of the same order of dimensions as the nanoscale domains of the BCPs, the pre-patterning step still needs to be performed using the low-throughput top-down lithographic approaches. Further research is underway to circumvent this issue whereby feature density multiplication and reduction in feature sizes may be achieved compared to current typical chemical pre-patterning routines [419].

In the graphoepitaxial method of DSA, topographically defined surfaces are utilized to control the lateral ordering of the BCP domains. This technique is simple and particularly advantageous over the epitaxial DSA method as the topographic features need not be of the same order as the domain dimensions of the BCPs, permitting one to use conventional photolithographic approaches to define the

surface topographies[422, 460]. Surface topographies as large as a few microns have been reported to yield well defined, ordered assemblies of the BCP blocks over arbitrarily large areas. For example, Sundrani *et al* demonstrated fabrication of parallel arrays of nanoscale domains aligned over macroscopic length scales by using a silicon nitride grating to guide the assembly of asymmetric polystyrene-*block*-poly(ethylene-*alt*-propylene) diblock copolymer cylinders.[462] In this work, silicon nitride grating was fabricated using electron beam lithography and reactive ion etching (top-down processes). Imaging by AFM showed that alignment was initiated on the vertical sidewalls of the lithographic patterns and extended throughout, even beyond, the confined volume. Cylinders exhibited significant conformity that enabled them to accommodate lithographic imperfections without introducing structural defects.

The convergence of top-down and bottom-up fabrication in the same BCP architecture has been demonstrated by several research groups. Russell and co-workers created cylindrical nanochannels at defined locations from PS-b-PMMA on the substrate, and thereby demonstrated its potential to generate integrated magnetoelectronic devices.[463] Ober and co-workers have successfully developed a novel BCP, poly(α-methylstyrene-b-4-hydroxystyrene) (PMS-b-PHOST), to achieve spatial control through high-resolution deep UV and e-beam lithographic processes, taking advantage of chemically amplified negative-tone resist materials (PHOST).[464-466] Maeda *et al* demonstrated the synthesis of patternable BCP, which is composed of both negative-tone and positive-tone resist blocks.[467, 468] The fluorine-containing BCP of poly(styrene-block-2,2,2-trifluoroethyl methacrylate) (PS-b-PTFEMA) and poly(4-hydroxystyrene-block-2,2,2-trifluoroethyl methacrylate) (PHOST-b-PTFEMA), which are capable of both top-down and bottom-up lithography, were developed in their work. Both PS and PHOST (negative-tone resist) are cross-linkable under deep-UV or e-beam radiation. PTFEMA (positive-tone) was selected to be a degradable segment under the same exposure conditions. Both these two systems were found to exhibit well-defined microphase separation in both the bulk and thin film forms. Through a combination of BCP self-assembly techniques and conventional top-down lithography, such integrated structures composed of “dots in lines” were successfully obtained from these BCP photoresists. It is clear that the integrated nanoscale patterns with a high degree of ordering cannot be obtained by conventional lithography or BCP lithography alone. Furthermore, the nanopatterns can also serve as patterned templates or scaffolds for the fabrication of various types of multifunctional nanomaterials.

Krishnamoorthy *et al* exploited the integration of nanostencil lithography, a high-throughput top-down tool, with micelle bottom-up self-assembly to produce complementary micro- and nano-patterning of surfaces.[469] The patterned nanostructures in this work were silicon nanopillars with smallest diameters of nearly 20 nm and heights up to 140 nm, resulting in an aspect ratio of up to 7. Nanostencils consist of a thin free standing Si_3N_4 membrane with 100–200 nm thickness, containing apertures defined

by photolithography and etching, or focused ion beam (FIB) milling. The versatility of this integrated approach includes the capability to pattern surfaces without using photoresist, the reusability of the nanostencil, and the feasibility of parallel processing, which reduces fabrication costs tremendously. The high production cost and low throughput of the conventional top-down lithography are major concerns. Previously, e-beam lithography has been used to create periodic patterns in combination with polystyrene-block-poly(2-vinylpyridine) (PS-b-P2VP) copolymer micelles.[432, 470] This work makes excellent use of nanostencils not only as a shadow mask for metal evaporation, but also as a mask for dry etching. Depending on the chosen process parameters (i.e. metal deposition or fluorine or oxygen plasma exposure of PS-b-P2VP-coated Si surfaces) in the presence of a shadow mask stencil and/or dry etch mask, an array of silicon nanopillers appear in either the masked or unmasked regions. A blurring of the boundaries and an increase in the polydispersity in the pillar dimensions is one problem that has been identified by the authors because of diffusion of the oxygen plasma beneath the stencils. Through optimization of the anisotropy of the plasma and the exposure duration, it may be possible to reduce the plasma diffusion below the stencils. This technique offers the possibility to create a nanopillar pattern that corresponds to either the positive or the negative image of the stencil mask. The positive image results from using fluorine plasma exposure through the stencil, the negative image from metal evaporation or oxygen plasma exposure through the stencil. The drawback to this technique however is the loss of surface area due to the pre-patterned, macro-scale topographies thereby reducing the over-all density of the BCP ordered domains.

The third technique combines the natural tendency of BCPs to form ordered assemblies over macroscopic length scales and the ability to control the segregation of functionalized nanoparticles or nanoparticle precursors to appropriate block of the copolymer. Long-range ordered arrangements of nanoparticles on substrates may thus be accomplished by utilizing the BCP assemblies as sacrificial scaffolds. Lopes *et al* reports on such a two-step assembly process to obtain striped patterns of isolated metal nanoparticles or interconnected metal chains on substrates by using pre-assembled thin films of polystyrene-block-poly(methylmethacrylate) (PS-b-PMMA) diblock copolymer as scaffolds.[437] Evaporation of ultra-thin metal films on these structures led to the selective deposition of the diffusing metal atoms along the stripe pattern. Here the authors note that, despite the large surface energies of metals, such a directional aggregation may be accomplished under non-equilibrium conditions; equilibrium conditions invariably driving the nanoparticles to coalesce into large spherical particles (in contrast to filling up the stripe patterns defined by the BCP domains (**Figure 25**)). Although contiguous stripe patterns were not obtained for metals such as Au, In, Pb, Sn and Bi under any deposition conditions on PS-b-PMMA, striped patterns were demonstrated in the case of Ag under non-equilibrium conditions.

This has been attributed to the remarkably high mobility of Ag on PMMA. As with other metals, driving the system to equilibrium disintegrates the wires into spherical, separated particles. The authors work is a classical example of a bottom up self assembly approach being integrated with conventional fabrication schemes to produce structures at the nanoscale.

Roman *et al* reported the ordered placement of Au nanoparticles using a similar technique exploiting the self-assembly of polystyrene-b-poly-[2-vinylpyridine ($HAuCl_4$)] on solid substrates (**Figure 26**).[424] The precursor-laden diblock copolymer self-assembles into uniform monomicellar films on substrates when deposited, following which chemical reduction of the Au precursor leads to the formation of metallic Au nanodots localized at the center of the diblock copolymer micelle. Subsequent removal of the diblock copolymer film from the substrate leaves behind ordered Au nanodot patterns across the substrates. The authors demonstrated a fine control on the size and placement of Au nanodots on the substrates through a combination of several techniques: nanodot sizes were controlled by the amount of $HAuCl_4$ precursor loaded into the micelles, inter-dot distances were controlled through tuning the molecular weight of the diblock copolymer, and directed assemblies of the nanodots into aperiodic structures were demonstrated though the use of top-down lithographically defined structures, exploiting the capillary forces of the retracting liquid solvent to force the micelles to the edge of the topographic structure. Continuous, electrically conducting lines of Au were subsequently patterned through the use of cylindrical micelle forming BCPs, thereby signifying the versatility of this approach.

Further developments in the synthesis of new BCP systems for nanopatterning using an integrated approach must take into account the stringent requirements demanded by modern semiconductor fabrication processing. It is evident that the bottom-up self-assembly complements a number of top-down fabrication techniques to enable production of hierarchically ordered functional materials with impressive characteristics. Moreover, successful integration of top-down and bottom-up approaches will open up exciting prospects in the areas of molecular electronics, bioelectronics, nanoelectromechanical systems and nanotechnology. It is evident that the application of integrated approaches is rapidly gaining prominence and is being explored at a hectic pace to elucidate further innovative technologies.

7. *In Situ* Characterization of Self-Assembly Processes

Harnessing self-assembly for furthering science and technology requires developing a comprehensive understanding of the associated phenomena at a fundamental level both qualitatively and quantitatively. Of specific interest is the quest for controlling the self-assembly of colloidal nanoparticle suspensions to enable formation of superlattices with desirable structural, optical, electronic, and magnetic properties. Employing *in situ* characterization methods allow data acquisition in real time during

the self-assembly, enabling one to determine the self-assembly formation mechanism and kinetics. Subsequently, this level of understanding will permit manipulation and tailoring of the physical processes and parameters associated with self-assembly. It is almost self-evident that employing *in situ* characterization tools is nontrivial as there are several challenges that arise from the ultra-fast kinetics of self-assembly, especially the stringent requirements for alignment and positioning of the samples with respect to the probe and inherent limitations of instrument resolution that can be observed/measured with a single technique compared to the assembly length and time scales. In this area, researchers have made substantial advancements toward developing suitable modifications to various sample cells and whole system designs to permit observation of the self-assembly process *in situ* either with a single probe or combination of probes. In this section, we summarize key developments and highlight the importance of using *in situ* measurements in the study of self-assembly with examples from recently reported literature.

With the advancement of second- and third-generation synchrotrons, X-ray probes are attractive for performing *in situ* reflectivity measurements to elucidate the growth of SAMs. The advantages of employing X-rays from a synchrotron source include: (i) availability of high beam energy with a small spot size for incidence at small angles, (ii) variable source energy permitting penetration to internal interfaces, and (iii) non-destructive nature of the methodology allowing *in situ* study without affecting the self-assembly process.[471] In this respect, Dutta and co-workers carried out an *in situ* X-ray reflectivity study to monitor and understand the growth of octadecyltrichlorosilane (OTS) SAM on oxidized Si(111) from solutions in heptane.[472] Prior to this study, several authors had conducted interrupted growth studies through *ex situ* measurements and concluded that OTS SAM grows in the form of islands [473, 474] while others had reported a uniform growth model.[475, 476] It is therefore evident that *ex situ* techniques were insufficient to reveal the actual mechanism. The important findings from the *in situ* study by Dutta *et al* were: (i) the thickness of the film remained constant at the expected thickness of a complete monolayer and (ii) the monolayer electron density increased continuously until it leveled off after nearly 20 h. Therefore, it was concluded that this system undergoes island-type growth with unique domains of the same thickness. This is different from the uniform growth model, in which the density of the incomplete film is close to that of the complete film while the thickness increases with deposition time. Dutta *et al* also performed *ex situ* measurements to determine the role of rinsing on the reported differences in the observations of the SAM formation.[472] Based on their findings, rinsing an incomplete film is said to remove the physisorbed molecules, which are only held in place by hydrogen bonding to neighboring molecules, allowing the reorganization of remaining molecules into tilted phases, which could explain the different observations reported by the other groups.[472] Besides disruption by *ex situ* characterization, several experimental parameters such as the surface energy and functionality of

the substrate, solution level, temperature, and clean room environmental conditions influence the film morphology, thereby leading to different interpretations on the mode of growth. In general, *in situ* monitoring of the growth kinetics of SAM is not easy with X-ray-based measurements. It requires careful choice of experimental parameters such as using extremely low concentrations of OTS to slow down the growth rate and permit meaningful measurements, using lower density solvents to reduce background, and specially constructed sample cells to prevent evaporation or leaking.

A quick review of recently published works tells us the importance of carrying out *in situ* characterization in the study of inter-particle interactions that may drive self-assembly of colloidal suspensions of nanoparticles into orderly structures such as superlattices.[477-481] It also drives home the point that understanding the fundamental interactions between particles and macroscopic (i.e. liquid–liquid or liquid–air) interfaces is critical, as these effects are particularly prominent in the self-assembly of thin films from colloidal suspensions. In general, the nature of the interactions between the particles and the interface is fundamentally different from the interactions among particles in the bulk. Presently, *in situ* studies are becoming increasingly important to understanding self-assembly mechanisms in these colloidal systems. In this respect, X-ray scattering measurements are versatile and gaining prominence. Specifically, synchrotron X-ray characterization techniques are very useful, as revealed by numerous recent works. [477-481] Such *in situ* studies are challenging and require suitable modification to the system design to incorporate desirable features. Development of an experimental chamber allowing *in situ* studies of solvent-mediated NP self-assembly has been reported in great detail recently.[471] The most significant feature is their injection system to deposit NP solutions on substrates without breaking the chamber's hermetic sealing. Such a sophisticated system with built-in capabilities for allowing *in situ* XRR and grazing-incidence small-angle X-ray scattering (GISAXS) is also shown to allow controlled evaporation rates of the solvent and thereby facilitate probing different stages of self-assembly, including macroscopic solution evaporation, thin film formation, and subsequent structural transformation. The value of this device was exemplified in a study of adsorption and desorption of a toluene film on a flat substrate, and study of the self-assembly process of gold nanoparticles on solid substrates.[471] Furthermore, this sample cell is shown to enable investigation of nanoparticle self-assembly kinetics both near-to and far-from thermodynamic equilibrium.

Recently, researchers at Cornell University have carried out an *in situ* synchrotron-based X-ray scattering study on the self-assembly of cubic PbSe nanocrystals (average edge length ~13.3 nm and relative polydispersity of ~8.2%) from colloidal suspensions stabilized by oleic acid.[482] Here they performed simultaneous *in situ* measurements of grazing incidence wide angle X-ray scattering (GIWAXS) and GISAXS for complete structural characterization of the nanocrystal superlattices. While

GISAXS reveals the translational ordering of the particles, GIWAXS provides information about the orientational ordering of nanocrystals in their superlattice sites. Analysis and indexing of such scattering patterns provides detailed information on the inter-particle spacing, possible lattice distortions, and average grain size. Furthermore, they found that these cubic PbSe nanocrystals assembled in a face-up (i.e. ⟨100⟩ normal to the interface) configuration at the liquid–substrate interface whereas nanocrystals at the liquid–air interface assume a corner-up (i.e. ⟨111⟩ normal to the interface) configuration (**Figure 27**). The authors explained the different orientations on the basis of thermodynamic considerations of particle orientations and the molecular configuration of the ligand near the interface.[482] This study also underscored the importance of kinetic aspects by monitoring the orientation as a function of drying rates. In the case of rapidly formed thin films, the hexagonal seed layer could not form at the gas–liquid interface and the emerging structure was dominated by ⟨100⟩ nanocrystal alignment induced by the interactions between the particles and the substrate. In slow drying times, the two orientations (⟨111⟩ and ⟨100⟩) coexisted. Meanwhile, in intermediate drying times, the ⟨111⟩ orientation was preferred over the ⟨100⟩ orientation as per the kinetic effects. These results suggest the importance of parameter manipulation to induce kinetic pathways favoring one orientation over another, enabling homogeneous superlattice structures. In short, *in situ* studies with X-ray scattering techniques can clearly bring out the role of interfacial effects as well the emphasis on the fundamental thermodynamic and kinetic factors governing the self-assembly of superstructures.

Recently, Wagner *et al* demonstrated the use of small angle neutron scattering (SANS) in probing the DSA of charge-stabilized colloidal dispersions by dielectrophoresis (DEP).[483] The importance of DSA and the various experimental routes used to realize DSA have been discussed in detail in preceding sections. Through the design and fabrication of a new suitable sample cell environment at the National Center for Neutron Research (National Institute of Standards and Technology in Gaithersburg, Maryland), *in situ* observation of electric field-driven crystallization of sub-micron particles has been enabled using SANS (**Figure 28**). In this work, two different aqueous suspensions of polystyrene particles stabilized with negatively charged sulfate groups (nominal diameters of 195.1 ± 9.6 nm and 539.9 ± 26.5 nm, respectively) were used for *in situ* DEP-SANS investigation. The *in situ* observations with SANS confirm a high degree of ordering of sub-micron colloidal particles with length scales on the order of millimeters. The importance of this work is underlined by the fact that most of the previous works were concerned with the creation of crystalline structures by DSA-DEP of micron-sized particles and the crystalline structure could be studied using optical microscopy and light scattering techniques.[207, 484] Furthermore, there is a fundamental challenge of assembling the nanoparticles as a result of the increasing importance of Brownian motion in conjunction with the DEP forces that order particles into periodic

structures under the influence of electric fields.[483] Therefore, significantly higher fields are therefore required to self-assemble nanoparticles, which is likely to cause problems such as electro-osmotic flow and electrode polarization effects that can interfere with DSA.[483] Hence, this study on the *in situ* SANS measurements of DSA by DEP is illuminating. The DEP-SANS cell fabricated in this work was shown to generate the high field strengths required to form large crystal sizes over millimeter length scales for permitting *in situ* studies. In conclusion, this work illustrates that performing *in situ* SANS measurements to study electric field-induced alignment and ordering of colloidal nanoparticles with varying particle size, chemical composition, and surface charge is advantageous to understand the fundamental science behind self-assembly.

Though X-ray and neutron scattering techniques are versatile for *in situ* studies to unravel mechanisms and kinetics of self-assembly, synchrotron and neutron beam facilities are available only at select locations and are far more sophisticated and require stringent alignment procedures compared to more prevalent instruments. On the other hand, simple techniques like real-time video recording of self-assembly events could be interesting and can be produced by custom-made equipment in a laboratory as demonstrated in a recent study on the evaporation-induced colloidal self-assembly (EISA) of polystyrene latex particles (average particle size of 1.09 μm).[485] The interesting aspect of this *in situ* study is the use of a custom-built setup composed of temperature (tolerance ± 0.1 °C) and pressure (tolerance ± 0.1 kPa) controller units connected directly to the sample cuvette. An optical microscope fitted to a CCD camera was then used to monitor the growth process *in situ* under different conditions of temperature and pressure. Interestingly, the authors employed two types of sample cuvettes with different slit sizes to determine the effect of evaporation rates on the growth process. The growth processes of colloidal crystals in different cuvettes recorded by direct video observations revealed that solvent flow around the pore space of the crystal played a key role in formation mechanics. By changing the environmental conditions of the self-assembly system and fluid properties (i.e. viscosity), different evaporation rates of solvent and growth rate of colloidal crystals were measured directly *in situ*. Previous studies used a sessile drop or the solvent exposed to the external environment [486-488] and, therefore, these works may not help to understand EISA as a result of uncontrolled evaporation rates. Hence, this work with real-time recording by a CCD camera reported by Yang *et al* is fascinating, not only from the perspective of providing a better understanding to EISA, but also from the viewpoint of using a simple, easily-built characterization tool [485]. Furthermore, this study confirms that both evaporation rate and growth rate are functions of temperature and pressure that fit Stefan's law well. The knowledge gained through this *in situ* study with a relatively simple experimental setup that allowed high degree of control in the evaporation rates could be very useful to fabricate colloidal photonic crystals with near-perfect order.

In recent years, there have been some efforts towards understanding self-assembly processes in biological systems using *in situ* probes.[489-491] Among these efforts, the recent work reported by Pfohl *et al* on the behavior of DNA/linker histone H1 assemblies under shear and elongational stress is very interesting.[491] Their work brings out the advantages of employing microfluidics in conjunction with synchrotron x-ray scattering and diffraction and micro-Raman spectroscopy. Employing microfluidics is advantageous because it permits the use only small sample volumes besides enabling shorter reaction and analysis times. Moreover, the challenge in the study of biological molecules with conventional X-ray scattering tool lies in their high sensitivity to damage caused by prolonged radiation exposure. In this respect, the tool based on a combination of microfluidics with x-ray scattering is a good proposition to reduce the radiation-related damage as the beam position is fixed and the macromolecules move with the flow. Micro-Raman spectroscopy together with microfluidics is another attractive method owing to its potential for chemical imaging without the need for additional marker molecules. Furthermore, this study illustrates the usefulness of combining structural and chemical mapping tools to probe dynamic formation of polycations/DNA assemblies.[491] The simultaneous orientation of macromolecules, during self-assembly in x-ray compatible hydrodynamic focusing microdevices, facilitates the exploration of reaction intermediates of DNA and proteins assemblies under physiological conditions in real time as shown in this work. Other techniques that have been employed for in situ investigation of self-assembly of colloidal nanoparticles and biological macromolecules include AFM[492], STM[493, 494], ellipsometer [495, 496], X-ray microscopy[497] and FTIR[498] and we refer the interested readers to these publications.

8. Conclusion

Self-assembly offers a comprehensive roadmap towards the next-generation of functional materials and devices formed from the hierarchical ordering of nanoscale objects. The overarching goal of this article has been to introduce the readers to the entire gamut of interaction forces, both internal to the system as well as externally applied, to drive the self-assembly of molecular or nanoscale objects within synthetic and biological systems. While self-assembly within biological systems is well established; nature having a clear advantage of time to perfect the evolutionary process, progress realized over the last decade in understanding and demonstrating self-assembly within synthetic systems, although in its nascent stage, is praiseworthy. Biomimetic approaches are certainly a key to help fast track our understanding and advancement of the science of self-assembly. Thus, this article has attempted to provide an unbiased glimpse into the progress made in the synthetic as well as in the biological domain. By biological domain, we imply biomimetic approaches towards synthetic materials. A logical progression is thus made to first provide a comprehensive discussion on the physics of self-assembly; the

various interaction forces that occur within systems of molecular/nanoscale constituents. Key illustrative examples have been provided from recent literature that exploits these interaction forces to derive self-assembly. On a broad level, this essentially entails engineering the interaction forces thereby exerting a level of control on the assembly process. Examples of such engineered approaches include: (i) assembly of colloidal systems through shape and surface engineering of colloids, (ii) exploitation of thermodynamic interplay between nanoparticle – polymer systems to drive controlled segregation of nanoparticles, and (iii) utilization of engineered macromolecular systems, in particular, BCP to guide self-assembly of nanoscale objects and in nanoscale lithography etc, all of which are presented in this article.

Directed self-assembly (DSA) through the use of pre-formed templates and/or external fields provide additional degrees of freedom to manipulate the assembly and thus form an important subject of discussion in this article. Several excellent reviews on DSA using templates have been previously published and hence this topic is not the focus of this article. On the other hand, DSA through application of external fields has gained more attention in recent years. This is attributed to the ability to apply and control the external fields to a high degree of precision and stability, thereby enabling scalable production of hierarchically assembled functional materials from nanoscale building blocks. The published works clearly demonstrate the usefulness of applying external fields such as electric, magnetic or flow fields as well as their combinations in guiding the assembly of nanobuilding blocks at all length scales (from nano- to micro- to macroscale). Interfacial self-assembly of nanoparticles is another promising technique underscored in this article due to the relative simplicity of the technique that can enable fabrication of 2-D monolayer ordered arrangement of nanoparticles (isotropic or anisotropic nanoparticles) over sufficiently large areas. This can have a broad technological implication, enabling the fabrication of free standing, ultra-thin membranes to 2-D electronic and photonics structures. It should be noted that, while the external forces are applied to direct the self-assembly, internal interaction forces still play an important role in dictating the overall dispersion stability of the individual constituents. Thus, appropriate surface engineering and other thermodynamic constraints imposed within the system have to be kept in mind for the design and engineering of the structures.

The advancement of the science of self-assembly critically depends on the development of suitable characterization tools that permit to investigate the various assembly steps in real time. In this respect, *in situ* characterization techniques play an important role in comprehending and substantiating the principle of self-assembly through a first-hand observation of the events as they unfold during self assembly. While the operating principle of the tools is the same as in *ex situ* measurements, the suitability of a specific characterization method for *in situ* measurements is dependent on achieving the desired spatial and temporal resolutions required to probe the assembling behavior. The real challenge lies in

modifying the tool appropriately to facilitate *in situ* study on self assembly mechanism. Recent publications demonstrate that significant advancement has been realized for employing X-ray scattering tool owing to the availability of synchrotron radiation. In particular, the simultaneous use of GISAXS and GIWAXS *in situ* during the assembly of colloidal nanocrystals is impressive to study the ordering at different length scales. In another study, SANS has been used *in situ* to probe the DSA of colloidal particles under the influence of AC field that enabled to carry out a fundamental study on the assembling behavior as a function of frequency and field. Other characterization tools explored for *in situ* study of the self assembly process include ellipsometer, AFM and STM. A detailed review on this topic with classic illustrations from recent works is discussed in this review. In short, there is a lot of scope for advancement in this field that will ultimately enable the scientists to engineer hierarchically assembled devices with desired functionality.

Mimicking the self-assembly processes observed in nature can lead to synthetic materials with biological functionality. As most of the biological self-assemblies occur under mild, non-toxic conditions, it poses additional constraints on the choice of the nanomaterials and their stability under physiological conditions. However, facile functionalization with various biological entities such as antibodies, peptides, enzymes, DNA molecules, and others will impart remarkable functionality and flexibility to these materials. Thus, a wide range of biocompatible chemical reactions have been used with a variety of analytical techniques for the analysis of chemical and biological molecules through self-assembly techniques. There are many different challenges involved for implementing these self-assembled nanostructures in real-world. Several problems based on size, shape, conductivity, and stability under varying experimental conditions have been reviewed. Despite these disadvantages or limitations, self-assembled materials have been performing a key role in various biological applications such as biosensing, optical imaging, and drug delivery. Detailed study of their unique properties will provide new opportunities to understand complex biological phenomena that are impossible with non-biological systems. Self-assembly is therefore an important tool in current technology and needs more attention to understand the relevant features such as stability and toxicity of the material in question for specific application in biomedical field.

The article also stresses the importance of employing integrated approaches towards hierarchical organization of nanoscale components on a large scale for fabrication of next generation of optical and electronic devices. The high degree of precision engineering and reliability required of patterned structures over macroscopic length scales demands a synergistic combination of top-down and bottom-up fabrication approaches. In this regard, the article places special emphasis on the various forms of BCP lithography towards obtaining large scale patterning of ordered structures, wherein BCPs are utilized as

lithographic masks, as integral structures of the final device or as scaffolds to direct the assembly of metal structures. Integration of bottom-up self-assembly and top-down approaches will surely open up exciting prospects in the next few years in the areas of molecular electronics, bioelectronics and biosensors, NEMS and lab-on-a-chip technologies, and nanotechnology, in general.

Acknowledgement

The authors would like to express their gratitude to Mr.Charles M.Darr (Graduate student in Department of Biological Engineering, University of Missouri) and Mrs. Rama Kannan (Graduate student in department of Biochemistry, University of Missouri) for their valuable suggestions and timely help in proofreading the manuscript thoroughly.

Figure Captions

Figure 1*. Variation of a typical colloidal potential, $U_{LJ}(r)$, as a function of interparticle separation. Plots are presented in dimensionless form whereby energy is measured in units of $2\varepsilon a/\sigma$ and distance in units of particle diameter, 2a. Here, r represents the distance between centers of two particles, ε is the depth of the potential well, 'a' is the particle radius and σ is the characteristic atomic diameter at which $U_{LJ}(\sigma) = 0$. Reprinted with permission from reference [36]. Copyright 2009, Wiley-VCH Verlag GmbH & Co. KGaA, Weinheim.*

Figure 2. (a) *Plot of Hamaker coefficient, A(L), as a function of surface separation L, calculated using the DLP theory for two semi-infinite gold surfaces interacting across water. Reprinted with permission from reference [36]. Copyright 2009, Wiley-VCH Verlag GmbH & Co. KGaA, Weinheim.* ***(b)*** *vdW force driven self-assembly of gold spherical nanoparticles separated from short nanorods (assembled at the outer layer). Reprinted with permission from reference [63]. Copyright 2005, American Chemical Society.* ***(c)*** *Formation of ribbon-like structure driven by favoring side-by-side arrangement of gold nanorods. Reprinted with permission from reference [63]. Copyright 2005, American Chemical Society.*

Figure 3 (a) *Schematic representation of gold and silver coated with self-assembled mono-layers (SAM) of alkane thiols, $HS(CH2)_{10}COOH$ (MUA) and $HS(CH2)_{11}NMe_3^+Cl^-$ (TMA) respectively. While the AuMUAs are negatively charged, the AgTMAs are positively charged. Reprinted with permission from reference [71]. Copyright 2006 The American Association for the Advancement of Science.* ***(b)*** *Electrostatic force driven self-assembly of nanoparticles to form diamond-like ZnS crystallites with octahedron morphology. This work also demonstrates the formation of other morphologies. Reprinted with permission from reference [71]. Copyright 2006 The American Association for the Advancement of Science.*

Figure 4*. Top panels: schematic representation of tube architectures formed with 5 and 10 nm Au nanoparticles placed on the surfaces of the DNA tile array. Bottom panels: the corresponding electron tomographic images are shown. Precise placement of Au nanoparticles on the DNA structures enables one to image true 3D conformations of DNA tubes, and overcome the limitations of electronic microscopic imaging techniques to study the same. Reprinted with permission from reference [92]. Copyright 2009 The American Association for the Advancement of Science.*

Figure 5. *Entropy-enthalpy interplay led to self-assembly within nanoparticle-polymer systems* ***(a)*** *Multilayer formation of assembled nanoparticles. Reprinted with permission from reference [164] Copyright 2007 Nature Publishing Group and* ***(b & c)*** *Application to the development of self-healing coating scale bar -50 µm. Reprinted with permission from reference [165]. Copyright 2006 Nature Publishing Group.*

Figure 6*. Cross-sectional TEM images showing the assembly of gold particles within PS-PVP block copolymer, assembly of gold nanoparticles surface functionalized with* ***(a)*** *100% PS groups and* ***(b)*** *20% PVP and 80% PS group. Reprinted with permission from reference [166] . Copyright 2005 American Chemical Society.* ***(c)*** *SEM image illustrating the cooperative self assembly between TOPO surface functionalized CdSe nanoparticles within PVP cylinders and* ***(d)*** *schematic of the assembly process. Reprinted with permission from reference [127]. Copyright 2005 Nature Publishing Group.*

Figure 7 (a) *Nanoparticle-polymer systems at high temperatures for spontaneous formation of high surface area organosilicate films. Reprinted with permission from reference [184]. Copyright 2009 IOP Publishing Ltd and* ***(b)*** *Fluorescent micrograph image of a fluorescent protein bound surface energy gated spontaneously patterned nanoporous thin films. Reprinted with permission from reference [185]. Copyright 2011 Elsevier Inc.*

Figure 8 (a) *Schematic of the experimental setup,* ***(b)*** *random distribution of 1.4µm latex particles before the application of the AC electric field (Scale 1 cm = 7 µm),* ***(c)*** *formation of 1D chains oriented in parallel to the field direction applied for 2 seconds Scale (1 cm = 7 µm) and* ***(d)*** *formation of hexagonally close packed arrays with the field applied for 15 seconds (1 cm = 3.5 microns). Reprinted with permission from reference [207]. Copyright 2004 American Chemical Society.*

Figure 9. *AFM images of* ***(a)*** *Ni nanoparticles cast on Si substrate,* ***(b)*** *Ni nanochains formed by self-organized nanoparticles in the presence of magnetic field (the inset shows higher magnification of a single nanochain, scale bar of 200 nm). Reprinted with permission from reference [225]. Copyright 2009 IOP Publishing Ltd.*

Figure 10. *Schematic illustration of the magnetic-field-dependent preparation of noble-metal hollow nanoparticle strucutures. Process (1) and (2) correspond to the presence and absence of the magnetic field, respectively.* M^{x+} *denotes* Au^{3+}, Pt^{4+}, *or* Pd^{2+}. *The SPR peak position of Au hollow nanoparticulate chain is seen to depend on external magnetic field. Reprinted with permission from reference [226]. Copyright 2007 WILEY-VCH Verlag GmbH & Co. KGaA, Weinheim.*

Figure 11. *Optical microscopy pictures of ellipsoidal particles trapped at the water-oil interface.* ***(a)*** *polystyrene (PS) ellipsoids coated with silica shell aggregate side to side (scale bar: 21 µm) and* ***(b)*** *PS ellipsoids without silica shell bind in a tip-to-tip manner (scale bar: 33 µm). Inset: polygon-like structure formed by PS ellipsoids (scale bar: 13.6 µm). Reprinted with permission from reference [259]. Copyright 2005 The American Physical Society.*

Figure 12 (A) *Schematic representation of the self-assembly during the early stages of drying (not to scale).* ***(B)*** *A TEM micrograph of a typical monolayer produced by drop-casting a solution of dodecanethiol-ligated 6-nm gold nanocrystals. Reprinted with permission from reference [268]. Copyright 2006 Publishing Group.* ***(C)*** *TEM image of a monolayer sheet self-assembled from 26.0 nm PS-Au nanoparticles and* ***(D)*** *Higher-magnification TEM image of the selected region from* ***(C)*** *showing that nanoparticles are hexagonally packed yet well spaced. Reprinted with permission from reference [269]. Copyright 2011 American Chemical Society.*

Figure 13. *Self-assembly of anisotropic* TiO_2 *particles as a consequence of electric field and flow induced effects. Reprinted with permission from reference [273]. Copyright 2009 WILEY-VCH Verlag GmbH & Co. KGaA, Weinheim.*

Figure 14. *Fabrication of 3D photonic crystals by self-assembly mediated by convective flow in a magnetic field. Reprinted with permission from reference [274]. Copyright 2009 WILEY-VCH Verlag GmbH & Co. KGaA, Weinheim.*

Figure 15*. Few examples of biological self-assembly towards ordered nanostructures.* ***(A)*** *Bone formation from collagen molecules incorporating hydroxyapatite crystals. Individual fibrils associate in a hierarchial pattern to generate the final bone structure. Reprinted with permission from reference [288] Copyright 1993 Nature Publishing Group.* ***(B)*** *Deep etch electron micrograph of cytoskeleton with origami inset (upper left) demonstrates the intricate patterns formed by cytoskeletal proteins that grants shape, support and flexibility to cells. Reprinted with permission from reference [286] Copyright 2006 The Rockefeller University Press. The inset in* ***(B)*** *is reprinted with permission from reference [116]. Copyright 2006 Nature Publishing Group* ***(C)*** *Highly ordered structure of muscle cell. Immunofluorescence image of myocytes labelled with antibodies against Actin (Blue) Actinin and Nebulin (merged orange) and fluorescent labelled phalloidin. Reprinted with permission from reference [287]. Copyright 2010 The Rockefeller University Press.* ***(D)*** *Immunofluorescence image of honeycomb like structure of lens fiber cells revealed by anti-Aquaporin-0 staining. (Source:* http://www.mc.vanderbilt.edu/root/vumc.php?site=msrcscheylab&doc=31159)

Figure 16*. Self assembled protein nanostructures.* ***(A)*** *Hexagonal hierarchical microtubular structures are produced by diphenylalanine self-assembly. Reprinted with permission from reference [337]. Copyright 2011 American Chemical Society)* ***(B)*** *The hexagonal tubular structures visualized by optical microscopy. Reprinted with permission from reference [335] Copyright 2011 Elsevier Ltd.* ***(C)*** *intermediate structures in the self-assembly of the peptide KFE8 (FKFEFKFE), designed with alternating polar and non-polar amino acids.* ***(D)*** *Atomic force microscopy (AFM) demonstrating ordered self-assembled KFE8 peptide and schematic top view. Images (****C-D****) reprinted with permission from reference [339]. Copyright 2002 American Chemical Society.*

Figure 17. (i-iii) *Patterned deposition of Au film on silicon (Si) substrate and* ***(iv-vi)*** *layer-by-layer assembly of gold nanoparticles on Au patterns.* ***(a-d)*** *Scanning electron micrographs of two layers of gold nanoparticles assembled onto lithographically defined gold patterns, taken at different magnifications, with the surrounding silicon being passivated with PEG silane. The first layer consists of 15 nm diameter particles and the second layer of 10 nm size particles. The oligonucleotides have been employed to perform nanoparticle assembly on lithographic patterns demonstrates the specificity and versatility of the multilayer process. Reprinted with permission from reference [343] Copyright 2004 American Chemical Society.*

Figure 18*.* ***(A)*** *Schematic presentation of DNA assisted assembly of nanowires. After DNA functionalization, the nanowires are assembled on the surface of the gold electrodes.* ***(B)*** *SEM image of an assembled Au/Pd/Au nanowire between electrodes. Reprinted with permission from reference [345] Copyright 2007 WILEY-VCH Verlag GmbH&Co. KGaA, Weinheim.*

Figure 19*. Self assembled RNA nanostructures. (****A-B****) Electron micrographs (EM) and schematics of 6 – stranded* ***(A)*** *and 10 - stranded* ***(B)*** *RNA cubes. Top left panels: EM of the RNA particles. Right panels: Average shapes of different classes Lower panel: Schematic projections of RNA nanostructures observed. Images* ***(A) & (B)*** *reprinted with permission from reference [354] Copyright 2010 Macmillan Publishers Limited****.*** ***(C)*** *Electron density map demonstrating the minor groove formed by the helical regions of the RNA nanosquare;* ***(D)*** *major groove view. Images* ***(C)*** *&* ***(D)*** *reprinted with permission from reference [353] Copyright 2012 by the National Academy of Sciences.*

Figure 20*. Self assembled lipid based bionanoparticles.* ***(A)*** *Liposomes fusing to particle surface after being mixed with hydrophilic particles. An anionic fluorescent dye (calcein) was incorporated by the fusion of a cationic lipid with an anionic silica particle. Fluorescence image demonstrating uptake of the calcein containing lipid nanoparticles. Image* ***(A)*** *reprinted with permission from reference [365] Copyright 2009 American Chemical Society.* ***(B)*** *Structure of Nanodiscs, modeled with POPC as lipid. Two amphipathic helices of MSP (gray ribbon) sarround the lipid bilayer (white space filling). The graphic was generated using the PyMOL Molecular Graphics system. Image* ***(B)*** *reprinted with permission from reference [378]. Copyright 2009 Elsevier Inc.*

Figure 21. (a) *Molecular model of the oligopeptide RADSC-14 with the sequence RADSRADSAAAAAC and of ethylene glycol thiolate (EG_6SH) and* ***(b)*** *an example of patterned surface using self-assembly and microcontact printing (top-down fabrication). Reprinted with permission from reference [393]. Copyright 1999 Elsevier Science Ltd.*

Figure 22. (a-c) *Schematic of the assembly mechanism for the formation of vertically aligned ADNTs. Using an inttegrated approach of top-down fabrication and bottom-up self-assembly. During evaporation, the diphenylalanine peptide, which is heated to 220^{o}C, attained a cyclic structure and then assembled on a substrate to form an ordered array of vertically aligned nanotubes. The aromatic π-stacking stabilizes the aligned nanotube architecture.* ***(d)*** *Cyclic voltammetry measurements of ADNT-coated (red line), carbon-nanotube-coated (black line) and uncoated (blue line) carbon electrodes and* ***(e)*** *Cross-sectional SEM image of vertically aligned ADNTs demonstrating the elongated micrometre tubes,*

with a thickness of 40 μm. Reprinted with permission from reference [30]. Copyright 2009 Macmillan Publishers Limited.

Figure 23. *Schematic representation of the hierarchical electrode fabrication using integrated top-down lithography and bottom-up self-assembly approach.* ***(a - c)*** *Patterning of gold pillars on silicon wafer using traditional photoresist process (top-down)* ***(d)*** *Tobacco mosaic virus (TMV) was self-assembled on the chip surface and metallized on the micropillars with Ni using an electroless plating and the active battery material, V_2O_5, was deposited using ALD.* ***(e-g)*** *– SEM images of the hierarchical electrodes recorded at different magnifications.* ***(f)*** *and* ***(g)*** *depict the side- and the top-views of one such pillar. Reprinted with permission from reference [33]. Copyright 2012 American Chemical Society.*

Figure 24 (a) *Schematic of the multi-layer structure used to create the nanomembrane based ultra-compact capacitors (UCCap) using a combined top-down and bottom-up strategy.* ***(b)*** *The multilayer nanomembrane exhibit self-rolling behavior due to strains.* ***(c)*** *The layer sequence for inorganic (Case I) and hybrid organic/inorganic (Case II) capacitors incorporating self-assembled monolayers is shown.* ***(d-e)*** *Typical SEM images of UCCaps demonstrating the reproducibility of the process to produce several such structures on a large area.* ***(f)*** *Cross-sectional SEM view of an UCCap comprising nearly 13 windings and rolled from a 600 μm long planar capacitor. Reprinted with permission from reference [32]. Copyright 2010 American Chemical Society.*

Figure 25. *Formation of metal nanochains and nanowires on PS-b-PMMA at different stages.* ***(a)*** *Aggregation of Au metal, vapor-deposited onto BCP film (3 nm nominal metal film thickness), into nanometer-sized islands.* ***(b)*** *Annealing at 180^{o}C for 1 min in an Ar ambient produces highly selective Au decoration of the PS domains forming metal nanochains.* ***(c)*** *Repeated deposition and short-time annealing at 180^{o}C leads to densely packed nanochains.* ***(d)*** *Large-scale TEM micrograph and* ***(e)*** *Magnified view of self-assembled Ag nanowires. Deposition with higher thickness of Ag film (12 nm) leads to nanowires while that of lower thickness (3 nm) self-assembles into nanochains. The varying grey levels in the image due to Bragg scattering is attributed to the different orientations of the nanocrystallites. All metal depositions were performed at base pressures of (1-2)× 10^{-6} Torr and rates of 0.005 ± 0.1 nm s^{-1}. Scale bars: 200 nm in (**a-c**) and 100 nm in **(d)** and **(e)**. Reprinted with permission from reference [437]. Copyright 2001 Macmillan Magazines Ltd.*

Figure 26. *SEM images of* ***(a)*** *PS(990)-b-P[2VP(HAuCl4)0.5] BCP micellar monolayer on a Si substrate after lifting-off the non-irradiated micelles (i.e. areas without electron beam exposures) and* ***(b)*** *after the hydrogen plasma treatment, which deposited 7 nm large Au-nanoparticles in a star pattern. Reprinted with permission from reference [424]. Copyright 2003 IOP Publishing Ltd.*

Figure 27*.* ***(A)*** *Schematic of the temporal and spatial evolution of self-assembled superstructures studied using in-situ X-ray scattering techniques. Slices at intermediate drying times reveal the process of ordering in different regions including at the interfaces. A low and high magnification TEM image of PbSe cubic nanocrystals (cNC) are also shown along with a SEM image of a monolayer of nanocrystals.* ***(B)*** *In-situ GISAXS reveals the evolution of the rhombohedral superlattice constant, a, and angle, α, as a function of hexane vapor concentration from wet (nearly saturated) to dry (pure He gas environment). GIWAXS* ***(C−E)*** *show the evolution of the orientational ordering from the wet film to the dry superlattice. Radially integrated intensity of the {111}NC reflection illustrates the preferential cNC orientation in the wet and dry films* ***(C−E)*** *as well as assemblies formed by slow (i) and fast (ii) evaporation. The monolayer film (iii) also illustrates preferential "face-up" alignment of the cNC. Reprinted with permission from reference [482]. Copyright 2012 American Chemical Society.*

Figure 28 (A) *Schematic of dielectrophoretic (DEP) sample cell (not to scale) integrated with small angle neutron scattering (SANs) probe to monitor the electric field directed self-assembly of polystyrene colloidal nanoparticles in-situ.* ***(B)*** *Scattering patterns in 2D and 3D for d = 195nm particles obtained at E = 1414V/cm 50 kHz shows six strong spot Bragg ordering confirming formation of crystal structures at*

very high field and low frequencies. Reprinted with permission from reference [483]. Copyright 2010 The Royal Society of Chemistry.

References

[1] Alivisatos P 2004 The use of nanocrystals in biological detection *Nat. Biotechnol.* **22** 47
[2] Anker J N, Hall W P, Lyandres O, Shah N C, Zhao J and Van Duyne R P 2008 Biosensing with plasmonic nanosensors *Nat. Mater.* **7** 442
[3] Atwater H A and Polman A 2010 Plasmonics for improved photovoltaic devices *Nat. Mater.* **9** 205
[4] Burda C, Chen X, Narayanan R and El-Sayed M A 2005 Chemistry and properties of nanocrystals of different shapes *Chem. Rev.* **105** 1025
[5] Cui Y, Wei Q, Park H and Lieber C M 2001 Nanowire nanosensors for highly sensitive and selective detection of biological and chemical species *Science* **293** 1289
[6] Hu J, Odom T W and Lieber C M 1999 Chemistry and physics in one dimension: Synthesis and properties of nanowires and nanotubes *Acc. Chem. Res.* **32** 435
[7] Katz E and Willner I 2004 Integrated nanoparticle-biomolecule hybrid systems: synthesis, properties, and applications *Angew. Chem. Int. Ed.* **43** 6042
[8] Patzke G R, Krumeich F and Nesper R 2002 Oxidic nanotubes and nanorods - Anisotropic modules for a future nanotechnology *Angew. Chem. Int. Ed.* **41** 2446
[9] Tartaj P, Del Puerto Morales M, Veintemillas-Verdaguer S, González-Carreño T and Serna C J 2003 The preparation of magnetic nanoparticles for applications in biomedicine *J. Phys. D: Appl. Phys.* **36** R182
[10] Trindade T, O'Brien P and Pickett N L 2001 Nanocrystalline semiconductors: Synthesis, properties, and perspectives *Chem. Mater.* **13** 3843
[11] Yin Y and Alivisatos A P 2005 Colloidal nanocrystal synthesis and the organic-inorganic interface *Nature* **437** 664
[12] Verwey E J W and Overbeek J T G 1948 *Theory of the Stability of Lyophobic Colloids* Elsevier Publishing Company Inc.
[13] Feldheim D L and Keating C D 1998 Self-assembly of single electron transistors and related devices *Chem. Soc. Rev.* **27** 1
[14] Fendler J H 1996 Self-assembled nanostructured materials *Chem. Mater.* **8** 1616
[15] Liu Y, Wang Y and Claus R O 1998 Layer-by-layer ionic self-assembly of Au colloids into multilayer thin-films with bulk metal conductivity *Chem. Phys. Lett.* **298** 315
[16] Martin B R, Dermody D J, Reiss B D, Fang M, Lyon L A, Natan M J and Mallouk T E 1999 Orthogonal self-assembly on colloidal gold-platinum nanorods *Adv. Mater.* **11** 1021
[17] Oldenburg S J, Averitt R D, Westcott S L and Halas N J 1998 Nanoengineering of optical resonances *Chem. Phys. Lett.* **288** 243
[18] Chen J T, Thomas E L, Ober C K and Mao G P 1996 Self-assembled smectic phases in rod-coil block copolymers *Science* **273** 343
[19] Emrick T and Fréchet J M 1999 Self-assembly of dendritic structures *Curr. Opin. Colloid Interface Sci.* **4** 15
[20] Ikkala O and Ten Brinke G 2002 Functional materials based on self-assembly of polymeric supramolecules *Science* **295** 2407
[21] Percec V, Ahn C H, Ungar G, Yeardley D J P, Möller M and Sheiko S S 1998 Controlling polymer shape through the self-assembly of dendritic side- groups *Nature* **391** 161
[22] Percec V, Glodde M, Beta T K, Miura Y, Shiyanovskaya I, Singer K D, Balagurusamy V S K, Heiney P A, Schnell I, Rapp A, Spiess H W, Hudson S D and Duan H 2002 Self-organization of supramolecular helical dendrimers into complex electronic materials *Nature* **419** 384

[23] Aggeli A, Bell M, Boden N, Keen J N, Knowles P F, McLeish T C B, Pitkeathly M and Radford S E 1997 Responsive gels formed by the spontaneous self-assembly of peptides into polymeric β-sheet tapes *Nature* **386** 259
[24] Philp D and Fraser Stoddart J 1996 Self-Assembly in natural and unnatural systems *Angew. Chem. Int. Ed.* **35** 1154
[25] Sarikaya M, Tamerler C, Jen A K Y, Schulten K and Baneyx F 2003 Molecular biomimetics: Nanotechnology through biology *Nat. Mater.* **2** 577
[26] Whitesides G M, Mathias J P and Seto C T 1991 Molecular self-assembly and nanochemistry: A chemical strategy for the synthesis of nanostructures *Science* **254** 1312
[27] Lee Y S 2007 *Self-Assembly and Nanotechnology: A Force Balance Approach* John Wiley & Sons, Inc.
[28] Liddle J A and Gallatin G M 2011 Lithography, metrology and nanomanufacturing *Nanoscale* **3** 2679
[29] Lu W and Sastry A M 2007 Self-assembly for semiconductor industry *IEEE T. Semiconduct. M.* **20** 421
[30] Adler-Abramovich L, Aronov D, Beker P, Yevnin M, Stempler S, Buzhansky L, Rosenman G and Gazit E 2009 Self-assembled arrays of peptide nanotubes by vapour deposition *Nat. Nanotechnol.* **4** 849
[31] Adler-Abramovich L and Gazit E 2008 Controlled patterning of peptide nanotubes and nanospheres using inkjet printing technology *J. Pept. Sci.* **14** 217
[32] Bof Bufon C C, Cojal González J D, Thurmer D J, Grimm D, Bauer M and Schmidt O G 2010 Self-assembled ultra-compact energy storage elements based on hybrid nanomembranes *Nano Lett.* **10** 2506
[33] Gerasopoulos K, Pomerantseva E, McCarthy M, Brown A, Wang C, Culver J and Ghodssi R 2012 Hierarchical three-dimensional microbattery electrodes combining bottom-up self-assembly and top-down micromachining *ACS Nano* **6** 6422
[34] Reches M and Gazit E 2006 Controlled patterning of aligned self-assembled peptide nanotubes *Nat. Nanotechnol.* **1** 195
[35] Wong T S, Brough B and Ho C M 2009 Creation of functional micro/nano systems through top-down and bottom-up approaches *Mol. Cell. Biomech.* **6** 1
[36] Bishop K J M, Wilmer C E, Soh S and Grzybowski B A 2009 Nanoscale forces and their uses in self-assembly *Small* **5** 1600
[37] Grzybowski B A, Wilmer C E, Kim J, Browne K P and Bishop K J M 2009 Self-assembly: From crystals to cells *Soft Matter* **5** 1110
[38] Whitesides G M and Grzybowski B 2002 Self-assembly at all scales *Science* **295** 2418
[39] Grzelczak M, Vermant J, Furst E M and Liz-Marzán L M 2010 Directed self-assembly of nanoparticles *ACS Nano* **4** 3591
[40] Palermo V and Samorì P 2007 Molecular self-assembly across multiple length scales *Angew. Chem. Int. Ed.* **46** 4428
[41] Rubinstein I, Steinberg S, Tor Y, Shanzer A and Sagiv J 1988 Ionic recognition and selective response in self-assembling monolayer membranes on electrodes *Nature* **332** 426
[42] Whitesides G M 2005 Nanoscience, nanotechnology, and chemistry *Small* **1** 172
[43] Reches M and Gazit E 2003 Casting metal nanowires within discrete self-assembled peptide nanotubes *Science* **300** 625
[44] Dawson K A 2002 The glass paradigm for colloidal glasses, gels, and other arrested states driven by attractive interactions *Curr. Opin. Colloid Interface Sci.* **7** 218
[45] Durbin S D and Feher G 1996 Protein crystallization *Annu. Rev. Phys. Chem.* **47** 171
[46] Foffi G, McCullagh G D, Lawlor A, Zaccarelli E, Dawson K A, Sciortino F, Tartaglia P, Pini D and Stell G 2002 Phase equilibria and glass transition in colloidal systems with short-ranged attractive interactions: Application to protein crystallization *Phys. Rev. E: Stat., Nonlinear, Soft Matter Phys.* **65** 031407/1
[47] Israelachvili J N 2011 *Intermolecular and surface forces* ^3rd Edition Burlington, MA: Academic Press

[48] Henderson D, Duh D M, Chu X and Wasan D 1997 An expression for the dispersion force between colloidal particles *J. Colloid Interface Sci.* **185** 265
[49] Derjaguin B V 1934 Friction and adhesion IV. The theory of adhesion of small particles *Kolloid Z.* **69** 155
[50] White L R 1983 On the deryaguin approximation for the interaction of macrobodies *J. Colloid Interface Sci.* **95** 286
[51] Hamaker H C 1937 The London-van der Waals attraction between spherical particles *Physica* **4** 1058
[52] Dzyaloshinskii I E, Lifshitz E M and Pitaevskii L P 1961 The general theory of van der Waals forces *Adv. Phys.* **10** 165
[53] Kim H Y, Sofo J O, Velegol D, Cole M W and Lucas A A 2006 Van der Waals forces between nanoclusters: Importance of many-body effects *J. Chem. Phys.* **124** 074504
[54] Kim H Y, Sofo J O, Velegol D, Cole M W and Lucas A A 2007 Van der waals dispersion forces between dielectric nanoclusters *Langmuir* **23** 1735
[55] Lee S W and Sigmund W M 2002 AFM study of repulsive van der Waals forces between Teflon AF™ thin film and silica or alumina *Colloids Surf., A* **204** 43
[56] Milling A, Mulvaney P and Larson I 1996 Direct measurement of repulsive van der Waals interactions using an atomic force microscope *J. Colloid Interface Sci.* **180** 460
[57] Blake T D 1975 Investigation of equilibrium wetting films of n-alkanes on α-alumina *J. Chem. Soc. Farad. Trans.* **71** 192
[58] Van Oss C J, Absolom D R and Neumann A W 1980 Applications of net repulsive van der Waals forces between different particles, macromolecules, or biological cells in liquids *Colloids Surf.* **1** 45
[59] Parsegian V A and Weiss G H 1981 Spectroscopic parameters for computation of van der waals forces *J. Colloid Interface Sci.* **81** 285
[60] Harfenist S A, Wang Z L, Alvarez M M, Vezmar I and Whetten R L 1996 Highly oriented molecular ag nanocrystal arrays *J. Phys. Chem.* **100** 13904
[61] Murray C B, Kagan C R and Bawendi M G 1995 Self-organization of CdSe nanocrystallites into three-dimensional quantum dot superlattices *Science* **270** 1335
[62] Ohara P C, Leff D V, Heath J R and Gelbart W M 1995 Crystallization of opals from polydisperse nanoparticles *Phys. Rev. Lett.* **75** 3466
[63] Sau T K and Murphy C J 2005 Self-assembly patterns formed upon solvent evaporation of aqueous cetyltrimethylammonium bromide-coated gold nanoparticles of various shapes *Langmuir* **21** 2923
[64] Stern O 1924 The theory of the electrolytic double-layer: *Z Elektrochem. Angew, Phys. Chem.* **30** 508
[65] Chapman D L 1913 A contribution to the theory of electrocapillarity *Philos. Mag.* **25** 475
[66] Gouy G 1910 Constitution of the Electric Charge at the Surface of an Electrolyte *J. Physique* **9** 457
[67] Duval J F L, Leermakers F A M and Van Leeuwen H P 2004 Electrostatic interactions between double layers: Influence of surface roughness, regulation, and chemical heterogeneities *Langmuir* **20** 5052
[68] Derjaguin B V and Landau D 1941 Theory of the stability of strongly charged lyophobic sols and of the adhesion of strongly charged particles in solutions of electrolytes *Acta Physicochim. URS.* **14** 733
[69] Todd B A and Eppell S J 2004 Probing the limits of the Derjaguin approximation with scanning force microscopy *Langmuir* **20** 4892
[70] Bhattacharjee S and Elimelech M 1997 Surface element integration: A novel technique for evaluation of DLVO interaction between a particle and a flat plate *J. Colloid Interface Sci.* **193** 273
[71] Kalsin A M, Fialkowski M, Paszewski M, Smoukov S K, Bishop K J M and Grzybowski B A 2006 Electrostatic self-assembly of binary nanoparticle crystals with a diamond-like lattice *Science* **312** 420
[72] Lekkerkerker H N W and Tuinier R 2011 *Stability of colloid-polymer mixtures* Springer Netherlands
[73] Sheiko S S, Sumerlin B S and Matyjaszewski K 2008 Cylindrical molecular brushes: Synthesis, characterization, and properties *Prog. Polym. Sci.* **33** 759

[74] Tadros T 2011 Interparticle interactions in concentrated suspensions and their bulk (Rheological) properties *Adv. Colloid Interface Sci.* **168** 263
[75] Ayres N 2010 Polymer brushes: Applications in biomaterials and nanotechnology *Polym. Chem.* **1** 769
[76] Cabane E, Zhang X, Langowska K, Palivan C G and Meier W 2012 Stimuli-responsive polymers and their applications in nanomedicine *Biointerphases* **7** 1
[77] Dai S, Ravi P and Tam K C 2008 pH-Responsive polymers: Synthesis, properties and applications *Soft Matter* **4** 435
[78] Woodle M C 1998 Controlling liposome blood clearance by surface-grafted polymers *Adv. Drug Delivery Rev.* **32** 139
[79] de Gennes P G 1987 Polymers at an interface; a simplified view *Adv. Colloid Interface Sci.* **27** 189
[80] Marsh D 2004 Scaling and Mean-Field Theories Applied to Polymer Brushes *Biophys. J.* **86** 2630
[81] Milner S T, Witten T A and Cates M E 1988 Theory of the grafted polymer brush *Macromolecules* **21** 2610
[82] Milner S T, Witten T A and Cates M E 1989 Effects of polydispersity in the end-grafted polymer brush *Macromolecules* **22** 853
[83] Lai P Y and Binder K 1992 Structure and dynamics of polymer brushes near the θ point: A Monte Carlo simulation *J. Chem. Phys.* **97** 586
[84] Lai P Y and Binder K 1993 Grafted polymer layers under shear: A Monte Carlo simulation *J. Chem. Phys.* **98** 2366
[85] Wittmer J, Johner A, Joanny J F and Binder K 1994 Chain desorption from a semidilute polymer brush: A Monte Carlo simulation *J. Chem. Phys.* **101** 4379
[86] Scheutjens J M H M and Fleer G J 1985 Interaction between two adsorbed polymer layers *Macromolecules* **18** 1882
[87] Poon W C K 2002 The physics of a model colloid-polymer mixture *J. Phys.- Condens. Mat.* **14** R859
[88] Chen Y L and Schweizer K S 2002 Depletion interactions in suspensions of spheres and rod-polymers *J. Chem. Phys.* **117** 1351
[89] Anderson T H, Donaldson S H, Zeng H and Israelachvili J N 2010 Direct measurement of double-layer, van der waals, and polymer depletion attraction forces between supported cationic bilayers *Langmuir* **26** 14458
[90] Odiachi Jr P C and Prieve D C 1999 Effect of added salt on the depletion attraction caused by non-adsorbing clay particles *Colloids Surf. A* **146** 315
[91] Pagac E S, Tilton R D and Prieve D C 1998 Depletion attraction caused by unadsorbed polyelectrolytes *Langmuir* **14** 5106
[92] Sharma J, Chhabra R, Cheng A, Brownell J, Liu Y and Yan H 2009 Control of self-assembly of DNA tubules through integration of gold nanoparticles *Science* **323** 112
[93] Baranov D, Fiore A, Van Huis M, Giannini C, Falqui A, Lafont U, Zandbergen H, Zanella M, Cingolani R and Manna L 2010 Assembly of colloidal semiconductor nanorods in solution by depletion attraction *Nano Lett.* **10** 743
[94] Nicholls A, Sharp K A and Honig B 1991 Protein folding and association: Insights from the interfacial and thermodynamic properties of hydrocarbons *Proteins: Struct., Funct., Genetics* **11** 281
[95] Lehtonen J Y A, Holopainen J M and Kinnunen P K J 1996 Evidence for the formation of microdomains in liquid crystalline large unilamellar vesicles caused by hydrophobic mismatch of the constituent phospholipids *Biophys. J.* **70** 1753
[96] Campelo F, McMahon H T and Kozlov M M 2008 The hydrophobic insertion mechanism of membrane curvature generation by proteins *Biophys. J.* **95** 2325

[97] Frank H S and Evans M W 1945 Free volume and entropy in condensed systems III. Entropy in binary liquid mixtures; Partial molal entropy in dilute solutions; Structure and thermodynamics in aqueous electrolytes *J. Chem. Phys.* **13** 507
[98] Yamaguchi T, Matsuoka T and Koda S 2004 Mode-coupling study on the dynamics of hydrophobic hydration *J. Chem. Phys.* **120** 7590
[99] Yamaguchi T, Matsuoka T and Koda S 2006 Mode-coupling study on the dynamics of hydrophobic hydration II: Aqueous solutions of benzene and rare gases *Phys. Chem. Chem. Phys.* **8** 737
[100] Parker J L, Claesson P M and Attard P 1994 Bubbles, cavities, and the long-ranged attraction between hydrophobic surfaces *J. Phys. Chem.* **98** 8468
[101] Tyrrell J W G and Attard P 2001 Images of nanobubbles on hydrophobic surfaces and their interactions *Phys. Rev. Lett.* **87** 1761041
[102] Steitz R, Gutberlet T, Hauss T, Klösgen B, Krastev R, Schemmel S, Simonsen A C and Findenegg G H 2003 Nanobubbles and their precursor layer at the interface of water against a hydrophobic substrate *Langmuir* **19** 2409
[103] Jensen T R, Jensen M O, Reitzel N, Balashev K, Peters G H, Kjaer K and Bjørnholm T 2003 Water in contact with extended hydrophobic surfaces: Direct evidence of weak dewetting *Phys. Rev. Lett.* **90** 086101/1
[104] Ball P 2003 How to keep dry in water *Nature* **423** 25
[105] Hu X, Cheng W, Wang T, Wang E and Dong S 2005 Well-ordered end-to-end linkage of gold nanorods *Nanotechnology* **16** 2164
[106] Johnson S R, Evans S D and Brydson R 1998 Influence of a terminal functionality on the physical properties of surfactant-stabilized gold nanoparticles *Langmuir* **14** 6639
[107] Thomas K G, Barazzouk S, Ipe B I, Joseph S T S and Kamat P V 2004 Uniaxial plasmon coupling through longitudinal self-assembly of gold nanorods *J. Phys. Chem. B* **108** 13066
[108] Ariga K, Hill J P, Lee M V, Vinu A, Charvet R and Acharya S 2008 Challenges and breakthroughs in recent research on self-assembly *Sci. Technol. Adv. Mat.* **9** 014109
[109] Ariga K, Nakanishi T and Hill J P 2007 Self-assembled microstructures of functional molecules *Curr. Opin. Colloid Interface Sci.* **12** 106
[110] Biswas A, Bayer I S, Biris A S, Wang T, Dervishi E and Faupel F 2012 Advances in top-down and bottom-up surface nanofabrication: Techniques, applications & future prospects *Adv. Colloid Interface Sci.* **170** 2
[111] Bogue R 2008 Self-assembly: A review of recent developments *Assembly Autom.* **28** 211
[112] Edler K J 2004 Soap and sand: Construction tools for nanotechnology *Philos. T. Roy. Soc. A.* **362** 2635
[113] He Q, Cui Y, Ai S, Tian Y and Li J 2009 Self-assembly of composite nanotubes and their applications *Curr. Opin. Colloid Interface Sci.* **14** 115
[114] Jeong W, Napier M E and Desimone J M 2010 Challenging nature's monopoly on the creation of well-defined nanoparticles *Nanomedicine* **5** 633
[115] Lazzari M, Rodríguez-Abreu C, Rivas J and Arturo López-Quintela M 2006 Self-assembly: A minimalist route to the fabrication of nanomaterials *J. Nanosci. Nanotechnol.* **6** 892
[116] Rothemund P W K 2006 Folding DNA to create nanoscale shapes and patterns *Nature* **440** 297
[117] Shimomura M and Sawadaishi T 2001 Bottom-up strategy of materials fabrication: A new trend in nanotechnology of soft materials *Curr. Opin. Colloid Interface Sci.* **6** 11
[118] Tang L, Li X, Ji R, Teng K S, Tai G, Ye J, Wei C and Lau S P 2012 Bottom-up synthesis of large-scale graphene oxide nanosheets *J. Mater. Chem.* **22** 5676
[119] Tu R S and Tirrell M 2004 Bottom-up design of biomimetic assemblies *Adv. Drug Delivery Rev.* **56** 1537

[120] Balazs A C, Emrick T and Russell T P 2006 Nanoparticle Polymer Composites: Where Two Small Worlds Meet *Science* **314** 1107
[121] Boal A K, Ilhan F, Derouchey J E, Thurn-Albrecht T, Russell T P and Rotello V M 2000 Self-assembly of nanoparticles into structured spherical and network aggregates *Nature* **404** 746
[122] Chen A, DePrince A E, Demortière A, Joshi-Imre A, Shevchenko E V, Gray S K, Welp U and Vlasko-Vlasov V K 2011 Self-Assembled Large Au Nanoparticle Arrays with Regular Hot Spots for SERS *Small* **7** 2365
[123] Fan J A, Wu C, Bao K, Bao J, Bardhan R, Halas N J, Manoharan V N, Nordlander P, Shvets G and Capasso F 2010 Self-Assembled Plasmonic Nanoparticle Clusters *Science* **328** 1135
[124] Jin R, Cao Y C, Hao E, Metraux G S, Schatz G C and Mirkin C A 2003 Controlling anisotropic nanoparticle growth through plasmon excitation *Nature* **425** 487
[125] Kowalczyk B, Bishop K J M, Lagzi I, Wang D, Wei Y, Han S and Grzybowski B A 2012 Charged nanoparticles as supramolecular surfactants for controlling the growth and stability of microcrystals *Nat. Mater.* **11** 227
[126] Li C Y 2009 Nanoparticle Assembly: Anisotropy unnecessary *Nat. Mater.* **8** 249
[127] Lin Y, Böker A, He J, Sill K, Xiang H, Abetz C, Li X, Wang J, Emrick T, Long S, Wang Q, Balazs A and Russell T P 2005 Self-directed self-assembly of nanoparticle/copolymer mixtures *Nature* **434** 55
[128] McCarthy S A, Davies G-L and Gun'ko Y K 2012 Preparation of multifunctional nanoparticles and their assemblies *Nat. Protocols* **7** 1677
[129] Qian C, Ni C, Yu W, Wu W, Mao H, Wang Y and Xu J 2011 Highly-Ordered, 3D Petal-Like Array for Surface-Enhanced Raman Scattering *Small* **7** 1801
[130] Tabakman S M, Chen Z, Casalongue H S, Wang H and Dai H 2011 A New Approach to Solution-Phase Gold Seeding for SERS Substrates *Small* **7** 499
[131] Thompson R B, Ginzburg V V, Matsen M W and Balazs A C 2001 Predicting the Mesophases of Copolymer-Nanoparticle Composites *Science* **292** 2469
[132] Warren S C, Messina L C, Slaughter L S, Kamperman M, Zhou Q, Gruner S M, DiSalvo F J and Wiesner U 2008 Ordered Mesoporous Materials from Metal Nanoparticle-Block Copolymer Self-Assembly *Science* **320** 1748
[133] Xia Y, Nguyen T D, Yang M, Lee B, Santos A, Podsiadlo P, Tang Z, Glotzer S C and Kotov N A 2011 Self-assembly of self-limiting monodisperse supraparticles from polydisperse nanoparticles *Nat. Nanotechnol.* **6** 580
[134] Grosso D, Cagnol F, Soler-Illia G J d A A, Crepaldi E L, Amenitsch H, Brunet-Bruneau A, Bourgeois A and Sanchez C 2004 Fundamentals of Mesostructuring Through Evaporation-Induced Self-Assembly *Adv. Funct. Mater.* **14** 309
[135] Brinker C J, Lu Y, Sellinger A and Fan H 1999 Evaporation-Induced Self-Assembly: Nanostructures Made Easy *Adv. Mater.* **11** 579
[136] Kresge C T, Leonowicz M E, Roth W J, Vartuli J C and Beck J S 1992 Ordered mesoporous molecular sieves synthesized by a liquid-crystal template mechanism *Nature* **359** 710
[137] Lu Y, Ganguli R, Drewien C A, Anderson M T, Brinker C J, Gong W, Guo Y, Soyez H, Dunn B, Huang M H and Zink J I 1997 Continuous formation of supported cubic and hexagonal mesoporous films by sol-gel dip-coating *Nature* **389** 364
[138] Bagshaw S A, Prouzet E and Pinnavaia T J 1995 Templating of Mesoporous Molecular Sieves by Nonionic Polyethylene Oxide Surfactants *Science* **269** 1242
[139] Zhao D, Feng J, Huo Q, Melosh N, Fredrickson G H, Chmelka B F and Stucky G D 1998 Triblock Copolymer Syntheses of Mesoporous Silica with Periodic 50 to 300 Angstrom Pores *Science* **279** 548
[140] Hedrick J L, Miller R D, Hawker C J, Carter K R, Volksen W, Yoon D Y and Trollsås M 1998 Templating nanoporosity in thin-film dielectric insulators *Adv. Mater.* **10** 1049

[141] Correa-Duarte M A, Pérez-Juste J, Sánchez-Iglesias A, Giersig M and Liz-Marzán L M 2005 Aligning Au nanorods by using carbon nanotubes as templates *Angew. Chem. Int. Ed.* **44** 4375
[142] Satishkumar B C, Govindaraj A, Nath M and Rao C N R 2000 Synthesis of metal oxide nanorods using carbon nanotubes as templates *J. Mater. Chem.* **10** 2115
[143] Thiruvengadathan R and Regev O 2005 Hierarchically Ordered Cadmium Sulfide Nanowires Dispersed in Aqueous Solution *Chem. Mater.* **17** 3281
[144] Park M, Harrison C, Chaikin P M, Register R A and Adamson D H 1997 Block Copolymer Lithography: Periodic Arrays of ~1011 Holes in 1 Square Centimeter *Science* **276** 1401
[145] Thorkelsson K, Mastroianni A J, Ercius P and Xu T 2011 Direct Nanorod Assembly Using Block Copolymer-Based Supramolecules *Nano Lett.* **12** 498
[146] Xiao Z L, Han C Y, Welp U, Wang H H, Kwok W K, Willing G A, Hiller J M, Cook R E, Miller D J and Crabtree G W 2002 Fabrication of Alumina Nanotubes and Nanowires by Etching Porous Alumina Membranes *Nano Lett.* **2** 1293
[147] Moll D, Huber C, Schlegel B, Pum D, Sleytr U B and Sára M 2002 S-layer-streptavidin fusion proteins as template for nanopatterned molecular arrays *Proc. Natl. Acad. Sci. U S A* **99** 14646
[148] Ma Y, Liang J, Sun H, Wu L, Dang Y and Wu Y 2012 Honeycomb micropatterning of proteins on polymer films through the inverse microemulsion approach *Chem . - Eur. J* **18** 526
[149] Farrell R A, Petkov N, Morris M A and Holmes J D 2010 Self-assembled templates for the generation of arrays of 1-dimensional nanostructures: From molecules to devices *J. Colloid Interface Sci.* **349** 449
[150] Mann S, Burkett S L, Davis S A, Fowler C E, Mendelson N H, Sims S D, Walsh D and Whilton N T 1997 Sol-Gel Synthesis of Organized Matter *Chem. Mater.* **9** 2300
[151] Wang D and Möhwald H 2004 Template-directed colloidal self-assembly - The route to 'top-down' nanochemical engineering *J. Mater. Chem.* **14** 459
[152] Stankovich S, Dikin D A, Dommett G H B, Kohlhaas K M, Zimney E J, Stach E A, Piner R D, Nguyen S T and Ruoff R S 2006 Graphene-based composite materials *Nature* **442** 282
[153] Chau J L H, Tung C T, Lin Y M and Li A K 2008 Preparation and optical properties of titania/epoxy nanocomposite coatings *Mater. Lett.* **62** 3416
[154] Bauer F, Sauerland V, Gläsel H-J, Ernst H, Findeisen M, Hartmann E, Langguth H, Marquardt B and Mehnert R 2002 Preparation of Scratch and Abrasion Resistant Polymeric Nanocomposites by Monomer Grafting onto Nanoparticles, 3. Effect of Filler Particles and Grafting Agents *Macromol. Mater. Eng.* **287** 546
[155] Wei Z, Blackburn R S and Dehghani-Sanij A A 2009 Carbon Black Reinforced Epoxy Resin Nanocomposites as Bending Sensors *J. Compos. Mater.* **43** 367
[156] Lee J Y, Buxton G A and Balazs A C 2004 Using nanoparticles to create self-healing composites *J. Chem. Phys.* **121** 5531
[157] Huang Q R, Volksen W, Huang E, Toney M, Frank C W and Miller R D 2002 Structure and Interaction of Organic/Inorganic Hybrid Nanocomposites for Microelectronic Applications. 1. MSSQ/P(MMA-co-DMAEMA) Nanocomposites *Chem. Mater.* **14** 3676
[158] Rafiee M A, Rafiee J, Wang Z, Song H, Yu Z-Z and Koratkar N 2009 Enhanced Mechanical Properties of Nanocomposites at Low Graphene Content *ACS Nano* **3** 3884
[159] Hogg P J 2006 Composites in Armor *Science* **314** 1100
[160] Sangho B, Venumadhav K, Luis P-P, Vamsi M, Gary A B, Keshab G, William R F, Purnendu K D and Shubhra G 2012 Confeito-like assembly of organosilicate-caged fluorophores: ultrabright suprananoparticles for fluorescence imaging *Nanotechnology* **23** 175601
[161] Trenkmann I, Bok S, Korampally V R, Gangopadhyay S, Graaf H and von Borczyskowski C 2012 Counting single Rhodamine 6G dye molecules in organosilicate nanoparticles *Chem. Phys.* **406** 41

[162] Hooper J B and Schweizer K S 2006 Theory of Phase Separation in Polymer Nanocomposites *Macromolecules* **39** 5133
[163] Mackay M E, Tuteja A, Duxbury P M, Hawker C J, Van Horn B, Guan Z, Chen G and Krishnan R S 2006 General Strategies for Nanoparticle Dispersion *Science* **311** 1740
[164] Stamm M and Sommer J-U 2007 Polymer-nanoparticle films: Entropy and enthalpy at play *Nat. Mater.* **6** 260
[165] Gupta S, Zhang Q, Emrick T, Balazs A C and Russell T P 2006 Entropy-driven segregation of nanoparticles to cracks in multilayered composite polymer structures *Nat. Mater.* **5** 229
[166] Chiu J J, Kim B J, Kramer E J and Pine D J 2005 Control of Nanoparticle Location in Block Copolymers *J. Am. Chem. Soc.* **127** 5036
[167] Krishnan R S, Mackay M E, Duxbury P M, Pastor A, Hawker C J, VanHorn B, Wong M S and Asokan S 2007 Self-Assembled Multilayers of Nanocomponents *Nano Lett.* **7** 484
[168] Krishnan R S, Mackay M E, Duxbury P M, Hawker C J, Asokan S, Wong M S, Goyette R and Thiyagarajan P 2007 Improved polymer thin-film wetting behavior through nanoparticle segregation to interfaces *J. Phys.- Condens. Mat.* **19** 356003
[169] Tyagi S, Lee J Y, Buxton G A and Balazs A C 2004 Using Nanocomposite Coatings To Heal Surface Defects *Macromolecules* **37** 9160
[170] Matsen M W and Bates F S 1996 Origins of Complex Self-Assembly in Block Copolymers *Macromolecules* **29** 7641
[171] Albert J N L and Epps Iii T H 2010 Self-assembly of block copolymer thin films *Mater. Today* **13** 24
[172] Park B-G, Guo W, Cui X, Park J and Ha C-S 2003 Preparation and characterization of organo-modified SBA-15 by using polypropylene glycol as a swelling agent *Micropor. Mesopor. Mat.* **66** 229
[173] Lin C-L, Pang Y-S, Chao M-C, Chen B-C, Lin H-P, Tang C-Y and Lin C-Y 2008 Synthesis of SBA-16 and SBA-15 mesoporous silica crystals templated with neutral block copolymer surfactants *J. Phys. Chem. Solids* **69** 415
[174] Margolese D, Melero J A, Christiansen S C, Chmelka B F and Stucky G D 2000 Direct Syntheses of Ordered SBA-15 Mesoporous Silica Containing Sulfonic Acid Groups *Chem. Mater.* **12** 2448
[175] Stoykovich M P, Müller M, Kim S O, Solak H H, Edwards E W, de Pablo J J and Nealey P F 2005 Directed Assembly of Block Copolymer Blends into Nonregular Device-Oriented Structures *Science* **308** 1442
[176] Kim B J, Bang J, Hawker C J and Kramer E J 2006 Effect of Areal Chain Density on the Location of Polymer-Modified Gold Nanoparticles in a Block Copolymer Template *Macromolecules* **39** 4108
[177] Chiu J J, Kim B J, Yi G-R, Bang J, Kramer E J and Pine D J 2007 Distribution of Nanoparticles in Lamellar Domains of Block Copolymers *Macromolecules* **40** 3361
[178] Jang S G, Khan A, Dimitriou M D, Kim B J, Lynd N A, Kramer E J and Hawker C J 2011 Synthesis of thermally stable Au-core/Pt-shell nanoparticles and their segregation behavior in diblock copolymer mixtures *Soft Matter* **7** 6255
[179] Kao J, Bai P, Chuang V P, Jiang Z, Ercius P and Xu T 2012 Nanoparticle Assemblies in Thin Films of Supramolecular Nanocomposites *Nano Lett.* **12** 2610
[180] Farrell R A, Kinahan N T, Hansel S, Stuen K O, Petkov N, Shaw M T, West L E, Djara V, Dunne R J, Varona O G, Gleeson P G, Jung S-J, Kim H-Y, Kolesnik M M, Lutz T, Murray C P, Holmes J D, Nealey P F, Duesberg G S, Krstic V and Morris M A 2012 Large-scale parallel arrays of silicon nanowires via block copolymer directed self-assembly *Nanoscale* **4** 3228
[181] Shuaigang X, XiaoMin Y, Kim Y L, Rene J M v d V, David K and Thomas P R 2011 Aligned nanowires and nanodots by directed block copolymer assembly *Nanotechnology* **22** 305302
[182] Wang X, Zhou Y, Ren J J, Hammer N D and Chapman M R 2010 Gatekeeper residues in the major curlin subunit modulate bacterial amyloid fiber biogenesis *Proc. Natl. Acad. Sci. U S A* **107** 163

[183] Kang H, Detcheverry F, ccedil, ois A, Mangham A N, Stoykovich M P, Daoulas K C, Hamers R J, uuml, ller M, de Pablo J J and Nealey P F 2008 Hierarchical Assembly of Nanoparticle Superstructures from Block Copolymer-Nanoparticle Composites *Phys. Rev. Lett.* **100** 148303
[184] Korampally V, Yun M, Rajagopalan T, Dasgupta P K, Gangopadhyay K and Gangopadhyay S 2009 Entropy driven spontaneous formation of highly porous films from polymer-nanoparticle composites *Nanotechnology* **20** 425602
[185] Korampally V, Mamidi V K, Harris B, Gangopadhyay K, Baker G A and Gangopadhyay S 2011 Sub-minute formation of supported nanoporous mesoscale patterns programmed by surface energy *J. Colloid Interface Sci.* **364** 546
[186] Bricarello D A, Smilowitz J T, Zivkovic A M, German J B and Parikh A N 2011 Reconstituted lipoprotein: A versatile class of biologically-inspired nanostructures *ACS Nano* **5** 42
[187] Cheng J Y, Mayes A M and Ross C A 2004 Nanostructure engineering by templated self-assembly of block copolymers *Nat. Mater.* **3** 823
[188] Maury P A, Reinhoudt D N and Huskens J 2008 Assembly of nanoparticles on patterned surfaces by noncovalent interactions *Curr. Opin. Colloid Interface Sci.* **13** 74
[189] Wade T L and Wegrowe J E 2005 Template synthesis of nanomaterials *EPJ Appl. Phys.* **29** 3
[190] Bae Y, Kim N H, Kim M, Lee K Y and Han S W 2008 Anisotropic Assembly of Ag Nanoprisms *J. Am. Chem. Soc.* **130** 5432
[191] Kim J-Y and Lee J-S 2010 Synthesis and Thermodynamically Controlled Anisotropic Assembly of DNA–Silver Nanoprism Conjugates for Diagnostic Applications *Chem. Mater.* **22** 6684
[192] Murphy C J, Sau T K, Gole A M, Orendorff C J, Gao J, Gou L, Hunyadi S E and Li T 2005 Anisotropic Metal Nanoparticles: Synthesis, Assembly, and Optical Applications *J. Phys. Chem. B* **109** 13857
[193] Polarz S 2011 Shape matters: Anisotropy of the morphology of inorganic colloidal particles - Synthesis and function *Adv. Funct. Mater.* **21** 3214
[194] Sajanlal P R, Sreeprasad T S, Samal A K and Pradeep T 2011 Anisotropic nanomaterials: structure, growth, assembly, and functions *Nano Reviews* **2** 5883
[195] Nagao D, Sugimoto M, Okada A, Ishii H, Konno M, Imhof A and Van Blaaderen A 2012 Directed orientation of asymmetric composite dumbbells by electric field induced assembly *Langmuir* **28** 6546
[196] Akcora P, Liu H, Kumar S K, Moll J, Li Y, Benicewicz B C, Schadler L S, Acehan D, Panagiotopoulos A Z, Pryamitsyn V, Ganesan V, Ilavsky J, Thiyagarajan P, Colby R H and Douglas J F 2009 Anisotropic self-assembly of spherical polymer-grafted nanoparticles *Nat. Mater.* **8** 354
[197] Pryamtisyn V, Ganesan V, Panagiotopoulos A Z, Liu H and Kumar S K 2009 Modeling the anisotropic self-assembly of spherical polymer-grafted nanoparticles *J. Chem. Phys.* **131** 221102
[198] Mang X, Zeng X, Tang B, Liu F, Ungar G, Zhang R, Cseh L and Mehl G H 2012 Control of anisotropic self-assembly of gold nanoparticles coated with mesogens *J. Mater. Chem.* **22** 11101
[199] O'Brien R W and White L R 1978 Electrophoretic mobility of a spherical colloidal particle *J. Chem. Soc. Faraday Trans.* **74** 1607
[200] Fraden S, Hurd A J and Meyer R B 1989 Electric-field-induced association of colloidal particles *Phys. Rev. Lett.* **63** 2373
[201] Gast A P and Zukoski C F 1989 Electrorheological fluids as colloidal suspensions *Adv. Colloid Interface Sci.* **30** 153
[202] Dassanayake U, Fraden S and Van Blaaderen A 2000 Structure of electrorheological fluids *J. Chem. Phys.* **112** 3851
[203] Gong T, Wu D T and Marr D W M 2003 Electric field-reversible three-dimensional colloidal crystals *Langmuir* **19** 5967
[204] Ristenpart W D, Aksay I A and Saville D A 2003 Electrically guided assembly of planar superlattices in binary colloidal suspensions *Phys. Rev. Lett.* **90** 128303/1

[205] Zhang B, Zhao W and Wang D 2012 Shape-controlled self-assembly of colloidal nanoparticles *Chem. Sci.* **3** 2252
[206] Halsey T C and Toor W 1990 Structure of electrorheological fluids *Phys. Rev. Lett.* **65** 2820
[207] Lumsdon S O, Kaler E W and Velev O D 2004 Two-Dimensional Crystallization of Microspheres by a Coplanar AC Electric Field *Langmuir* **20** 2108
[208] Fagan J A, Sides P J and Prieve D C 2005 Evidence of multiple electrohydrodynamic forces acting on a colloidal particle near an electrode due to an alternating current electric field *Langmuir* **21** 1784
[209] Gong T, Wu D T and Marr D W M 2002 Two-dimensional electrohydrodynamically induced colloidal phases *Langmuir* **18** 10064
[210] Thompson D A and Best J S 2000 Future of magnetic data storage technology *IBM J. Res. Dev.* **44** 311
[211] Shylesh S, Schünemann V and Thiel W R 2010 Magnetically separable nanocatalysts: Bridges between homogeneous and heterogeneous catalysis *Angew. Chem. Int. Ed.* **49** 3428
[212] Berry C C and Curtis A S G 2003 Functionalisation of magnetic nanoparticles for applications in biomedicine *J. Phys. D: Appl. Phys.* **36** R198
[213] Shenhar R and Rotello V M 2003 Nanoparticles: Scaffolds and building blocks *Acc. Chem. Res.* **36** 549
[214] Frey N A, Peng S, Cheng K and Sun S 2009 Magnetic nanoparticles: Synthesis, functionalization, and applications in bioimaging and magnetic energy storage *Chem. Soc. Rev.* **38** 2532
[215] Jinhao G A O, Hongwei G U and Bing X U 2009 Multifunctional magnetic nanoparticles: design, synthesis, and biomedical applications *Acc. Chem. Res.* **42** 1097
[216] Lu A H, Salabas E L and Schüth F 2007 Magnetic nanoparticles: Synthesis, protection, functionalization, and application *Angew. Chem. Int. Ed.* **46** 1222
[217] Roca A G, Costo R, Rebolledo A F, Veintemillas-Verdaguer S, Tartaj P, González-Carreño T, Morales M P and Serna C J 2009 Progress in the preparation of magnetic nanoparticles for applications in biomedicine *J. Phys. D: Appl. Phys.* **42**
[218] Lalatonne Y, Richardi J and Pileni M P 2004 Van der Waals versus dipolar forces controlling mesoscopic organizations of magnetic nanocrystals *Nat. Mater.* **3** 121
[219] Niu H, Chen Q, Zhu H, Lin Y and Zhang X 2003 Magnetic field-induced growth and self-assembly of cobalt nanocrystallites *J. Mater. Chem.* **13** 1803
[220] Tanase M, Bauer L A, Hultgren A, Silevitch D M, Sun L, Reich D H, Searson P C and Meyer G J 2001 Magnetic Alignment of Fluorescent Nanowires *Nano Lett.* **1** 155
[221] Tanase M, Silevitch D M, Hultgren A, Bauer L A, Searson P C, Meyer G J and Reich D H 2002 Magnetic trapping and self-assembly of multicomponent nanowires *J. Appl. Phys.* **91** 8549
[222] Tripp S L, Dunin-Borkowski R E and Wei A 2003 Flux Closure in Self-Assembled Cobalt Nanoparticle Rings *Angew. Chem. Int. Ed.* **42** 5591
[223] Tripp S L, Pusztay S V, Ribbe A E and Wei A 2002 Self-assembly of cobalt nanoparticle rings *J. Am. Chem. Soc.* **124** 7914
[224] Goyal A, Hall C K and Velev O D 2008 Phase diagram for stimulus-responsive materials containing dipolar colloidal particles *Phys. Rev. E: Stat., Nonlinear, Soft Matter Phys.* **77** 031401
[225] Bliznyuk V, Singamaneni S, Sahoo S, Polisetty S, He X and Binek C 2009 Self-assembly of magnetic Ni nanoparticles into 1D arrays with antiferromagnetic order *Nanotechnology* **20** 105606
[226] Zeng J, Huang J, Lu W, Wang X, Wang B, Zhang S and Hou J 2007 Necklace-like noble-metal hollow nanoparticle chains: synthesis and tunable optical properties *Adv. Mater.* **19** 2172
[227] Bao Y, Beerman M and Krishnan K M 2003 Controlled self-assembly of colloidal cobalt nanocrystals *J. Magn. Magn. Mater.* **266** L245

[228] Krishnan K M, Pakhomov A B, Bao Y, Blomqvist P, Chun Y, Gonzales M, Griffin K, Ji X and Roberts B K 2006 Nanomagnetism and spin electronics: Materials, microstructure and novel properties *J. Mater. Sci.* **41** 793
[229] Zhang F and Wang C C 2008 Fabrication of one-dimensional iron oxide/silica nanostructures with high magnetic sensitivity by dipole-directed self-assembly *J. Phys. Chem. C* **112** 15151
[230] Prasad V, Semwogerere D and Weeks E R 2007 Confocal microscopy of colloids *J. Phys.- Condens. Mat.* **19**
[231] Chen L B, Ackerson B J and Zukoski C F 1994 Rheological consequences of microstructural transitions in colloidal crystals *J. Rheol.* **38** 193
[232] Chen L B, Zukoski C F, Ackerson B J, Hanley H J M, Straty G C, Barker J and Glinka C J 1992 Structural changes and orientaional order in a sheared colloidal suspension *Phys. Rev. Lett.* **69** 688
[233] Eberle A P R and Porcar L 2012 Flow-SANS and Rheo-SANS applied to soft matter *Curr. Opin. Colloid Interface Sci.* **17** 33
[234] Fry D, Langhorst B, Wang H, Becker M L, Bauer B J, Grulke E A and Hobbie E K 2006 Rheo-optical studies of carbon nanotube suspensions *J. Chem. Phys.* **124** 1
[235] Gunes D Z, Scirocco R, Mewis J and Vermant J 2008 Flow-induced orientation of non-spherical particles: Effect of aspect ratio and medium rheology *J. Non-Newton. Fluid Mech.* **155** 39
[236] McConnell G A, Gast A P, Huang J S and Smith S D 1993 Disorder-order transitions in soft sphere polymer micelles *Phys. Rev. Lett.* **71** 2102
[237] McConnell G A, Lin M Y and Gast A P 1995 Long range order in polymeric micelles under steady shear *Macromolecules* **28** 6754
[238] Panine P, Narayanan T, Vermant J and Mewis J 2002 Structure and rheology during shear-induced crystallization of a latex suspension *Phys. Rev. E: Stat., Nonlinear, Soft Matter Phys.* **66** 022401/1
[239] Pujari S, Rahatekar S S, Gilman J W, Koziol K K, Windle A H and Burghardt W R 2009 Orientation dynamics in multiwalled carbon nanotube dispersions under shear flow *J. Chem. Phys.* **130** 214903
[240] Schmidt G and Malwitz M M 2003 Properties of polymer-nanoparticle composites *Curr. Opin. Colloid Interface Sci.* **8** 103
[241] Vermant J 2001 Large-scale structures in sheared colloidal dispersions *Curr. Opin. Colloid Interface Sci.* **6** 489
[242] Vermant J and Solomon M J 2005 Flow-induced structure in colloidal suspensions *J. Phys.-Condens. Mat.* **17** R187
[243] Yan Y D, Dhont J K G, Smits C and Lekkerkerker H N W 1994 Oscillatory-shear-induced order in nonaqueous dispersions of charged colloidal spheres *Physica A* **202** 68
[244] Stancik E J, Gavranovic G T, Widenbrant M J O, Laschitsch A T, Vermant J and Fuller G G 2003 Structure and dynamics of particle monolayers at a liquid-liquid interface subjected to shear flow *Faraday Discuss.* **123** 145
[245] Scirocco R, Vermant J and Mewis J 2004 Effect of the viscoelasticity of the suspending fluid on structure formation in suspensions *J. Non-Newton. Fluid Mech.* **117** 183
[246] Pasquino R, Snijkers F, Grizzuti N and Vermant J 2010 Directed self-assembly of spheres into a two-dimensional colloidal crystal by viscoelastic stresses *Langmuir* **26** 3016
[247] Nativ-Roth E, Yerushalmi-Rozen R and Regev O 2008 Phase behavior and shear alignment in SWNT-surfactant dispersions *Small* **4** 1459
[248] Weiss V, Thiruvengadathan R and Regev O 2006 Preparation and characterization of a carbon nanotube - Lyotropic liquid crystal composite *Langmuir* **22** 854
[249] Hobbie E K 2007 Shape of the isotropic-(para)nematic coexistence curve in sheared nanotube suspensions *Phys. Rev. E: Stat., Nonlinear, Soft Matter Phys.* **75** 012501

[250] Hobbie E K and Fry D J 2006 Nonequilibrium phase diagram of sticky nanotube suspensions *Phys. Rev. Lett.* **97** 036101
[251] Hobbie E K and Fry D J 2007 Rheology of concentrated carbon nanotube suspensions *J. Chem. Phys.* **126** 124907
[252] Ma A W K, Mackley M R and Rahatekar S S 2007 Experimental observation on the flow-induced assembly of Carbon nanotube suspensions to form helical bands *Rheol. Acta* **46** 979
[253] Vigolo B, Penicaud A, Coulon C, Sauder C, Pailler R, Journet C, Bernier P and Poulin P 2000 Macroscopic fibers and ribbons of oriented carbon nanotubes *Science* **290** 1331
[254] Janes D W, Katzenstein J M, Shanmuganathan K and Ellison C J 2013 Directing convection to pattern thin polymer films *J. Polym. Sci., Part B: Polym. Phys.* **51** 535
[255] Kralchevsky P A and Denkov N D 2001 Capillary forces and structuring in layers of colloid particles *Curr. Opin. Colloid Interface Sci.* **6** 383
[256] Kralchevsky P A, Denkov N D and Danov K D 2001 Particles with an undulated contact line at a fluid interface: Interaction between capillary quadrupoles and rheology of particulate monolayers *Langmuir* **17** 7694
[257] Lehle H, Noruzifar E and Oettel M 2008 Ellipsoidal particles at fluid interfaces *Eur. Phys. J. E* **26** 151
[258] Lewandowski E P, Bernate J A, Tseng A, Searson P C and Stebe K J 2009 Oriented assembly of anisotropic particles by capillary interactions *Soft Matter* **5** 886
[259] Loudet J C, Alsayed A M, Zhang J and Yodh A G 2005 Capillary interactions between anisotropic colloidal particles *Phys. Rev. Lett.* **94**
[260] Madivala B, Fransaer J and Vermant J 2009 Self-assembly and rheology of ellipsoidal particles at interfaces *Langmuir* **25** 2718
[261] Böker A, He J, Emrick T and Russell T P 2007 Self-assembly of nanoparticles at interfaces *Soft Matter* **3** 1231
[262] Stamou D, Duschl C and Johannsmann D 2000 Long-range attraction between colloidal spheres at the air-water interface: The consequence of an irregular meniscus *Phys. Rev. E* **62** 5263
[263] Binder W H 2005 Supramolecular Assembly of Nanoparticles at Liquid–Liquid Interfaces *Angew. Chem. Int. Ed.* **44** 5172
[264] Lin Y, Skaff H, Emrick T, Dinsmore A D and Russell T P 2003 Nanoparticle Assembly and Transport at Liquid-Liquid Interfaces *Science* **299** 226
[265] Duan H, Wang D, Kurth D G and Möhwald H 2004 Directing Self-Assembly of Nanoparticles at Water/Oil Interfaces *Angew. Chem. Int. Ed.* **43** 5639
[266] Russell J T, Lin Y, Böker A, Su L, Carl P, Zettl H, He J, Sill K, Tangirala R, Emrick T, Littrell K, Thiyagarajan P, Cookson D, Fery A, Wang Q and Russell T P 2005 Self-Assembly and Cross-Linking of Bionanoparticles at Liquid–Liquid Interfaces *Angew. Chem. Int. Ed.* **117** 2472
[267] Hellsing M S, Kapaklis V, Rennie A R, Hughes A V and Porcar L 2012 Crystalline order of polymer nanoparticles over large areas at solid/liquid interfaces *Appl. Phys. Lett.* **100** 221601
[268] Bigioni T P, Lin X-M, Nguyen T T, Corwin E I, Witten T A and Jaeger H M 2006 Kinetically driven self assembly of highly ordered nanoparticle monolayers *Nat. Mater.* **5** 265
[269] Chen Y, Fu J, Ng K C, Tang Y and Cheng W 2011 Free-Standing Polymer–Nanoparticle Superlattice Sheets Self-Assembled at the Air–Liquid Interface *Cryst. Growth Des.* **11** 4742
[270] Ng K C, Udagedara I B, Rukhlenko I D, Chen Y, Tang Y, Premaratne M and Cheng W 2011 Free-Standing Plasmonic-Nanorod Superlattice Sheets *ACS Nano* **6** 925
[271] Cheng W, Campolongo M J, Cha J J, Tan S J, Umbach C C, Muller D A and Luo D 2009 Free-standing nanoparticle superlattice sheets controlled by DNA *Nat. Mater.* **8** 519
[272] Cheng W, Campolongo M J, Tan S J and Luo D 2009 Freestanding ultrathin nano-membranes via self-assembly *Nano Today* **4** 482

[273] Mittal M and Fürst E M 2009 Electric field-directed convective assembly of ellipsoidal colloidal particles to create optically and mechanically anisotropic thin films *Adv. Funct. Mater.* **19** 3271
[274] Ding T, Song K, Clays K and Tung C H 2009 Fabrication of 3D photonic crystals of ellipsoids: Convective self-assembly in magnetic field *Adv. Mater.* **21** 1936
[275] Csoka L, Hoeger I C, Peralta P, Peszlen I and Rojas O J 2011 Dielectrophoresis of cellulose nanocrystals and alignment in ultrathin films by electric field-assisted shear assembly *J. Colloid Interface Sci.* **363** 206
[276] Berry R M 2000 Theories of rotary motors *Philos. Trans. Roy. Soc. B* **355** 503
[277] Casjens S R 2011 The DNA-packaging nanomotor of tailed bacteriophages *Nat. Rev. Microbiol.* **9** 647
[278] Lee T J and Guo P 2006 Interaction of gp16 with pRNA and DNA for genome packaging by the motor of bacterial virus phi29 *J. Mol. Biol.* **356** 589
[279] Wang H and Oster G 1998 Energy transduction in the F1 motor of ATP synthase *Nature* **396** 279
[280] Zandonella C 2003 Cell nanotechnology: The tiny toolkit *Nature* **423** 10
[281] Epstein J R, Leung A P, Lee K H and Walt D R 2003 High-density, microsphere-based fiber optic DNA microarrays *Biosens. Bioelectron.* **18** 541
[282] Wittenberg N J, Im H, Johnson T W, Xu X, Warrington A E, Rodriguez M and Oh S H 2011 Facile assembly of micro- and nanoarrays for sensing with natural cell membranes *ACS Nano* **5** 7555
[283] Yeakley J M, Fan J B, Doucet D, Luo L, Wickham E, Ye Z, Chee M S and Fu X D 2002 Profiling alternative splicing on fiber-optic arrays *Nat. Biotechnol.* **20** 353
[284] Hildebrand M, Holton G, Joy D C, Doktycz M J and Allison D P 2009 Diverse and conserved nano- and mesoscale structures of diatom silica revealed by atomic force microscopy *J. Microsc.* **235** 172
[285] Yoo S Y, Lee T, Chung Y H, Min J and Choi J W 2011 Fabrication of biofilm in nanoscale consisting of cytochrome f/2-MAA bilayer on Au surface for bioelectronic devices by self-assembly technique *J. Nanosci. Nanotechnol.* **11** 7069
[286] Morone N, Fujiwara T, Murase K, Kasai R S, Ike H, Yuasa S, Usukura J and Kusumi A 2006 Three-dimensional reconstruction of the membrane skeleton at the plasma membrane interface by electron tomography *J. Cell. Biol.* **174** 851
[287] Pappas C T, Krieg P A and Gregorio C C 2010 Nebulin regulates actin filament lengths by a stabilization mechanism *J. Cell Biol.* **189** 859
[288] Lakes R 1993 Materials with structural hierarchy *Nature* **361** 511
[289] Nicolis G and Prigogine I 1989 *Exploring complexity : an introduction* W.H. Freeman
[290] Nuzzo R G and Allara D L 1983 Adsorption of bifunctional organic disulfides on gold surfaces *J. Am. Chem. Soc.* **105** 4481
[291] Tamerler C and Sarikaya M 2007 Molecular biomimetics: Utilizing nature's molecular ways in practical engineering *Acta Biomaterialia* **3** 289
[292] Srinivasan A, Haritos G and Hedberg F 1991 Biomimetics: Advancing man-made materials through guidance from nature *Appl. Mech. Rev.* **44** 463
[293] Gao H, Ji B, Jäger I L, Arzt E and Fratzl P 2003 Materials become insensitive to flaws at nanoscale: Lessons from nature *Proc. Natl. Acad. Sci. U S A* **100** 5597
[294] Nalla R K, Kinney J H and Ritchie R O 2003 Mechanistic fracture criteria for the failure of human cortical bone *Nat. Mater.* **2** 164
[295] Arzt E 2006 Biological and artificial attachment devices: Lessons for materials scientists from flies and geckos *Mat. Sci. Eng., C* **26** 1245
[296] Mann S 2009 Self-assembly and transformation of hybrid nano-objects and nanostructures under equilibrium and non-equilibrium conditions *Nat. Mater.* **8** 781

[297] Welte L, Calzolari A, Di Felice R, Zamora F and Gomez-Herrero J 2010 Highly conductive self-assembled nanoribbons of coordination polymers *Nat. Nanotechnol.* **5** 110
[298] Kisailus D, Truong Q, Amemiya Y, Weaver J C and Morse D E 2006 Self-assembled bifunctional surface mimics an enzymatic and templating protein for the synthesis of a metal oxide semiconductor *Proc. Natl. Acad. Sci. U S A* **103** 5652
[299] Baneyx G, Baugh L and Vogel V 2002 Fibronectin extension and unfolding within cell matrix fibrils controlled by cytoskeletal tension *Proc. Natl. Acad. Sci. U. S. A.* **99** 5139
[300] Hyman P, Valluzzi R and Goldberg E 2002 Design of protein struts for self-assembling nanoconstructs *Proc. Natl. Acad. Sci. U S A* **99** 8488
[301] Niemeyer C M 2002 The developments of semisynthetic DNA-protein conjugates *Trends Biotechnol.* **20** 395
[302] Soong R K, Bachand G D, Neves H P, Olkhovets A G, Craighead H G and Montemagno C D 2000 Powering an inorganic nanodevice with a biomolecular motor *Science* **290** 1555
[303] van den Heuvel M G and Dekker C 2007 Motor proteins at work for nanotechnology *Science* **317** 333
[304] Popov A M, Lozovik Y E, Fiorito S and Yahia L 2007 Biocompatibility and applications of carbon nanotubes in medical nanorobots *Int. J. Nanomed.* **2** 361
[305] Yeri A and Gao D 2011 Biosensing using nanoelectromechanical systems *Methods Mol. Biol.* **726** 119
[306] Fennimore A M, Yuzvinsky T D, Han W Q, Fuhrer M S, Cumings J and Zettl A 2003 Rotational actuators based on carbon nanotubes *Nature* **424** 408
[307] Ho D, Fung A O and Montemagno C D 2006 Engineering novel diagnostic modalities and implantable cytomimetic nanomaterials for next-generation medicine *Biol. Blood Marrow Tr.* **12** 92
[308] Lin C T, Kao M T, Kurabayashi K and Meyhofer E 2006 Efficient designs for powering microscale devices with nanoscale biomolecular motors *Small* **2** 281
[309] Liu H, Guo S, Roll R, Li J, Diao Z, Shao N, Riley M R, Cole A M, Robinson J P, Snead N M, Shen G and Guo P 2007 Phi29 pRNA vector for efficient escort of hammerhead ribozyme targeting survivin in multiple cancer cells *Cancer Biol. Ther.* **6** 697
[310] Bhushan B 2008 Nanotribology and nanomechanics in nano/biotechnology *Philos. Trans. Roy. Soc. A* **366** 1499
[311] Craighead H G 2000 Nanoelectromechanical systems *Science* **290** 1532
[312] Abe S, Hikage T, Watanabe Y, Kitagawa S and Ueno T 2010 Mechanism of accumulation and incorporation of organometallic Pd complexes into the protein nanocage of apo-ferritin *Inorg. Chem.* **49** 6967
[313] Ueno T, Abe M, Hirata K, Abe S, Suzuki M, Shimizu N, Yamamoto M, Takata M and Watanabe Y 2009 Process of accumulation of metal ions on the interior surface of apo-ferritin: crystal structures of a series of apo-ferritins containing variable quantities of Pd(II) ions *J. Am. Chem. Soc.* **131** 5094
[314] Minteer S D, Liaw B Y and Cooney M J 2007 Enzyme-based biofuel cells *Curr. Opin. Biotechnol.* **18** 228
[315] Boland S, Barriere F and Leech D 2008 Designing stable redox-active surfaces: chemical attachment of an osmium complex to glassy carbon electrodes prefunctionalized by electrochemical reduction of an in situ-generated aryldiazonium cation *Langmuir* **24** 6351
[316] Kavanagh P and Leech D 2006 Redox polymer and probe DNA tethered to gold electrodes for enzyme-amplified amperometric detection of DNA hybridization *Anal. Chem.* **78** 2710
[317] Xiao Y, Patolsky F, Katz E, Hainfeld J F and Willner I 2003 "Plugging into Enzymes": nanowiring of redox enzymes by a gold nanoparticle *Science* **299** 1877

[318] Vamvakaki V, Tsagaraki K and Chaniotakis N 2006 Carbon nanofiber-based glucose biosensor *Anal. Chem.* **78** 5538
[319] Grueninger D, Treiber N, Ziegler M O, Koetter J W, Schulze M S and Schulz G E 2008 Designed protein-protein association *Science* **319** 206
[320] Heyman A, Levy I, Altman A and Shoseyov O 2007 SP1 as a novel scaffold building block for self-assembly nanofabrication of submicron enzymatic structures *Nano Lett.* **7** 1575
[321] Dgany O, Gonzalez A, Sofer O, Wang W, Zolotnitsky G, Wolf A, Shoham Y, Altman A, Wolf S G, Shoseyov O and Almog O 2004 The structural basis of the thermostability of SP1, a novel plant (Populus tremula) boiling stable protein *J. Biol. Chem.* **279** 51516
[322] Medalsy I, Klein M, Heyman A, Shoseyov O, Remacle F, Levine R D and Porath D 2010 Logic implementations using a single nanoparticle-protein hybrid *Nat. Nanotechnol.* **5** 451
[323] Horton P and Ruban A 2005 Molecular design of the photosystem II light-harvesting antenna: photosynthesis and photoprotection *J. Exp. Bot.* **56** 365
[324] Li X P, Bjorkman O, Shih C, Grossman A R, Rosenquist M, Jansson S and Niyogi K K 2000 A pigment-binding protein essential for regulation of photosynthetic light harvesting *Nature* **403** 391
[325] Harvey P D, Brégier F, Aly S M, Szmytkowski J, Paige M F and Steer R P 2013 Dendron to central core S1-S1 and S 2-Sn (n>1) energy transfers in artificial special pairs containing dendrimers with limited numbers of conformations *Chem . - Eur. J* **19** 4352
[326] Jang W D, Lee C H, Choi M S and Osada M 2009 Synthesis of multi-porphyrin dendrimer as artificial light-harvesting antennae *J. Porphyr. Phthalocya.* **13** 787
[327] Kim J H, Lee E, Jeong Y H and Jang W D 2012 Unique photoluminescence of diacetylene containing dendrimer self-assemblies: Application in positive and negative luminescence patterning *Chem. Mater.* **24** 2356
[328] Nam Y S, Shin T, Park H, Magyar A P, Choi K, Fantner G, Nelson K A and Belcher A M 2010 Virus-templated assembly of porphyrins into light-harvesting nanoantennae *J. Am. Chem. Soc.* **132** 1462
[329] Klug A 1983 From Macromolecules to Biological Assemblies (Nobel Lecture) *Angew. Chem. Int. Ed.* **22** 565
[330] Klug A 1999 The tobacco mosaic virus particle: Structure and assembly *Philos. Trans. R. Soc. Lond. B Biol. Sci.* **354** 531
[331] Chiti F and Dobson C M 2006 Protein misfolding, functional amyloid, and human disease *Annu. Rev. Biochem.* **75** 333
[332] Lansbury P T and Lashuel H A 2006 A century-old debate on protein aggregation and neurodegeneration enters the clinic *Nature* **443** 774
[333] Chapman M R, Robinson L S, Pinkner J S, Roth R, Heuser J, Hammar M, Normark S and Hultgren S J 2002 Role of Escherichia coli curli operons in directing amyloid fiber formation *Science* **295** 851
[334] Hartgerink J D, Beniash E and Stupp S I 2001 Self-assembly and mineralization of peptide-amphiphile nanofibers *Science* **294** 1684
[335] Lakshmanan A, Zhang S and Hauser C A E 2012 Short self-assembling peptides as building blocks for modern nanodevices *Trends Biotechnol.* **30** 155
[336] Palmer L C, Newcomb C J, Kaltz S R, Spoerke E D and Stupp S I 2008 Biomimetic systems for hydroxyapatite mineralization inspired by bone and enamel *Chem. Rev.* **108** 4754
[337] Wang M, Du L, Wu X, Xiong S and Chu P K 2011 Charged diphenylalanine nanotubes and controlled hierarchical self-assembly *ACS Nano* **5** 4448
[338] Xu H, Cao B, George A and Mao C 2011 Self-assembly and mineralization of genetically modifiable biological nanofibers driven by beta-structure formation *Biomacromolecules* **12** 2193
[339] Marini D M, Hwang W, Lauffenburger D A, Zhang S and Kamm R D 2002 Left-Handed Helical Ribbon Intermediates in the Self-Assembly of a β–Sheet Peptide *Nano Lett.* **2** 295

[340] Duan X, Huang Y, Agarwal R and Lieber C M 2003 Single-nanowire elecctrically driven lasers *Nature* **421** 241
[341] Lalander C H, Zheng Y, Dhuey S, Cabrini S and Bach U 2010 DNA-directed self-assembly of gold nanoparticles onto nanopatterned surfaces: Controlled placement of individual nanoparticles into regular arrays *ACS Nano* **4** 6153
[342] Elghanian R, Storhoff J J, Mucic R C, Letsinger R L and Mirkin C A 1997 Selective colorimetric detection of polynucleotides based on the distance-dependent optical properties of gold nanoparticles *Science* **277** 1078
[343] Kannan B, Kulkarni R P and Majumdar A 2004 DNA-based programmed assembly of gold nanoparticles on lithographic patterns with extraordinary specificity *Nano Lett.* **4** 1521
[344] Kim S I, Chang Y W and Yoo K H 2007 Temperature dependence of coulomb oscillations on DNA-mediated Au nanoparticle assembly *IEEE. T. Nanotechnol.* **6** 718
[345] Lee J, Wang A A, Rheem Y, Yoo B, Mulchandani A, Chen W and Myung N V 2007 DNA assisted assembly of multisegmented nanowires *Electroanalysis* **19** 2287
[346] Kim D H and Rossi J J 2007 Strategies for silencing human disease using RNA interference *Nat. Rev. Genet.* **8** 173
[347] Joyce G F 2004 Directed evolution of nucleic acid enzymes *Annu. Rev. Biochem.* **73** 791
[348] Davidson E A and Ellington A D 2005 Engineering regulatory RNAs *Trends Biotechnol* **23** 109
[349] Khaled A, Guo S, Li F and Guo P 2005 Controllable self-assembly of nanoparticles for specific delivery of multiple therapeutic molecules to cancer cells using RNA nanotechnology *Nano Lett.* **5** 1797
[350] Chworos A, Severcan I, Koyfman A Y, Weinkam P, Oroudjev E, Hansma H G and Jaeger L 2004 Building programmable jigsaw puzzles with RNA *Science* **306** 2068
[351] Severcan I, Geary C, Verzemnieks E, Chworos A and Jaeger L 2009 Square-shaped RNA particles from different RNA folds *Nano Lett.* **9** 1270
[352] Nasalean L, Baudrey S, Leontis N B and Jaeger L 2006 Controlling RNA self-assembly to form filaments *Nucleic Acids Res.* **34** 1381
[353] Dibrov S M, McLean J, Parsons J and Hermann T 2011 Self-assembling RNA square *Proc. Natl. Acad. Sci. U S A* **108** 6405
[354] Afonin K A, Bindewald E, Yaghoubian A J, Voss N, Jacovetty E, Shapiro B A and Jaeger L 2010 In vitro assembly of cubic RNA-based scaffolds designed in silico *Nat. Nanotechnol.* **5** 676
[355] Severcan I, Geary C, Chworos A, Voss N, Jacovetty E and Jaeger L 2010 A polyhedron made of tRNAs *Nat. Chem.* **2** 772
[356] Holbrook S R, Cheong C, Tinoco I, Jr. and Kim S H 1991 Crystal structure of an RNA double helix incorporating a track of non-Watson-Crick base pairs *Nature* **353** 579
[357] Woodson S A 2010 Compact intermediates in RNA folding *Annu. Rev. Biophys.* **39** 61
[358] Jaeger L, Westhof E and Leontis N B 2001 TectoRNA: modular assembly units for the construction of RNA nano-objects *Nucleic Acids Res.* **29** 455
[359] Smalley M K and Silverman S K 2006 Fluorescence of covalently attached pyrene as a general RNA folding probe *Nucleic Acids Res.* **34** 152
[360] Shapiro B A, Bindewald E, Kasprzak W and Yingling Y 2008 Protocols for the in silico design of RNA nanostructures *Methods Mol. Biol.* **474** 93
[361] Guo P 2005 RNA nanotechnology: engineering, assembly and applications in detection, gene delivery and therapy *J. Nanosci. Nanotechnol.* **5** 1964
[362] Simons K and Sampaio J L 2011 Membrane organization and lipid rafts *Cold Spring Harb. Perspect. Biol.* **3** a004697

[363] Escriba P V, Gonzalez-Ros J M, Goni F M, Kinnunen P K, Vigh L, Sanchez-Magraner L, Fernandez A M, Busquets X, Horvath I and Barcelo-Coblijn G 2008 Membranes: a meeting point for lipids, proteins and therapies *J. Cell. Mol. Med.* **12** 829
[364] Wisniewska A, Draus J and Subczynski W K 2003 Is a fluid-mosaic model of biological membranes fully relevant? Studies on lipid organization in model and biological membranes *Cell. Mol. Biol. Lett.* **8** 147
[365] Liu J, Stace-Naughton A, Jiang X and Brinker C J 2009 Porous nanoparticle supported lipid bilayers (protocells) as delivery vehicles *J. Am. Chem. Soc.* **131** 1354
[366] Tanner P, Baumann P, Enea R, Onaca O, Palivan C and Meier W 2011 Polymeric vesicles: from drug carriers to nanoreactors and artificial organelles *Acc. Chem. Res.* **44** 1039
[367] Bangham A D 1995 Surrogate cells or Trojan horses. The discovery of liposomes *BioEssays : news and reviews in molecular, cellular and developmental biology* **17** 1081
[368] Sun B, Lim D S, Kuo J S, Kuyper C L and Chiu D T 2004 Fast initiation of chemical reactions with laser-induced breakdown of a nanoscale partition *Langmuir* **20** 9437
[369] Verma S, Dent S, Chow B J, Rayson D and Safra T 2008 Metastatic breast cancer: the role of pegylated liposomal doxorubicin after conventional anthracyclines *Cancer Treat. Rev.* **34** 391
[370] Tian B, Al-Jamal W T, Al-Jamal K T and Kostarelos K 2011 Doxorubicin-loaded lipid-quantum dot hybrids: surface topography and release properties *Int. J. Pharm.* **416** 443
[371] Garg G and Saraf S 2007 Cubosomes: An overview *Biol. Pharm. Bull.* **30** 350
[372] Nazaruk E and Bilewicz R 2007 Catalytic activity of oxidases hosted in lipidic cubic phases on electrodes *Bioelectrochemistry* **71** 8
[373] Spicer P T 2005 Progress in liquid crystalline dispersions: Cubosomes *Curr. Opin. Colloid Interface Sci.* **10** 274
[374] Barauskas J, Johnsson M, Joabsson F and Tiberg F 2005 Cubic phase nanoparticles (Cubosome): principles for controlling size, structure, and stability *Langmuir* **21** 2569
[375] Barauskas J, Johnsson M and Tiberg F 2005 Self-assembled lipid superstructures: beyond vesicles and liposomes *Nano Lett.* **5** 1615
[376] Engstrom S, Ericsson B and Landh T 1996 A cubosome formulation for intravenous administration of somatostatin *Proc. Control. Release Soc.* 89
[377] Chung H, Kim J, Um J Y, Kwon I C and Jeong S Y 2002 Self-assembled "nanocubicle" as a carrier for peroral insulin delivery *Diabetologia* **45** 448
[378] Ritchie T K, Grinkova Y V, Bayburt T H, Denisov I G, Zolnerciks J K, Atkins W M and Sligar S G 2009 Chapter 11 Reconstitution of Membrane Proteins in Phospholipid Bilayer Nanodiscs in Methods in Enzymology Ed.N. Duzgunes 464 211
[379] Denisov I G, Grinkova Y V, Lazarides A A and Sligar S G 2004 Directed self-assembly of monodisperse phospholipid bilayer Nanodiscs with controlled size *J. Am. Chem. Soc.* **126** 3477
[380] Bayburt T H and Sligar S G 2010 Membrane protein assembly into Nanodiscs *Febs Lett.* **584** 1721
[381] Baas B J, Denisov I G and Sligar S G 2004 Homotropic cooperativity of monomeric cytochrome P450 3A4 in a nanoscale native bilayer environment *Arch. Biochem. Biophys.* **430** 218
[382] Duan H, Civjan N R, Sligar S G and Schuler M A 2004 Co-incorporation of heterologously expressed Arabidopsis cytochrome P450 and P450 reductase into soluble nanoscale lipid bilayers *Arch. Biochem. Biophys.* **424** 141
[383] Bayburt T H, Grinkova Y V and Sligar S G 2006 Assembly of single bacteriorhodopsin trimers in bilayer nanodiscs *Arch. Biochem. Biophys.* **450** 215
[384] Sharma M K and Gilchrist M L 2007 Templated assembly of biomembranes on silica microspheres using bacteriorhodopsin conjugates as structural anchors *Langmuir* **23** 7101

[385] Leitz A J, Bayburt T H, Barnakov A N, Springer B A and Sligar S G 2006 Functional reconstitution of Beta2-adrenergic receptors utilizing self-assembling Nanodisc technology *Biotechniques* **40** 601
[386] Boldog T, Li M and Hazelbauer G L 2007 Using Nanodiscs to create water-soluble transmembrane chemoreceptors inserted in lipid bilayers *Method Enzymol.* **423** 317
[387] Nath A, Atkins W M and Sligar S G 2007 Applications of phospholipid bilayer nanodiscs in the study of membranes and membrane proteins *Biochemistry* **46** 2059
[388] Pease R F and Chou S Y 2008 Lithography and other patterning techniques for future electronics *P. IEEE* **96** 248
[389] Pimpin A and Srituravanich W 2012 Reviews on micro- and nanolithography techniques and their applications *Eng. J.* **16** 37
[390] Aggeli A, Nyrkova I A, Bell M, Harding R, Carrick L, McLeish T C B, Semenov A N and Boden N 2001 Hierarchical self-assembly of chiral rod-like molecules as a model for peptide β-sheet tapes, ribbons, fibrils, and fibers *Proc. Natl. Acad. Sci. U. S. A.* **98** 11857
[391] Childers W S, Mehta A K, Ni R, Taylor J V and Lynn D G 2010 Peptides organized as bilayer membranes *Angew. Chem. Int. Ed.* **49** 4104
[392] Cui H, Muraoka T, Cheetham A G and Stupp S I 2009 Self-assembly of giant peptide nanobelts *Nano Lett.* **9** 945
[393] Zhang S, Lin Y, Altman M, Lässle M, Nugent H, Frankel F, Lauffenburger D A, Whitesides G M and Rich A 1999 Biological surface engineering: A simple system for cell pattern formation *Biomaterials* **20** 1213
[394] Kim M S, Yeon J H and Park J K 2007 A microfluidic platform for 3-dimensional cell culture and cell-based assays *Biomed. Microdevices* **9** 25
[395] Hungt A M and Stupp S I 2007 Simultaneous self-assembly, orientation, and patterning of peptide-amphiphile nanofibers by soft lithography *Nano Lett.* **7** 1165
[396] Martín L, Arias F J, Alonso M, García-Arévalo C and Rodríguez-Cabello J C 2010 Rapid micropatterning by temperature-triggered reversible gelation of a recombinant smart elastin-like tetrablock-copolymer *Soft Matter* **6** 1121
[397] Jiang H and Stupp S I 2005 Dip-pen patterning and surface assembly of peptide amphiphiles *Langmuir* **21** 5242
[398] Perry H, Gopinath A, Kaplan D L, Negro L D and Omenetto F G 2008 Nano- and micropatterning of optically transparent, mechanically robust, biocompatible silk fibroin films *Adv. Mater.* **20** 3070
[399] Wilson D L, Martin R, Hong S, Cronin-Golomb M, Mirkin C A and Kaplan D L 2001 Surface organization and nanopatterning of collagen by dip-pen nanolithography *Proc. Natl. Acad. Sci. U S A* **98** 13660
[400] Zhang S, Greenfield M A, Mata A, Palmer L C, Bitton R, Mantei J R, Aparicio C, De La Cruz M O and Stupp S I 2010 A self-assembly pathway to aligned monodomain gels *Nat. Mater.* **9** 594
[401] Zhao Z, Banerjee I A and Matsui H 2005 Simultaneous targeted immobilization of anti-human IgG-coated nanotubes and anti-mouse IgG-coated nanotubes on the complementary antigen-patterned surfaces via biological molecular recognition *J. Am. Chem. Soc.* **127** 8930
[402] Miller J S, Béthencourt M I, Hahn M, Lee T R and West J L 2006 Laser-scanning lithography (LSL) for the soft lithographic patterning of cell-adhesive self-assembled monolayers *Biotechnol. Bioeng.* **93** 1060
[403] Orner B P, Derda R, Lewis R L, Thomson J A and Kiessling L L 2004 Arrays for the combinatorial exploration of cell adhesion *J. Am. Chem. Soc.* **126** 10808
[404] Yeo W S, Hodneland C D and Mrksich M 2001 Electroactive monolayer substrates that selectively release adherent cells *ChemBioChem* **2** 590
[405] Derda R, Musah S, Orner B P, Klim J R, Li N and Kiessling L L 2010 High-throughput discovery of synthetic surfaces that support proliferation of pluripotent cells *J. Am. Chem. Soc.* **132** 1289

[406] Arthur T S, Bates D J, Cirigliano N, Johnson D C, Malati P, Mosby J M, Perre E, Rawls M T, Prieto A L and Dunn B 2011 Three-dimensional electrodes and battery architectures *MRS Bull.* **36** 523
[407] Chamran F, Yeh Y, Min H S, Dunn B and Kim C J 2007 Fabrication of high-aspect-ratio electrode arrays for three-dimensional microbatteries *J. Microelectromech. S.* **16** 844
[408] Nathan M, Golodnitsky D, Yufit V, Strauss E, Ripenbein T, Shechtman I, Menkin S and Peled E 2005 Three-dimensional thin-film Li-ion microbatteries for autonomous MEMS *J. Microelectromech. S.* **14** 879
[409] Wang C, Taherabadi L, Jia G, Madou M, Yeh Y and Dunn B 2004 C-MEMS for the manufacture of 3D microbatteries *Electrochem. Solid-State Lett.* **7** A435
[410] Bruce P G, Scrosati B and Tarascon J M 2008 Nanomaterials for rechargeable lithium batteries *Angew. Chem. Int. Ed.* **47** 2930
[411] Guo Y G, Hu J S and Wan L J 2008 Nanostructured materials for electrochemical energy conversion and storage devices *Adv. Mater.* **20** 2877
[412] Jiang C, Hosono E and Zhou H 2006 Nanomaterials for lithium ion batteries *Nano Today* **1** 28
[413] Teki R, Krishnan R, Parker T C, Lu T M, Kumta P N and Koratkar N 2009 Nanostructured silicon anodes for lithium Ion rechargeable batteries *Small* **5** 2236
[414] Navone C, Pereira-Ramos J P, Baddour-Hadjean R and Salot R 2006 High-capacity crystalline V2O5 thick films prepared by RF sputtering as positive electrodes for rechargeable lithium microbatteries *J. Electrochem. Soc.* **153** A2287
[415] Patrissi C J and Martin C R 2001 Improving the Volumetric Energy Densities of Nanostructured V 2O 5 Electrodes Prepared Using the Template Method *J. Electrochem. Soc.* **148** A1247
[416] Stoney G G 1909 The tension of metallic films deposited by electrolysis *Proc. R. Soc. London, Ser. A* **82** 172
[417] Mei Y, Huang G, Solovev A A, Ureña E B, Mönch I, Ding F, Reindl T, Fu R K Y, Chu P K and Schmidt O G 2008 Versatile approach for integrative and functionalized tubes by strain engineering of nanomembranes on polymers *Adv. Mater.* **20** 4085
[418] Kim S O, Solak H H, Stoykovich M P, Ferrier N J, De Pablo J J and Nealey P F 2003 Epitaxial self-assembly of block copolymers on lithographically defined nanopatterned substrates *Nature* **424** 411
[419] Ruiz R, Kang H, Detcheverry F A, Dobisz E, Kercher D S, Albrecht T R, De Pablo J J and Nealey P F 2008 Density multiplication and improved lithography by directed block copolymer assembly *Science* **321** 936
[420] Ryu D Y, Shin K, Drockenmuller E, Hawker C J and Russell T P 2005 A generalized approach to the modification of solid surfaces *Science* **308** 236
[421] Segalman R A, Yokoyama H and Kramer E J 2001 Graphoepitaxy of spherical domain block copolymer films *Adv. Mater.* **13** 1152
[422] Black C T and Bezencenet O 2004 Nanometer-scale pattern registration and alignment by directed diblock copolymer self-assembly *IEEE T. Nanotechnol.* **3** 412
[423] Nunns A, Gwyther J and Manners I 2013 Inorganic block copolymer lithography *Polymer* **54** 1269
[424] Roman G, Martin M and Joachim P S 2003 Block copolymer micelle nanolithography *Nanotechnology* **14** 1153
[425] Farrell R A, Fitzgerald T G, Borah D, Holmes J D and Morris M A 2009 Chemical interactions and their role in the microphase separation of block copolymer thin films *Int. J. Mol. Sci.* **10** 3671
[426] Hamley I W 2000 Cell dynamics simulations of block copolymers *Macromol. Theor. Simul.* **9** 363
[427] Krausch G 1995 Surface induced self assembly in thin polymer films *Mat. Sci. Eng. R* **14** 1
[428] Olsen B D and Segalman R A 2008 Self-assembly of rod-coil block copolymers *Mat. Sci. Eng. R* **62** 37
[429] Sakurai S 1995 Control of morphology in block copolymers *Trends Polym. Sci.* **3** 90
[430] Segalman R A 2005 Patterning with block copolymer thin films *Mat. Sci. Eng. R* **48** 191

[431] Darling S B 2007 Directing the self-assembly of block copolymers *Prog. Polym. Sci.* **32** 1152
[432] Glass R, Möller M and Spatz J P 2003 Block copolymer micelle nanolithography *Nanotechnology* **14** 1153
[433] Hamley I 1998 *The Physics of block copolymers* Oxford University Press, Incorporated
[434] Hamley I W 2003 Nanotechnology with soft materials *Angew. Chem. Int. Ed.* **42** 1692
[435] Hamley I W 2005 *Block Copolymers in Solution: Fundamentals and Applications* Wiley
[436] Hawker C J and Russell T P 2005 Block copolymer lithography: Merging "bottom-up" with "top-down" processes *MRS Bull.* **30** 952
[437] Lopes W A and Jaeger H M 2001 Hierarchical self-assembly of metal nanostructures on diblock copolymer scaffolds *Nature* **414** 735
[438] Melenkevitz J and Muthukumar M 1991 Density functional theory of Lamellar ordering in diblock copolymers *Macromolecules* **24** 4199
[439] Matsen M W and Bates F S 1996 Unifying weak- and strong-segregation block copolymer theories *Macromolecules* **29** 1091
[440] Hamley I W, Koppi K A, Rosedale J H, Bates F S, Almdal K and Mortensen K 1993 Hexagonal mesophases between lamellae and cylinders in a diblock copolymer melt *Macromolecules* **26** 5959
[441] Knoll A, Horvat A, Lyaldaova K S, Krausch G, Sevink G J A, Zvelindovsky A V and Magerle R 2002 Phase behavior in thin films of cylinder-forming block copolymers *Phys. Rev. Lett.* **89** 355011
[442] Arora H, Du P, Tan K W, Hyun J K, Grazul J, Xin H L, Muller D A, Thompson M O and Wiesner U 2010 Block copolymer self-assembly-directed single-crystal homo- and heteroepitaxial nanostructures *Science* **330** 214
[443] Bratton D, Yang D, Dai J and Ober C K 2006 Recent progress in high resolution lithography *Polym. Adv. Technol.* **17** 94
[444] Cheng J Y, Ross C A, Smith H I and Thomas E L 2006 Templated self-assembly of block copolymers: Top-down helps bottom-up *Adv. Mater.* **18** 2505
[445] Malinova V, Belegrinou S, De Bruyn Ouboter D and Meier W P 2010 Biomimetic block copolymer membranes *Adv. Polym. Sci.* **224** 113
[446] Tada Y, Akasaka S, Yoshida H, Hasegawa H, Dobisz E, Kercher D and Takenaka M 2008 Directed Self-Assembly of Diblock Copolymer Thin Films on Chemically-Patterned Substrates for Defect-Free Nano-Patterning *Macromolecules* **41** 9267
[447] Gokan H, Esho S and Ohnishi Y 1983 Dry Etch Resistance of Organic Materials *J. Electrochem. Soc.* **130** 143
[448] Guarini K W, Black C T and Yeung S H I 2002 Optimization of Diblock Copolymer Thin Film Self Assembly *Adv. Mater.* **14** 1290
[449] Zschech D, Kim D H, Milenin A P, Scholz R, Hillebrand R, Hawker C J, Russell T P, Steinhart M and Gösele U 2007 Ordered Arrays of <100> - Oriented Silicon Nanorods by CMOS-Compatible Block Copolymer Lithography *Nano Lett.* **7** 1516
[450] Nitta S, Ponoth S, Breyta G, Colburn M, Clevenger L, Horak D, Bhushan M, Casey J, Chan E, Cohen S, Colt J, Flaitz P, Fluhr E, Fuller N, Kniffin A, Huang E, Hu C K, Kumar K, Landis H, Li B, Li W K, Liniger E, Lisi A, Liu X, Lloyd J R, Melville I, Muncy J, Nogami T, Ramachandran V, Rath D L, Standaert T, Sucharitaves J T, Tumbull D, Crabbe E, McCredie B, Lane M, Purushothaman S and Edelstein D A multilevel copper/low-k/airgap BEOL technology 2008, 329
[451] Black C T 2005 Self-aligned self assembly of multi-nanowire silicon field effect transistors *Appl. Phys. Lett.* **87** 163116
[452] Black C T, Ruiz R, Breyta G, Cheng J Y, Colburn M E, Guarini K W, Kim H C and Zhang Y 2007 Polymer self assembly in semiconductor microelectronics *IBM J. Res. Dev.* **51** 605

[453] Jung Y S, Jung W, Tuller H L and Ross C A 2008 Nanowire Conductive Polymer Gas Sensor Patterned Using Self-Assembled Block Copolymer Lithography *Nano Lett.* **8** 3776
[454] Shin D O, Jeong J-R, Han T H, Koo C M, Park H-J, Lim Y T and Kim S O 2010 A plasmonic biosensor array by block copolymer lithography *J. Mater. Chem.* **20** 7241
[455] Yang C Y P, Yang E L, Steinhaus C A, Liu C-C, Nealey P F and Skinner J L 2012 Planar-localized surface plasmon resonance device by block-copolymer and nanoimprint lithography fabrication methods *J. Vac. Sci. Technol., B* **30** 026801
[456] Cheng J Y, Ross C A, Chan V Z H, Thomas E L, Lammertink R G H and Vancso G J 2001 Formation of a cobalt magnetic dot array via block copolymer lithography *Adv. Mater.* **13** 1174
[457] Olszowka V, Hund M, Kuntermann V, Scherdel S, Tsarkova L and Böker A 2009 Electric Field Alignment of a Block Copolymer Nanopattern: Direct Observation of the Microscopic Mechanism *ACS Nano* **3** 1091
[458] Keller A, Pedemonte E and Willmouth F M 1970 Macro-lattice from Segregated Amorphous Phases of a Three Block Copolymer *Nature* **225** 538
[459] Ouk Kim S, Solak H H, Stoykovich M P, Ferrier N J, de Pablo J J and Nealey P F 2003 Epitaxial self-assembly of block copolymers on lithographically defined nanopatterned substrates *Nature* **424** 411
[460] Bita I, Yang J K W, Jung Y S, Ross C A, Thomas E L and Berggren K K 2008 Graphoepitaxy of Self-Assembled Block Copolymers on Two-Dimensional Periodic Patterned Templates *Science* **321** 939
[461] Jeong S-J and Kim S O 2011 Ultralarge-area block copolymer lithography via soft graphoepitaxy *J. Mater. Chem.* **21** 5856
[462] Sundrani D, Darling S B and Sibener S J 2004 Hierarchical assembly and compliance of aligned nanoscale polymer cylinders in confinement *Langmuir* **20** 5091
[463] Bal M, Ursache A, Tuominen M T, Goldbach J T and Russell T P 2002 Nanofabrication of integrated magnetoelectronic devices using patterned self-assembled copolymer templates *Appl. Phys. Lett.* **81** 3479
[464] Bosworth J K, Black C T and Ober C K 2009 Selective area control of self-assembled pattern architecture using a lithographically patternable block copolymer *ACS Nano* **3** 1761
[465] Bosworth J K, Paik M Y, Ruiz R, Schwartz E L, Huang J Q, Ko A W, Smilgies D M, Black C T and Ober C K 2008 Control of self-assembly of lithographically patternable block copolymer films *ACS Nano* **2** 1396
[466] Li M, Douki K, Goto K, Li X, Coenjarts C, Smilgies D M and Ober C K 2004 Spatially controlled fabrication of nanoporous block copolymers *Chem. Mater.* **16** 3800
[467] Maeda R, Chavis M, You N H and Ober C K 2012 Top-down meets bottom up: Block copolymers with photoreactive segments *J. Photopolym. Sci. Technol.* **25** 17
[468] Maeda R, Hayakawa T and Ober C K 2012 Dual mode patterning of fluorine-containing block copolymers through combined top-down and bottom-up lithography *Chem. Mater.* **24** 1454
[469] Krishnamoorthy S, Van Den Boogaart M A F, Brugger J, Hibert C, Pugin R, Hinderling C and Heinzelmann H 2008 Combining micelle self-assembly with nanostencil lithography to create periodic/aperiodic micro-/nanopatterns on surfaces *Adv. Mater.* **20** 3533
[470] Glass R, Arnold M, Cavalcanti-Adam E A, Blümmel J, Haferkemper C, Dodd C and Spatz J P 2004 Block copolymer micelle nanolithography on non-conductive substrates *New J. Phys.* **6** 1
[471] Calzolari D C E, Pontoni D, Daillant J and Reichert H 2013 An X-ray chamber for in situ structural studies of solvent-mediated nanoparticle self-assembly *J. Synchrotron Radiat.* **20** 306
[472] Richter A G, Yu C J, Datta A, Kmetko J and Dutta P 2002 Using X-rays to characterize the process of self-assembly in real time *Colloids Surf. A* **198-200** 3
[473] Britt D W and Hlady V 1996 An AFM study of the effects of silanization temperature, hydration, and annealing on the nucleation and aggregation of condensed OTS domains on mica *J. Colloid Interface Sci.* **178** 775

[474] Parikh A N, Liedberg B, Atre S V, Ho M and Allara D L 1995 Correlation of molecular organization and substrate wettability in the self-assembly of n-alkylsiloxane monolayers *J. Phys. Chem.* **99** 9996
[475] Tidswell I M, Rabedeau T A, Pershan P S, Kosowsky S D, Folkers J P and Whitesides G M 1991 X-ray grazing incidence diffraction from alkylsiloxane monolayers on silicon wafers *J. Chem. Phys.* **95** 2854
[476] Wasserman S R, Whitesides G M, Tidswell I M, Ocko B M, Pershan P S and Axe J D 1989 The structure of self-assembled monolayers of alkylsiloxanes on silicon: A comparison of results from ellipsometry and low-angle X-ray reflectivity *J. Am. Chem. Soc.* **111** 5852
[477] Daillant J 2009 Recent developments and applications of grazing incidence scattering *Curr. Opin. Colloid Interface Sci.* **14** 396
[478] Giner-Casares J J, Brezesinski G, Möhwald H, Landsmann S and Polarz S 2012 Polyoxometalate surfactants as unique molecules for interfacial self-assembly *J. Phys. Chem. Lett.* **3** 322
[479] Narayanan S, Wang J and Lin X M 2004 Dynamical self-assembly of nanocrystal superlattices during colloidal droplet evaporation by in situ small angle x-ray scattering *Phys. Rev. Lett.* **93** 135503
[480] Pontoni D, Alvine K J, Checco A, Gang O, Ocko B M and Pershan P S 2009 Equilibrating nanoparticle monolayers using wetting films *Phys. Rev. Lett.* **102**
[481] Roth S V, Rothkirch A, Autenrieth T, Gehrke R, Wroblewski T, Burghammer M C, Riekel C, Schulz L, Hengstler R and Müller-Buschbaum P 2010 Spatially resolved investigation of solution cast nanoparticle films by X-ray scattering and multidimensional data set classification *Langmuir* **26** 1496
[482] Choi J J, Bian K, Baumgardner W J, Smilgies D M and Hanrath T 2012 Interface-induced nucleation, orientational alignment and symmetry transformations in nanocube superlattices *Nano Lett.* **12** 4791
[483] McMullan J M and Wagner N J 2010 Directed self-assembly of colloidal crystals by dielectrophoretic ordering observed with small angle neutron scattering (SANS) *Soft Matter* **6** 5443
[484] Van Blaaderen A, Ruel R and Wiltzius P 1997 Template-directed colloidal crystallization *Nature* **385** 321
[485] Yang L, Gao K, Luo Y, Luo J, Li D and Meng Q 2011 In situ observation and measurement of evaporation-induced self-assembly under controlled pressure and temperature *Langmuir* **27** 1700
[486] Jiang Z, Lin X M, Sprung M, Narayanan S and Wang J 2010 Capturing the crystalline phase of two-dimensional nanocrystal superlattices in action *Nano Lett.* **10** 799
[487] Koh Y K and Wong C C 2006 In situ monitoring of structural changes during colloidal self-assembly *Langmuir* **22** 897
[488] Yan Q, Gao L, Sharma V, Chiang Y M and Wong C C 2008 Particle and substrate charge effects on colloidal self-assembly in a sessile drop *Langmuir* **24** 11518
[489] Bancelin S, Aimé C, Coradin T and Schanne-Klein M C 2012 In situ three-dimensional monitoring of collagen fibrillogenesis using SHG microscopy *Biomed Opt Express* **3** 1446
[490] Köster S, Evans H M, Wong J Y and Pfohl T 2008 An in situ study of collagen self-assembly processes *Biomacromolecules* **9** 199
[491] Toma A C, Dootz R and Pfohl T 2013 Analysis of complex fluids using microfluidics: The particular case of DNA/polycations assemblies *J. Phys. D: Appl. Phys.* **46**
[492] Chen C L, Bromley K M, Moradian-Oldak J and Deyoreo J J 2011 In situ AFM study of amelogenin assembly and disassembly dynamics on charged surfaces provides insights on matrix protein self-assembly *J. Am. Chem. Soc.* **133** 17406
[493] Loglio F, Schweizer M and Kolb D M 2003 In situ characterization of self-assembled butanethiol monolayers on Au(100) electrodes *Langmuir* **19** 830
[494] Surin M and Samorì P 2007 Multicomponent monolayer architectures at the solid-liquid interface: Towards controlled space-confined properties and reactivity of functional building blocks *Small* **3** 190

[495] Körstgens V, Wiedersich J, Meier R, Perlich J, Roth S V, Gehrke R and Müller-Buschbaum P 2010 Combining imaging ellipsometry and grazing incidence small angle X-ray scattering for in situ characterization of polymer nanostructures *Anal. Bioanal. Chem.* **396** 139
[496] Walker M L, Vanderah D J and Rubinson K A 2011 In-situ characterization of self-assembled monolayers of water-soluble oligo(ethylene oxide) compounds *Colloids Surf B Biointerfaces* **82** 450
[497] Weon B M, Lee J S, Kim J T, Pyo J and Je J H 2012 Colloidal wettability probed with X-ray microscopy *Curr. Opin. Colloid Interface Sci.* **17** 388
[498] De Paz-Simon H, Chemtob A, Croutxé-Barghorn C, Rigolet S, Michelin L, Vidal L and Lebeau B 2013 Block copolymer self-assembly in mesostructured silica films revealed by real-time ftir and solid-state NMR *Langmuir* **29** 1963

List of Figures

Manuscript Title: Nanomaterial Processing using Self Assembly - Bottom-Up Chemical and Biological Approaches

Revised Manuscript # ROP/397087/REV/270775

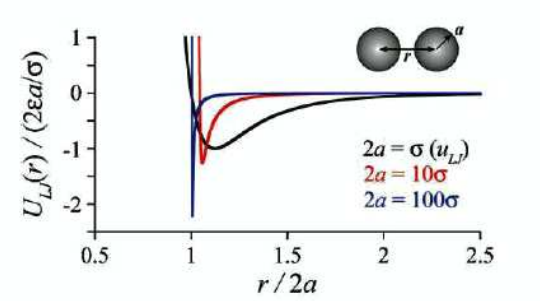

Figure 1 of 28*. Shubhra Gangopadhyay et al*

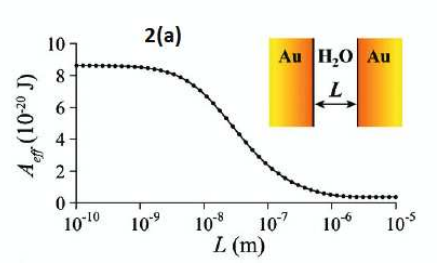

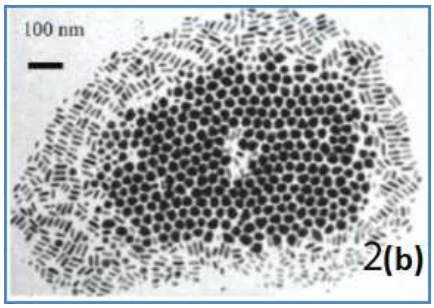

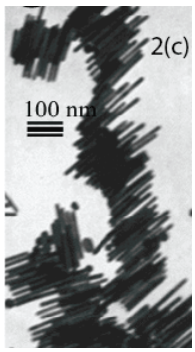

Figure 2 of 28*. Shubhra Gangopadhyay et al*

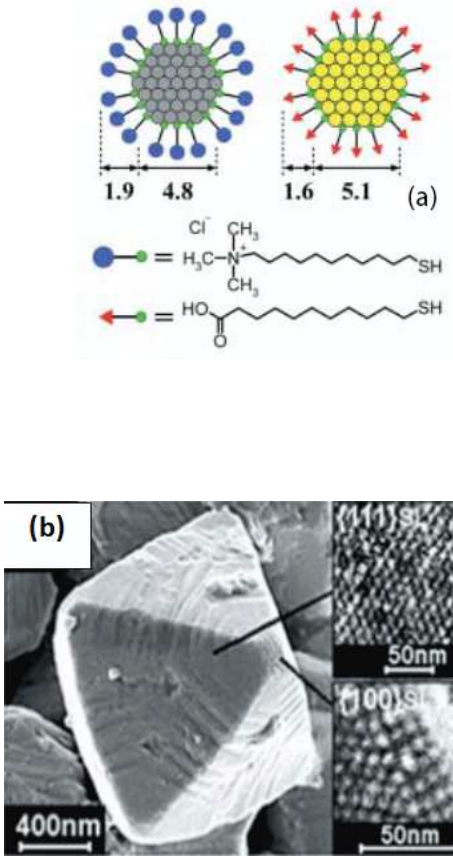

Figure 3 of 28. *Shubhra Gangopadhyay et al*

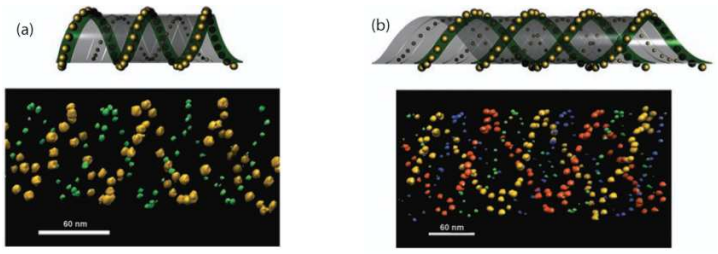

Figure 4 of 28. *Shubhra Gangopadhyay et al*

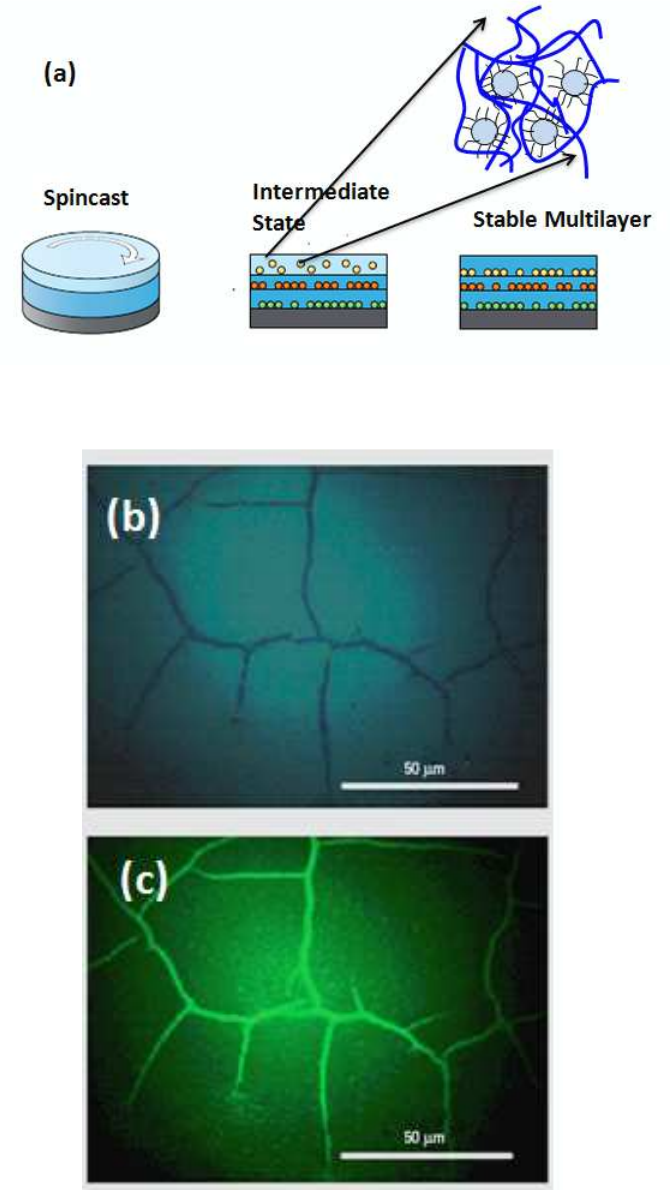

Figure 5 of 28. *Shubhra Gangopadhyay et al*

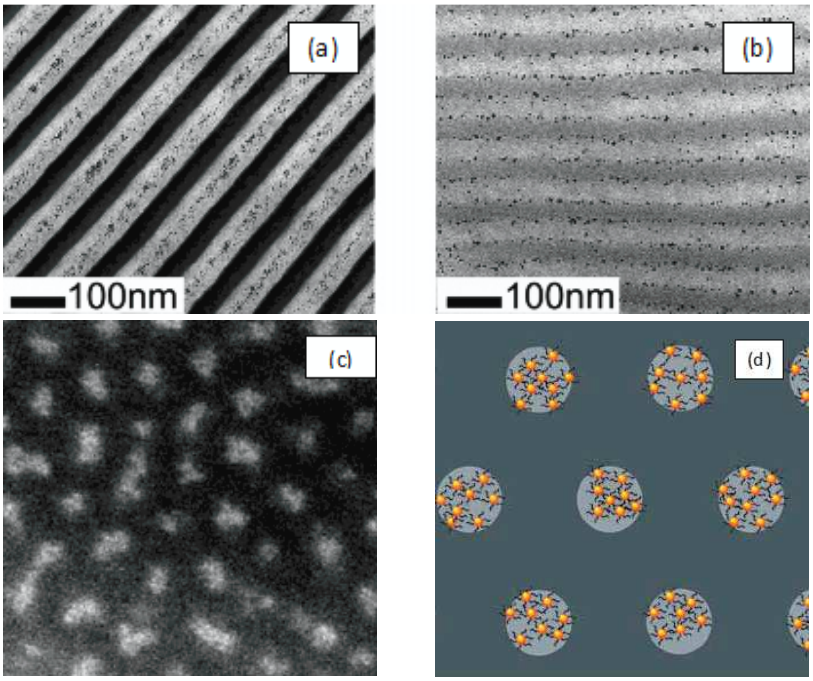

Figure 6 of 28. *Shubhra Gangopadhyay et al*

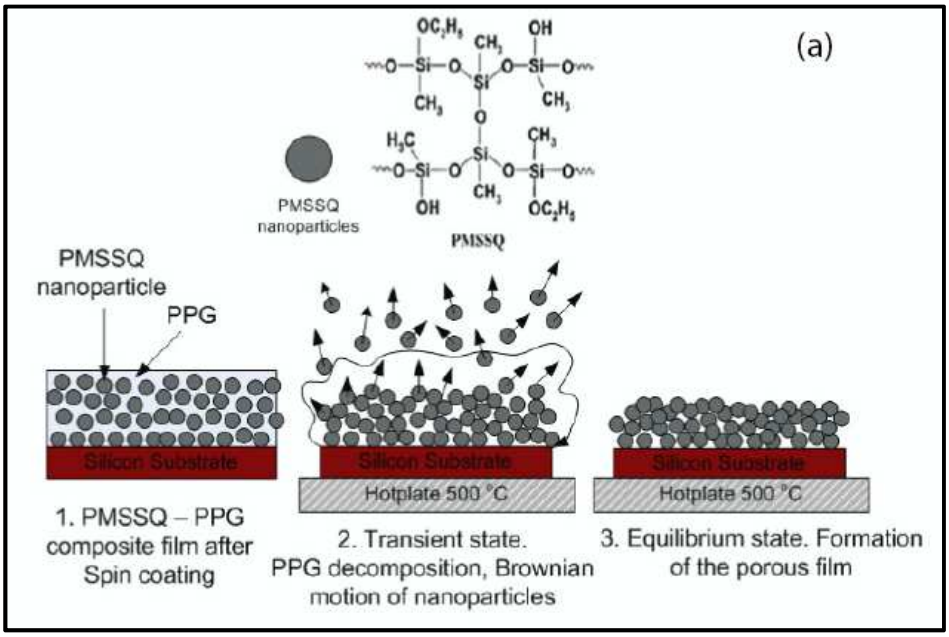

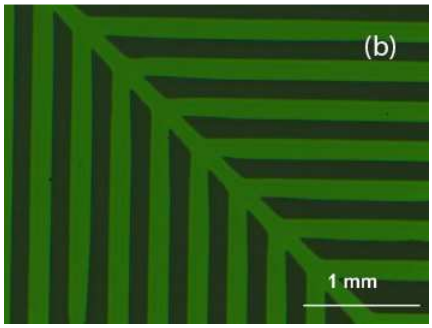

Figure 7 of 28. *Shubhra Gangopadhyay et al*

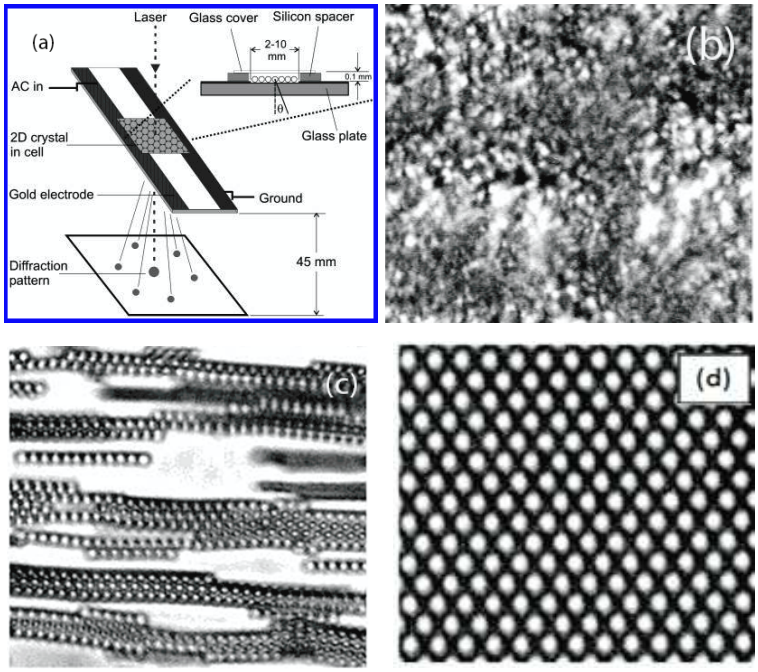

Figure 8 of 28. *Shubhra Gangopadhyay et al*

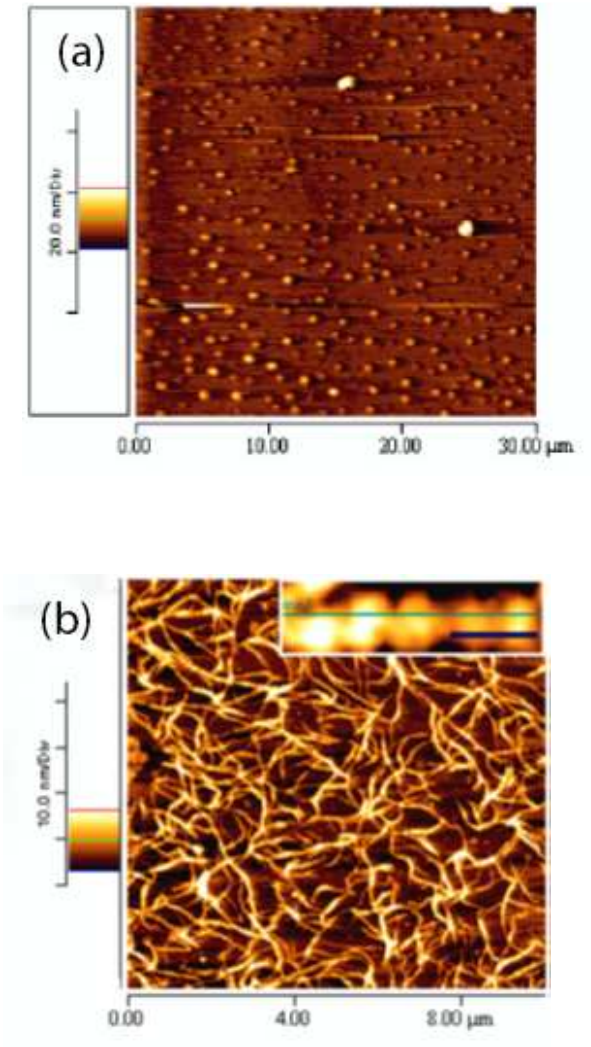

Figure 9 of 28. *Shubhra Gangopadhyay et al*

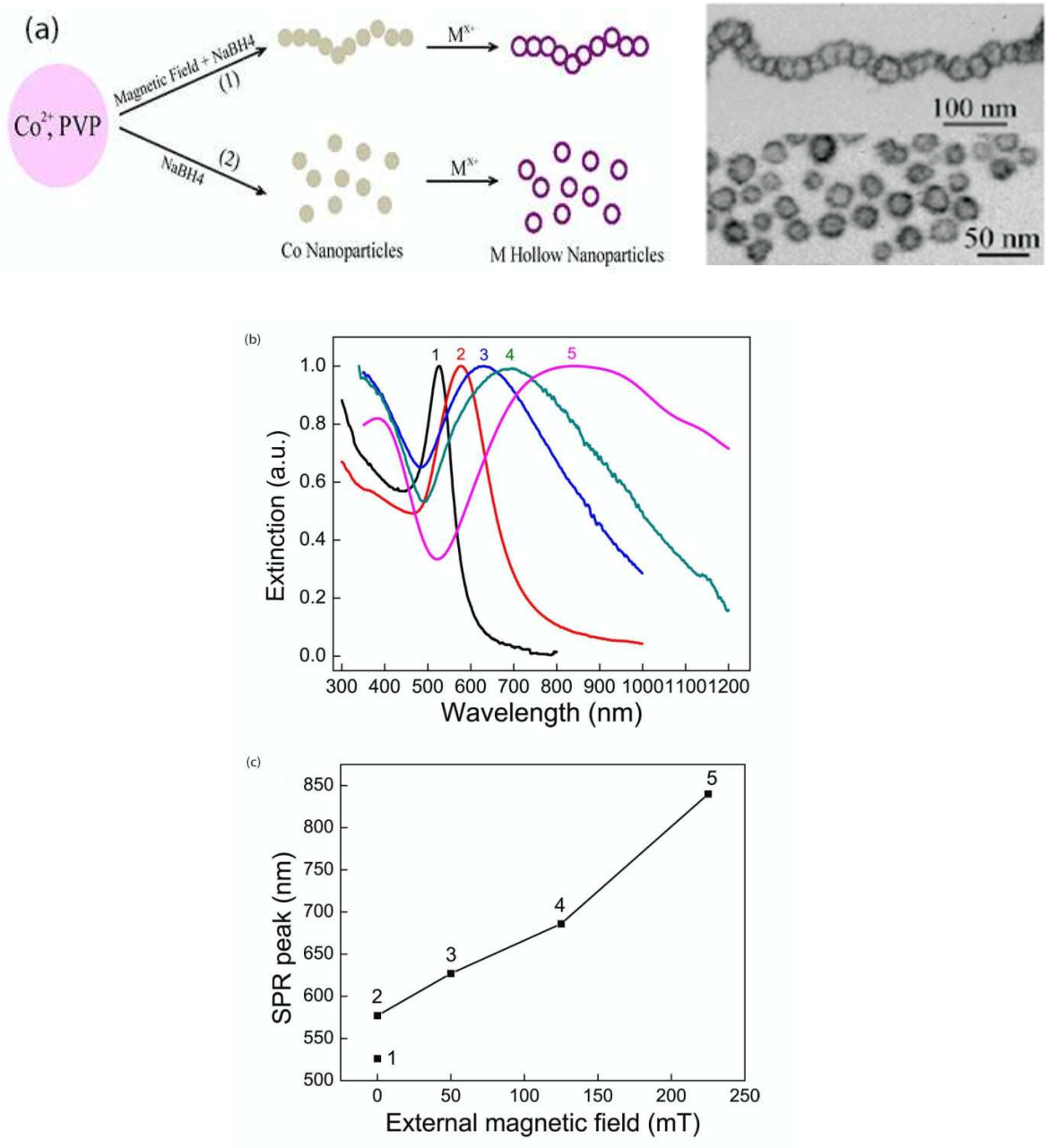

Figure 10 of 28. *Shubhra Gangopadhyay et al*

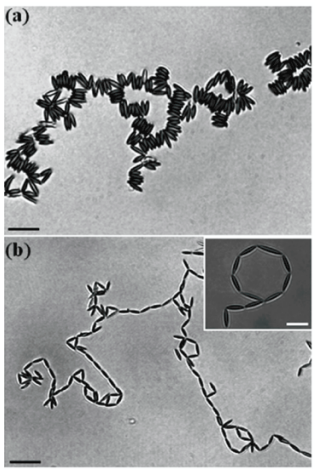

Figure 11 of 28. *Shubhra Gangopadhyay et al*

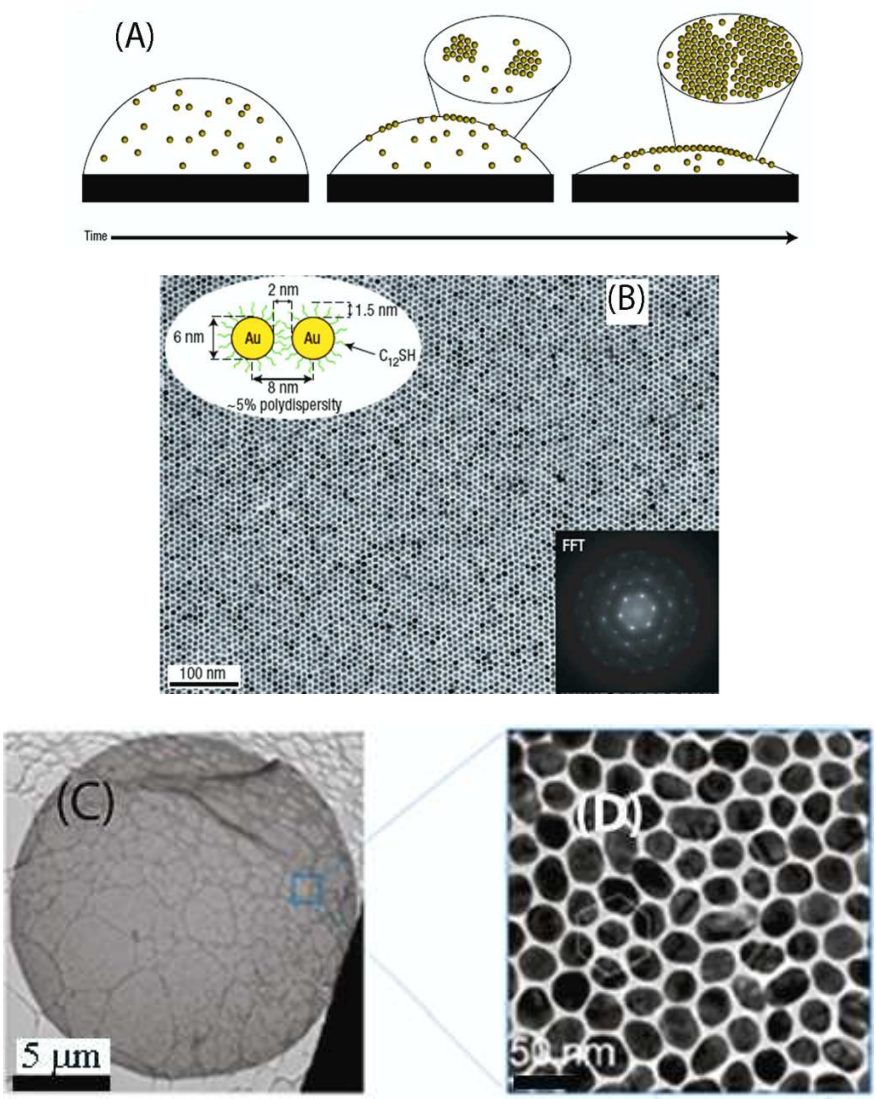

Figure 12 of 28*. Shubhra Gangopadhyay et al*

Random orientation of TiO_2 particles before application of field.

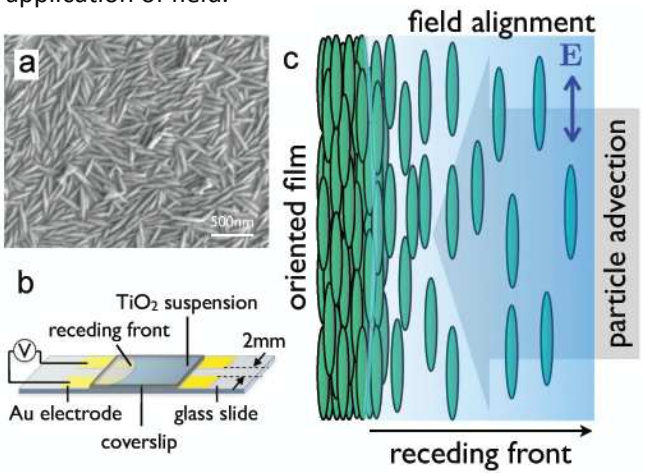

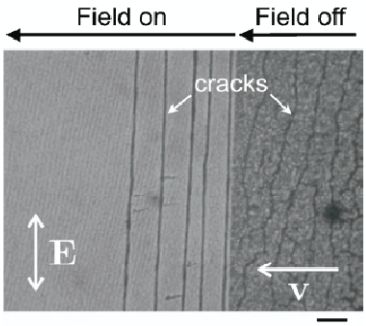

SEM images of films assembled with application of field as a function of intensity and frequency (below) and highly anisotropic cracking of the films along the direction of the field (above).

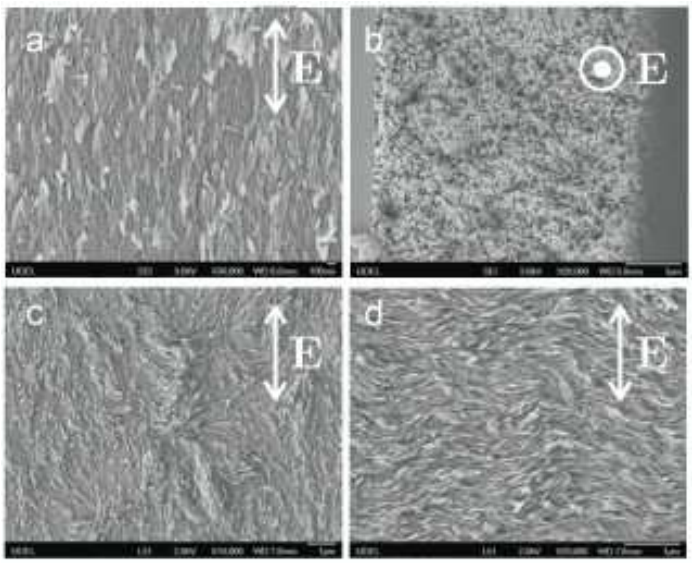

***Figure 13 of 28**. Shubhra Gangopadhyay et al*

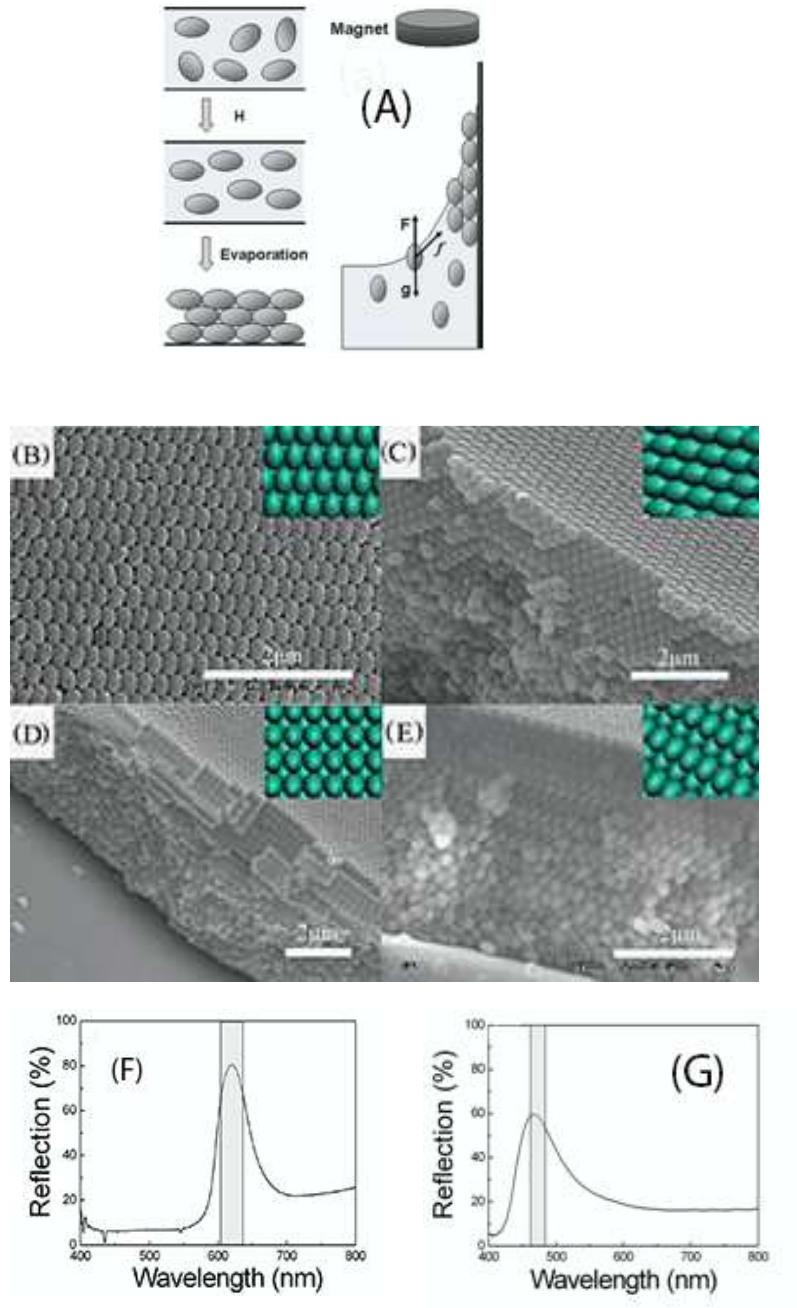

Figure 14 of 28. *Shubhra Gangopadhyay et al*

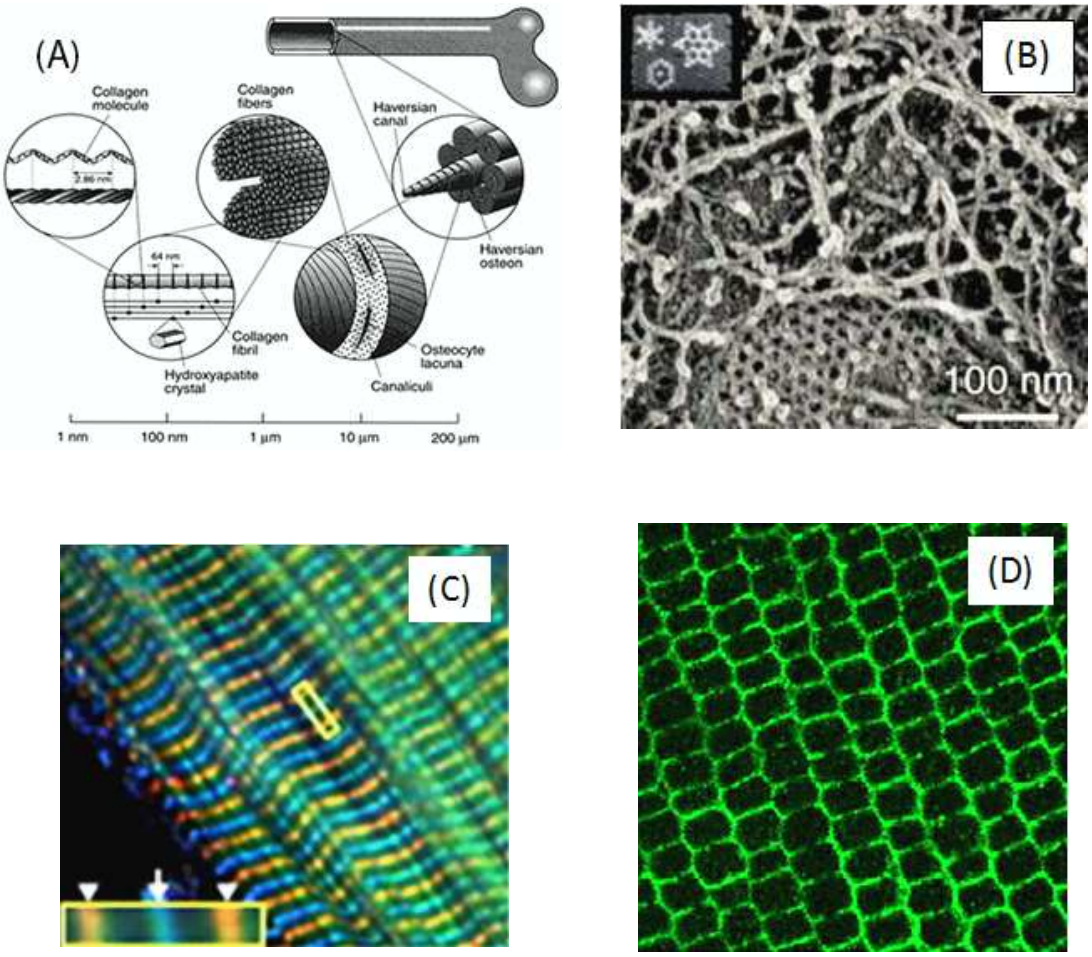

Figure 15 of 28. *Shubhra Gangopadhyay et al*

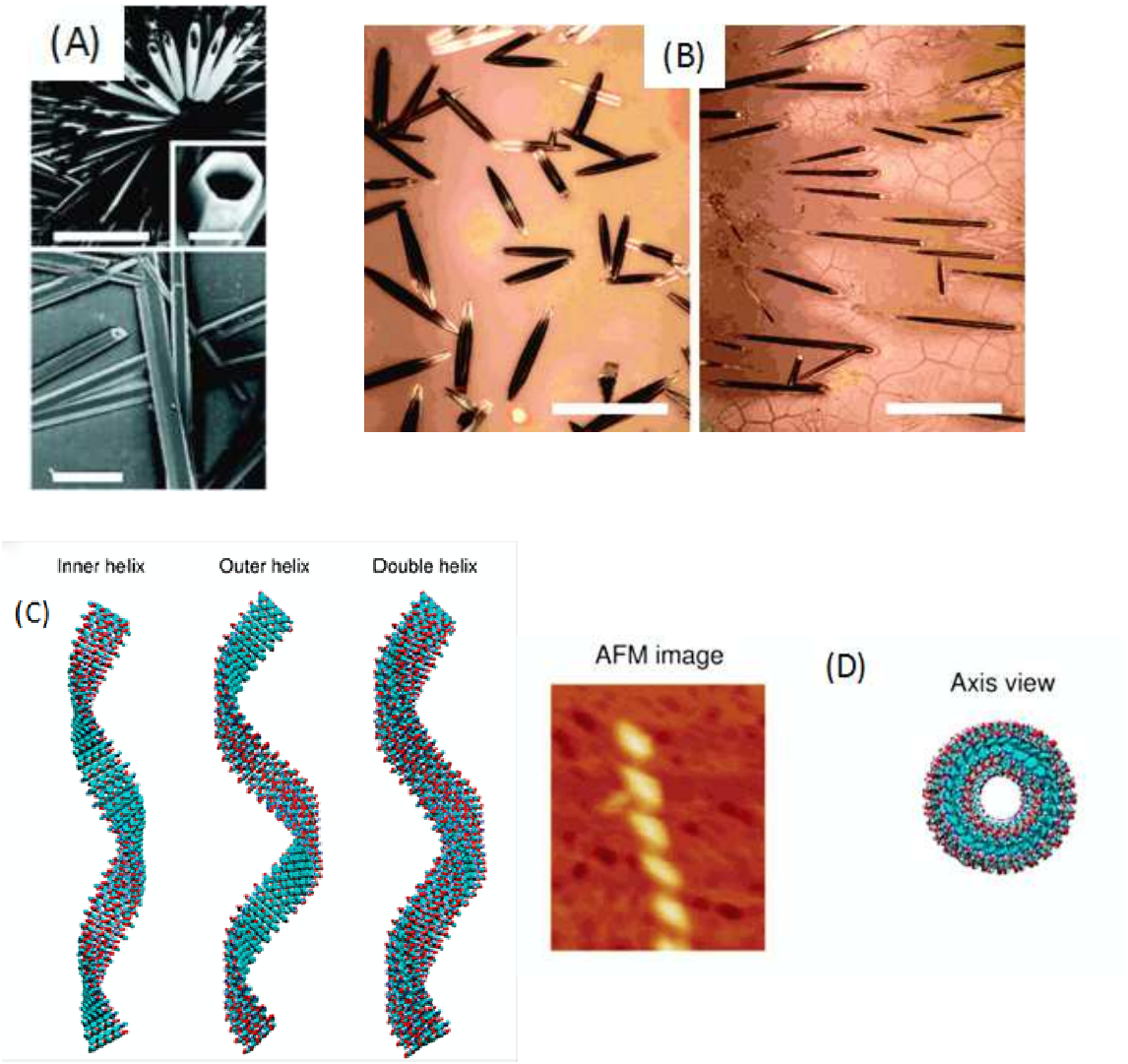

Figure 16 of 28*. Shubhra Gangopadhyay et al*

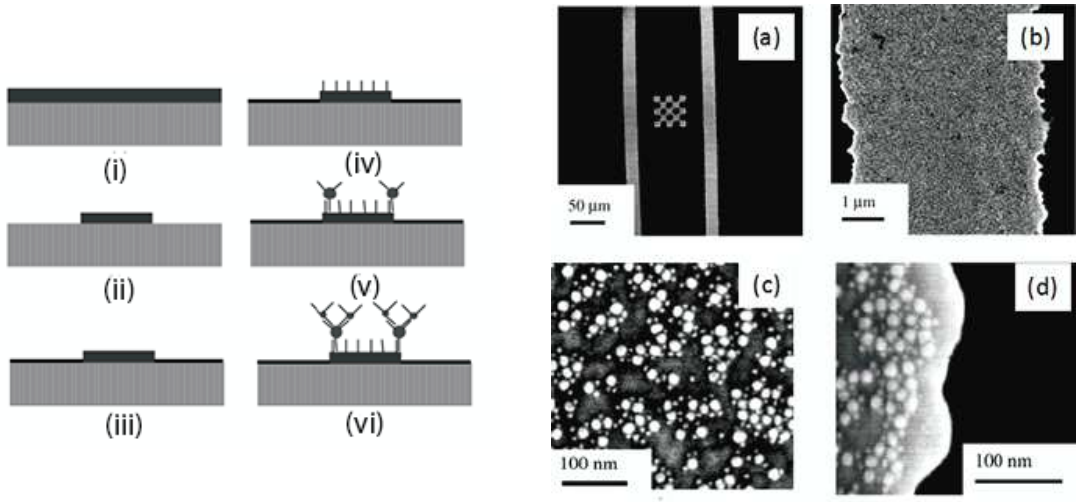

Figure 17 of 28*. Shubhra Gangopadhyay et al*

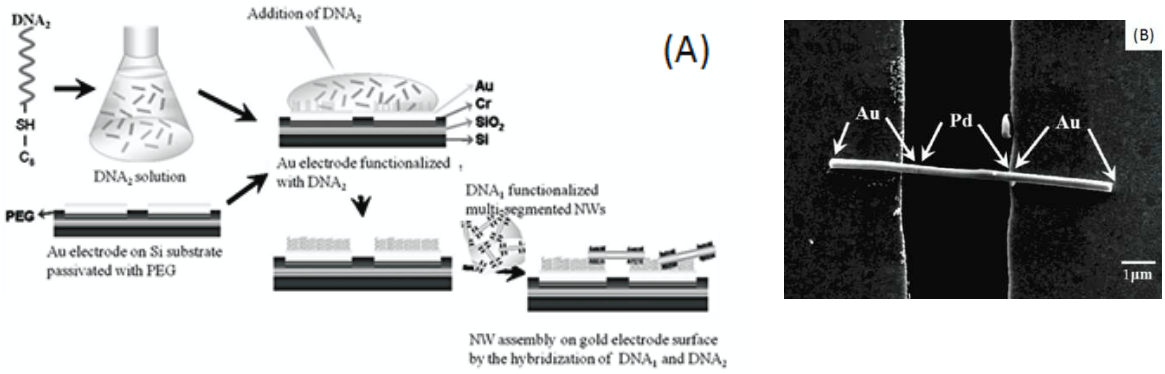

Figure 18 of 28. *Shubhra Gangopadhyay et al*

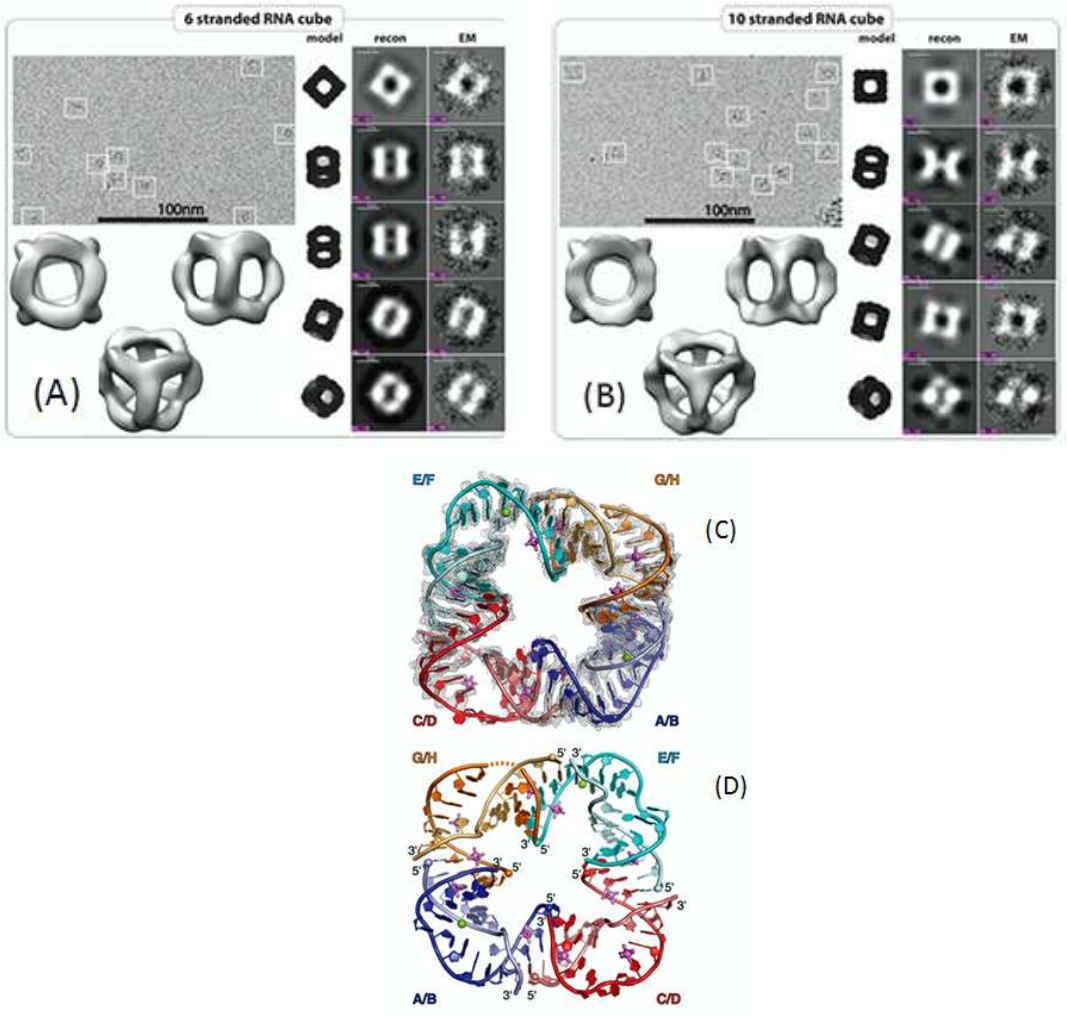

Figure 19 of 28. *Shubhra Gangopadhyay et al*

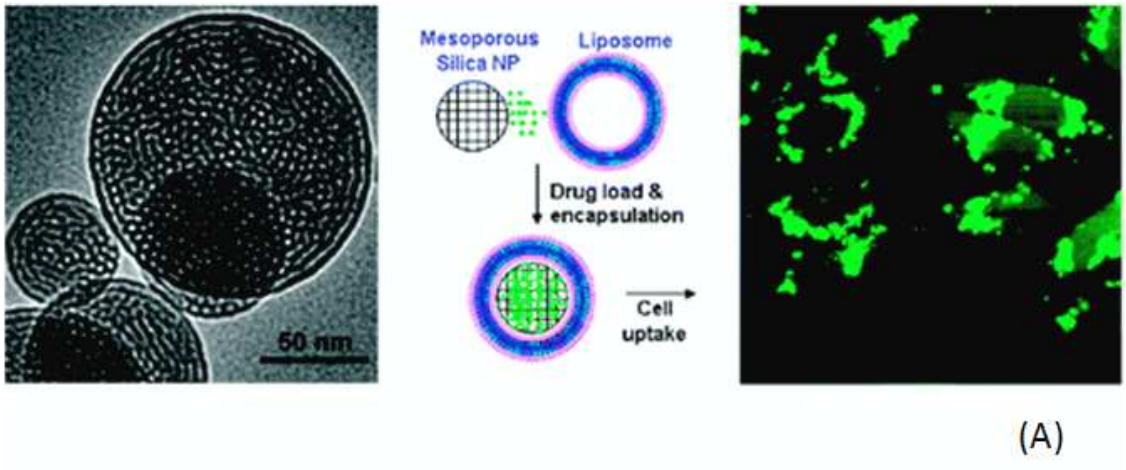

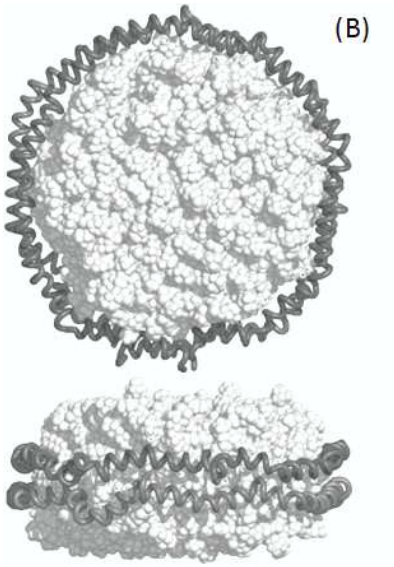

Figure 20 of 28. *Shubhra Gangopadhyay et al*

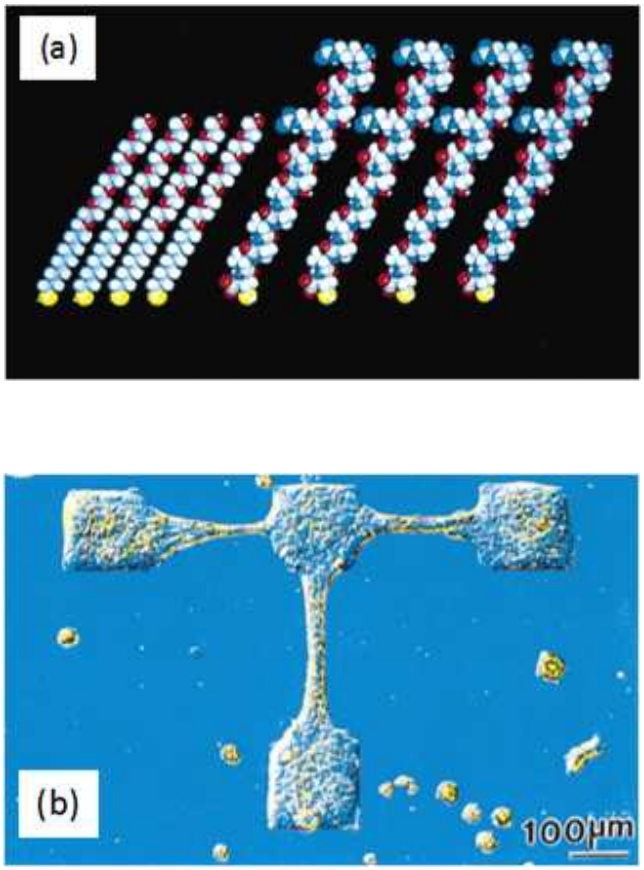

Figure 21 of 28*. Shubhra Gangopadhyay et al*

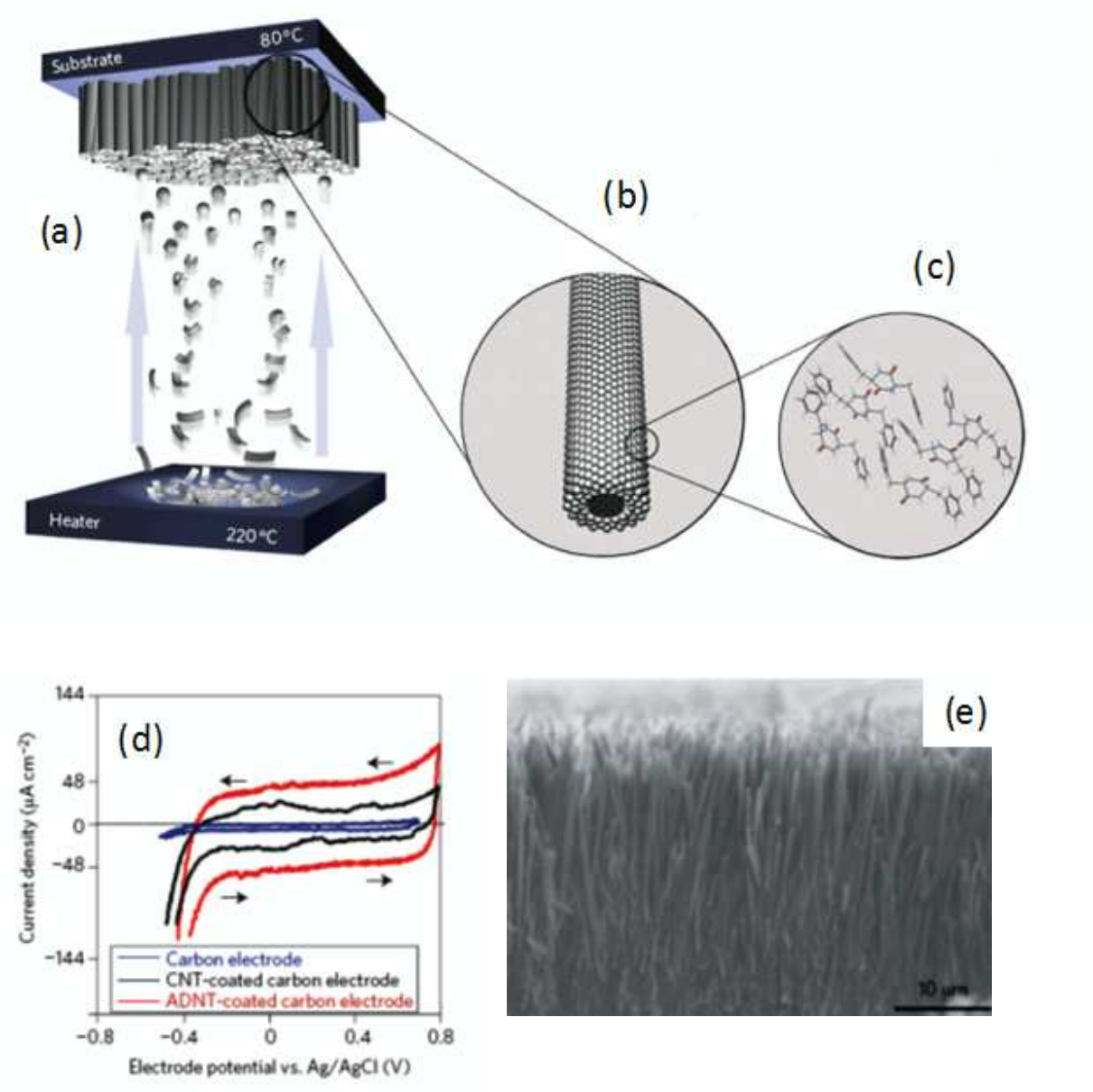

Figure 22 of 28. *Shubhra Gangopadhyay et al*

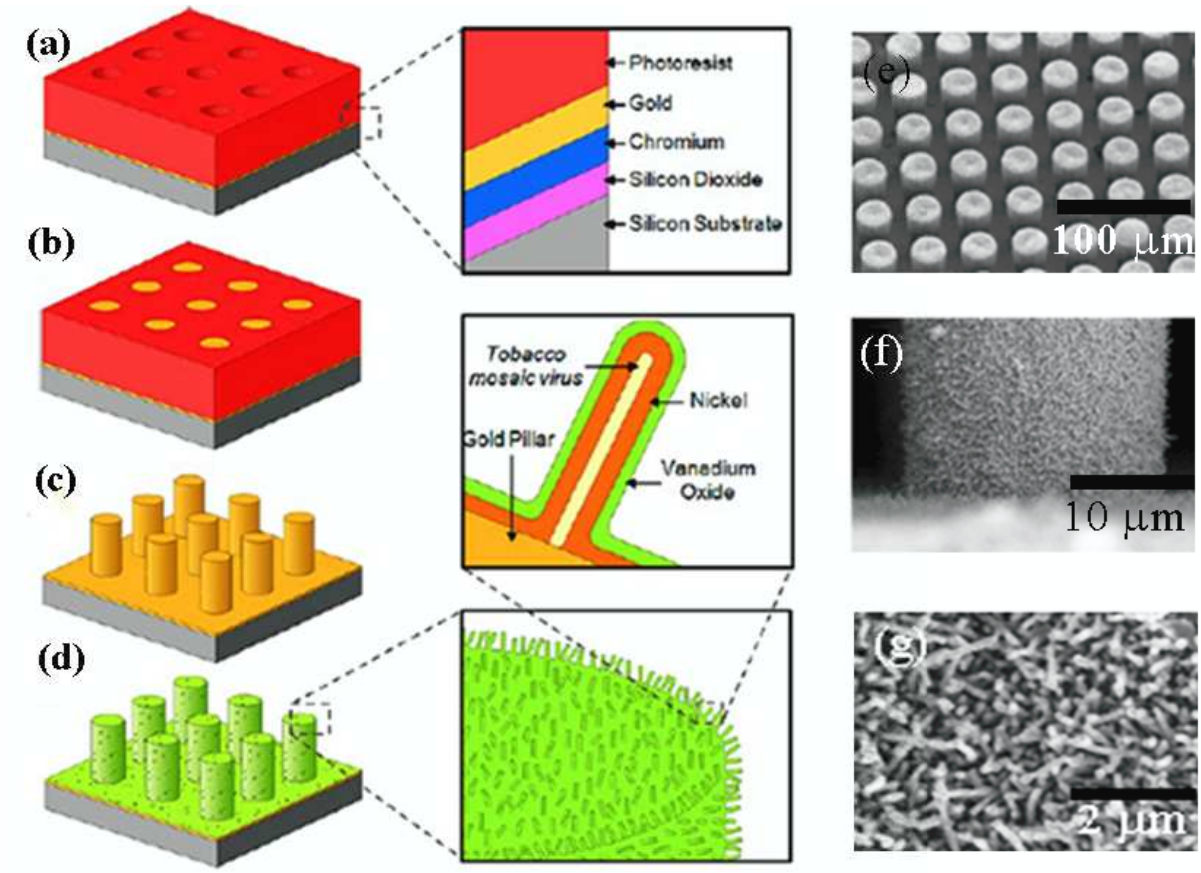

Figure 23 of 28. *Shubhra Gangopadhyay et al*

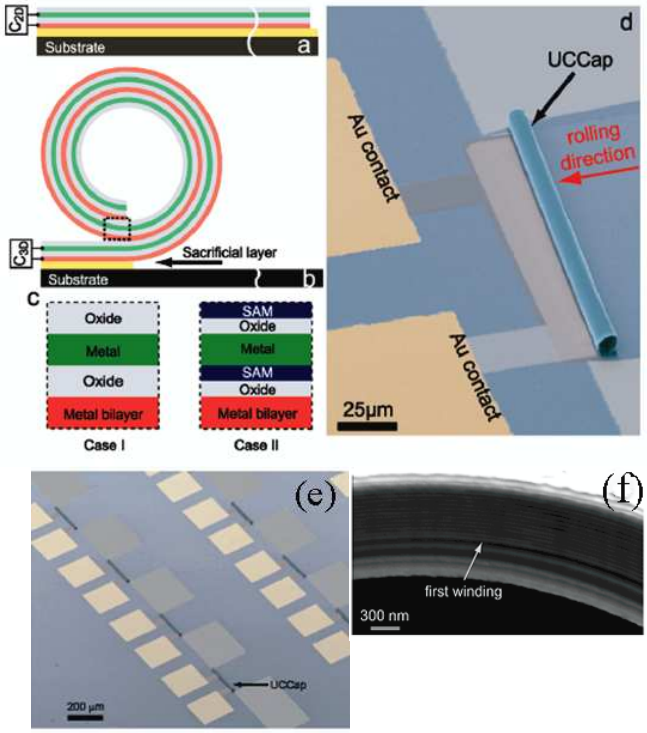

Figure 24 of 28. *Shubhra Gangopadhyay et al*

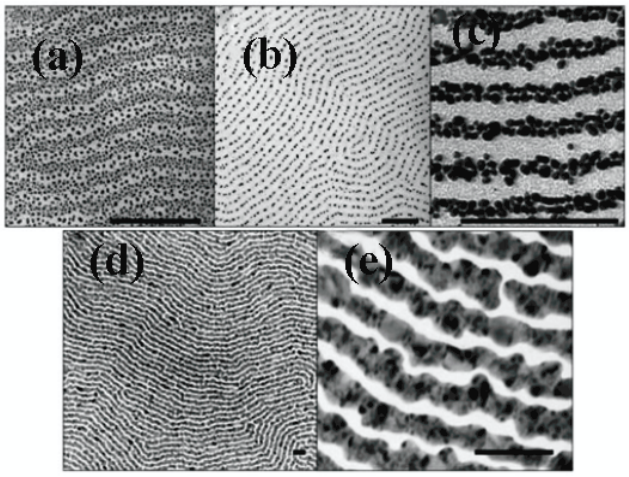

Figure 25 of 28. *Shubhra Gangopadhyay et al*

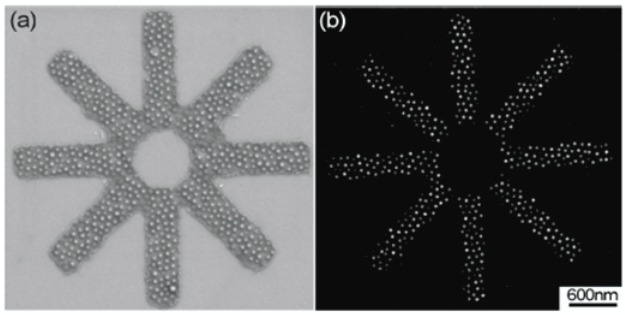

Figure 26 of 28. *Shubhra Gangopadhyay et al*

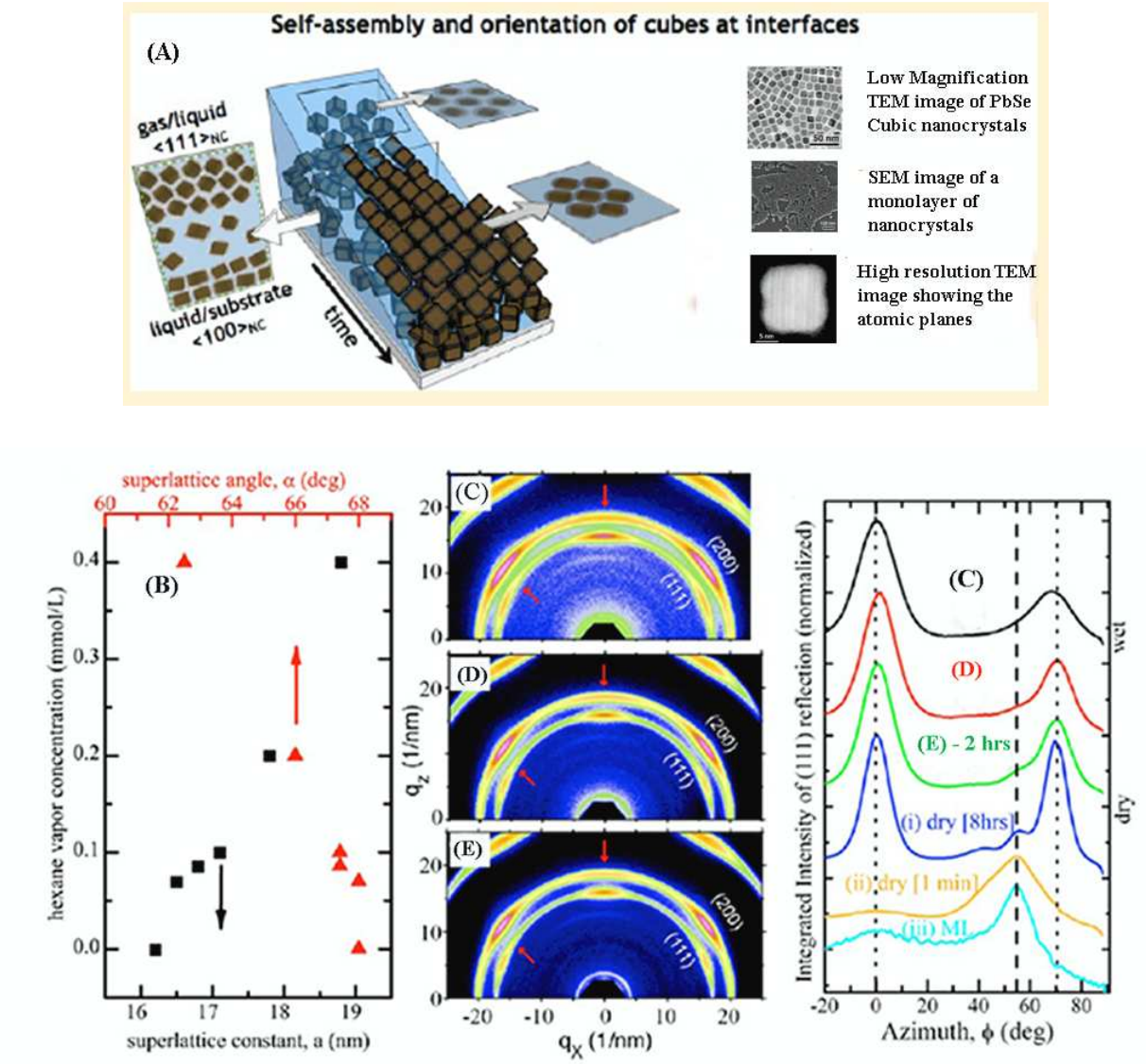

Figure 27 of 28 *Shubhra Gangopadhyay et al*

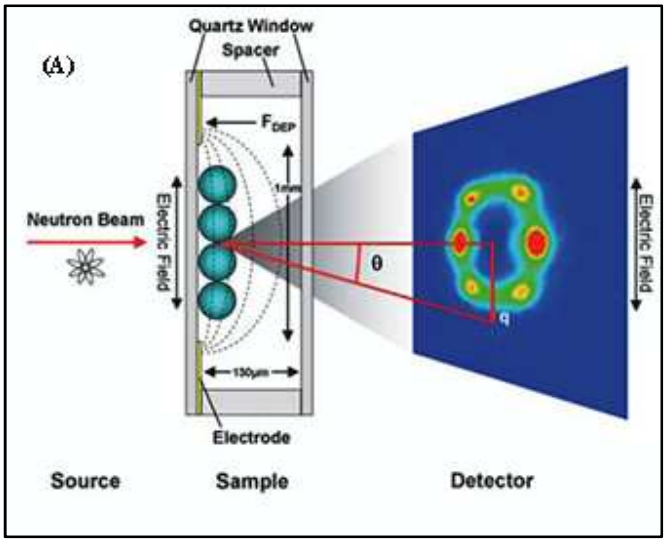

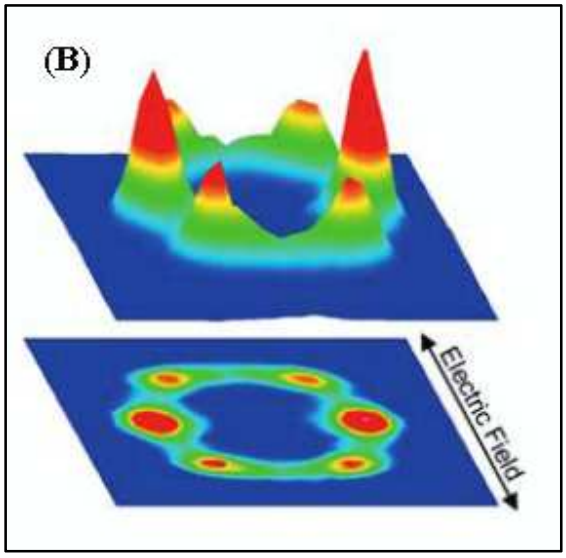

Figure 28 of 28 *Shubhra Gangopadhyay et al*